To Fold or Not to Fold:
The Role of Protein Triage in Dictating Neural Cell Fate Following Acute Injury

By

Amy Marie Palubinsky

Dissertation

Submitted to the Faculty of the

Graduate School of Vanderbilt University

in partial fulfillment of the requirements

for the degree of

DOCTOR OF PHILOSOPHY

in

Neuroscience

June 30, 2019

Nashville, Tennessee

Approved:

Eugenia Gurevich, Ph.D., Chair

BethAnn McLaughlin, Ph.D., Advisor

Rebecca Sappington, Ph.D.

Tyler Abel, M.D., Ph.D.

To my best friend and husband, Scott, and our amazing children,

Aubrianna Marie,
Jackson James
&
Baby P #3

This family of ours was only a dream when this all began,
But your smiles, laughter and love saw me through…

ACKNOWLEDGEMENTS

This work was made possible through the guidance of the most dedicated and passionate scientist I have ever known. Dr. McLaughlin's mentorship, encouragement and support have made me the researcher I only ever dreamt I could be. She has instilled in me, through example, not just scientific knowledge and know-how but life skills like patience and resilience. She has been a constant reminder that science is not everything; that health and wellbeing are extremely important and that family comes first. But for her, these are not just things you say, they are things that as a mentor, you make possible. In doing so, she provided a training environment that challenged me to think outside of the box, to try things that I never would have seen myself doing (Mass Spec anyone?), to think big but stay streamlined, and to always stand up for what is right no matter what the consequences. It is these intangibles that I could never thank her for enough…but I'll try. THANKS BOSS!!!

To Ms. Amelia Stanwood, whose tenacity shines through in everything she does. I thank you for being you. For always having a smile, hug or cookie to give. For offering to help in so so so many ways and for being a shining example of what it means to be a truly good human! To the members of the McLaughlin lab (past and present), I am forever grateful for being able to "science" with such an amazing group of people. Research is hard and can be draining, but having lab mates with passion and heart makes it all worthwhile. I am proud to have worked with each and every one of you!!! I am especially grateful to Dr. Jeannette Stankowski for taking me under her wing as an early graduate student, and demonstrating just how important hard work, perseverance and friendship are for survival, thanks Stink!

My thesis committee has played an integral role throughout my training at Vanderbilt and I sincerely appreciate the willingness of Drs. Eugenia Gurevich, Rebecca Sappington and Ty Abel, to always provide their help and support. My committee encouraged me to become a better scientist, challenged me to think about my project in different ways and I am extremely thankful for their unwavering faith in my abilities as a scientist. I also want to thank my clinical mentors, Dr. Robert Singer and Dr. Lori Jordan for introducing me to the realities of pediatric stroke, for steering me through uncountable brain scans, teaching me that there really is no "normal" brains and for being amazing sounding boards during my many trips towards giant rabbit holes – thank you!

I would also like to thank my collaborators, Dr. Dan Liebler and Dr. Ned Porter. The Liebler lab took in a neuroscience student with no knowledge whatsoever regarding mass spec, gave me exceptional guidance and allowed me to bloom. My experience with you all gave me confidence I that I could learn something extremely challenging and succeed. To the Porter lab, and in particular, Dr. Phil Wages, thank you for helping me think outside the box, for teaching me new techniques, for sending me papers I still can't really decipher, and for being an outstanding role model and an amazing friend.

A giant thank you also to my first science family – The Ronnett Lab. To Dr. Gabrielle Ronnett for taking a chance on a kid fresh out of undergrad with very little real-life lab experience and trusting her to (at least attempt) to manage such an amazing lab. To the entire Ronnett lab: Susan McTeer, Leslie, Amy P ☺, Rajaa, Santosh, Jerry, Yajun, Susan Aja and Jing – I thank you all for teaching me so much about what it means to be a scientist and for encouraging me to keep reaching higher. A special thanks to Leslie who spent much of

her time teaching me the ins and outs of, well, pretty much everything. For having confidence in my skills and abilities even when I didn't. You showed me that being a good scientist, a decent human and a mom was possible without completely losing your mind and your continued support means the world to me.

To my lab sister, Dr. Britney Lizama, you have taught me so much about how to be strong and fierce (yet silent ☺). You made lab and life bearable on days when I wanted to jump, picked up my pieces only God knows how many times and helped put me back together and for that and so much more I am forever grateful… I also want to thank my best friend, Mrs. Jill Barlow (Bean), for unfiltered commentary, hilarious stories, wine and of course for making countless trips to Nashville just when I needed you…

My family has always been by biggest support and there are no words that can express how much they mean to me and how grateful I am for everything they have done so that I could succeed. They have made sacrifices that are in no way lost on me… I'm pretty sure my mom did not dream of being a school cafeteria worker, but her taking that post allowed me to attend a school with amazing science teachers. I'm also pretty sure my dad didn't necessarily want to come home after working grueling shifts at the plant to sit with me and do math homework. But they did this, and so much more, so that I could pursue my dreams. To my mom and dad, thank you, thank you, thank you, from the bottom of my heart for always being there for me, in good times and in bad, and for setting the absolute best example of what it means to be a family and to love with abandon.

To my baby brother, Brian, thank you for always having my back even when you don't really want to. For being the one person I can trust to tell me when I'm being an ass but who I know will stick by my anyways. Thank you also to my Aunt Sal, for so many things, but in the context of this thesis, for buying me my first microscope and for constantly reminding me that if attaining a Ph.D. was easy, everyone would have one. I have learned so much from you on so many levels. I have relied on you and aunt Jan for way too much over the years, but please know that your kindness, love and unwavering support have seen me through and I am forever grateful.

My family means more to me than anything in this world and I would be lost without them. To my husband, Scott - my one and only, my rock… Each and every day I am thankful to have you by my side. You have given me strength in times of weakness, reminded me of my success when imposter syndrome rears its head, and have been my number one fan through it all. You have allowed me to grow as a person, to be a better human and given me the chance to be a mother… Abby and Jack, you are my greatest gifts. Your smiles and laughter can break through even the darkest of days and make them bright. As you grow, and reach for the stars, I hope that you will find family, friends and mentors as amazing as mine to prop you up from below.

Lastly, I express sincere thanks to my funding sources that supported this work including: the Vanderbilt Neuroscience Training Program (AMP), pre-doctoral fellowships funded by the American Heart Association 12PRE11640010 (AMP) and 15PRE25100000 (AMP), NIH grants NS050396 (BAM) R01ES022936 (BAM) and travel and professional development scholarships funded by Vanderbilt Graduate School, the Vanderbilt Clinical Neuroscience Scholars Program and the Dan Marino Foundation.

TABLE OF CONTENTS

LIST OF TABLES

Table

LIST OF FIGURES

Figure

LIST OF ABBREVIATIONS

4-HNE	4-hydroxy-2-nonenal
Aβ	Amyloid-beta
ADH	Alcohol dehydrogenase
ADP	Adenosine diphosphate
AMPA	alpha-amino-3-hydroxy-5-methyl-4-isoxazolepropionic acid
ANOVA	Analysis of variance
ATP	Adenosine triphosphate
BAG-1	Bcl-2-associated athanogene 2
BBB	Blood brain barrier
BSA	Bovine serum albumin
CHIP	C-terminus of HSC70 interacting protein
CNS	Central nervous system
C-terminus	Carboxy terminus
COX IV	Cytochrome oxidase IV
Cyt c	Cytochrome c
DAPI	4,6-diamidino-2-phenylindole
DIV	Days in vitro
DJ-1	*PARK7* protein
DMEM	Dulbecco's modified eagle medium
DMSO	Dimethyl sulfoxide
DR	Derivitization reaction
Drp1	Dynamin-related protein 1
DTT	Dithiothreitol
E	Eluate
EDTA	Ethylenediaminetetraacetic acid
EGTA	Ethyl glycol tetraacetic acid
ER	Endoplasmic reticulum
ETC	Electron transport chain
FBS	Fetal bovine serum

FDA	Federal drug agency
Fk2	Antibody against mono and poly-ubiquitinated proteins
FT	Flow through
F_{2t}-IsoPs	F_{2t}-Isoprostanes
GAPDH	Glyceraldehyde 3-phosphate dehydrogenase
GSH	Reduced glutathione
GSSG	Oxidized glutathione
GSTα4	Glutathione S-transferase α4
HBSS	Hank's balanced salt solution
HEPES	4-(2-hydroxyethyl)-1-piperazineethaanesulfonic acid
Het	Heterozygous
HIP	HSP70 interacting protein
HOP	HSP70 organizing protein
HPLC	High performance liquid chromatography
HRP	Horseradish peroxidase
HSC70	Heat shock cognate 70
HSF1	Heat shock factor 1
HSP	Heat shock protein
HSP40	Heat shock protein 40
HSP70	Heat shock protein 70
IMM	Inner mitochondrial membrane
In	Input
IV	Intravenous
KO	Knockout
LC3	Microtubule-associated protein light chain III
LDH	Lactate dehydrogenase
LN_2	Liquid nitrogen
MAP2	Microtubule-associated protein 2
MDH	Malate dehydrogenase
MEM	Minimum essential medium
Mfn1	Mitofusin 1
Mfn2	Mitofusin 2
MRI	Magnetic resonance imaging

MTS	Mitochondrial targeting sequence
NC	Negative control
NMDA	*N*-methyl-D-aspartate
OGD	Oxygen glucose deprivation
OMM	Outer mitochondrial membrane
OPA1	Optic atrophy 1
PBS	Phosphate buffer saline
PCR	Polymerase chain reaction
PC	Preconditioning
PD	Parkinson's disease
PINK1	PTEN-inducible putative kinase 1
PND	Post-natal day
PVDF	Polyvinylidene difluoride
ROS	Reactive oxygen species
RT	Room temperature
SDS	Sodium dodecyl sulfate
SEM	Standard error of the mean
siRNA	Small interfering RNA
SOD	Superoxide dismutase
tPA	Tissue plasminogen activator
TBS	Tris-buffered saline
TBST	Tris-buffered saline/Tween 20
TIA	Transient ischemic attack
TOM20	Translocase of outer membrane 20
TPR	Tetratricopeptide repeat domain
UBL	Ubiquitin-like
UPR	Unfolded protein response
VDAC	Voltage-dependent anion channel
WT	Wildtype

ABSTRACT

Neuronal protein refolding and degradation in response to stress is largely mediated by the HSP70 chaperone complex and is critical for maintaining cell function and survival. While some components of the triage machinery have been identified, we lack both a fundamental understanding of the triage responses that neurons evoke in response to an acute, ischemic stress and an ability to leverage this response to improve protein triage. In this work we have identified changes in known and novel molecules that are part of the chaperone machinery in response to oxygen and glucose deprivation (OGD) that may represent new targets for therapeutic intervention. We find that immediately following a short period of OGD, neurons endogenously attempt to refold damaged proteins but are unable to maintain these increased folding rates. Using an allosteric modulator of the HSP70 complex, 115-7c, which promotes protein refolding, we were able to improve both neuronal protein and lipid integrity. Additionally, cholesterol biosynthesis, bioenergetic status and membrane architecture were all improved by 115-7c while levels of oxidized and ubiquitinated proteins were decreased. Priming naive neurons with 115-7c mimics the endogenous response to low level stress and neuroprotective effects of ischemic preconditioning (PC) in the absence of new protein synthesis. Taken together with our proteomic and metabolic data, we hypothesize that the endogenous response to acute injury is to promote protein refolding and that pharmacological augmentation of this response will allow neurons to better maintain proteostasis, decrease cell injury and maximize energetic capacity in order to survive ischemic stress. Given that stroke is a leading cause of death worldwide, and that there is currently only one FDA-approved treatment for the ischemic stroke, these data are particularly compelling and warrant continued exploration.

CHAPTER 1

INTRODUCTION

1.1 Stroke: A Statistical Overview[1]

According to the American Heart Association (AHA), stroke is the 5th leading cause of fatality in the United States, accounting for 1 in every 20 deaths. Current projections predict that in 2018 alone, roughly 800,000 people will suffer from a stroke, resulting in the death of 130,000 individuals (Benjamin, 2017). As global life expectancy increases, an additional 3.4 million people over the age of 18 years are expected to have a stroke by 2030, a 20.5% increase from 2012 (Benjamin, 2017).

Stroke survivors often experience lasting and extensive medical complications making stroke the leading cause of long-term disability. One in every four people whom have had a stroke will have another without intervention. Best practices dictate that clinicians manage the most common risk factors of stroke including: controlling blood pressure and cholesterol levels, normalizing glucose levels, increasing activity, eating well, losing weight, refraining from smoking and adding low aspirin or other medical therapies (Benjamin, 2017).

Ischemic strokes account for 87% of all strokes and occur when a vessel supplying blood to the brain is obstructed, resulting in the loss of oxygen and glucose and neuronal cell death. Despite being so devastating, there is only one FDA-approved treatment for ischemic stroke, intravenous (IV) administration of the thrombolytic agent, tPA (tissue plasminogen activator). However, treatment rates are low with only 3.4% of patients receiving IV tPA due

[1] In presenting these statistics during a 3 Minute Thesis competition I was informed that these data were, "extremely compelling." I chose to begin my thesis with these same stats for just that reason.

to the narrow therapeutic time window (administration within 3.5 hours of stroke onset) (Adeoye, 2011). This narrow treatment window makes delays in activating emergency medical services, suboptimal hospital infrastructure, poor communication and transportation real risks to positive patient outcomes (Cheng and Kim, 2015).

Both the National Institutes of Heath (NIH) and the AHA are committed to expanding the number of stroke centers throughout the US. The unmet needs of rural Americans are now being met with telemedicine to triage and treat the most critically ill patients. As of 2012, there were 56 tele-stroke programs across the US (Silva, 2012). Increased access to these centers has resulted in increased treatment rates (14%-15.5%) and fewer hospital transfers (down from 44% to 19%) (Cheng and Kim, 2015; Hess, 2005). There are also numerous clinical trials in place to determine whether the treatment window for tPA can be effectively and safely extended (Benjamin, 2017; Del Zoppo, 2009; Hacke, 2008).

One of the biggest gaps in neurotherapeutics lies in our ability to not just reperfuse the brain, as tPA does, but to protect the tissue that was without oxygen and glucose from reperfusion injury. Our team works diligently to identify new therapies, understand which factors limit cell survival and to improve neuronal viability and functional outcomes following stroke. Within this body of work, I hope to convey my role in the research and discovery efforts highlighting the cellular and molecular cues that contribute to determining cell fate following oxygen and glucose deprivation.

1.2 The Molecular Underpinnings of Ischemic Stroke

The classical framework in which we dissect the molecular mechanisms associated with stroke are by evaluating the energetic changes resulting from glucose deprivation and

oxidative imbalances. As such, both energetic and oxidative[2] stressors have been found to result in an increasingly well-understood pathway of 'excitotoxic' cell death (Hayashi, 1954; Olney, 1969; Watkins and Jane, 2006).

Energetic Stress

The brain constitutes only 2% of the body's weight yet accounts for 20% of oxygen consumption and 25% of glucose utilization (Hofmeijer and van Putten, 2012; Kety, 1963). Glucose is the main substrate for cerebral energy production. Following transport across the blood brain barrier (BBB) and cell membrane, glucose is converted into pyruvate via the anaerobic glycolytic pathway in the cytosol producing 2 ATP. Pyruvate is then transported into the mitochondria and converted into acetyl-CoA, which can then enter the Krebs cycle. In subsequent steps, and following oxidative phosphorylation, an additional 30 molecules of ATP are produced. Loss of glucose supply / consumption as during an ischemic event consequently results in a rapid (within 5 minutes) decrease in ATP levels (Folbergrova, 1992; Kalogeris, 2012; Sims and Muyderman, 2010).

Depleted bioenergetic stores result in failure of ATPase-dependent ion transporters which contribute to increased intracellular and mitochondrial calcium (Ca^{2+}) levels and consequent mitochondrial failure (Kalogeris, 2012). When oxygen and glucose levels are restored, ischemia-damaged mitochondria are unable to immediately couple oxidative phosphorylation with ATP production resulting in a surge in the generation of reactive oxygen species (ROS) (Quarrie, 2014).

[2] A key McLaughlin lab publication isolated the oxidative and energetic components of ischemia as a means to identify the potentially neuroprotective role of the Krebs cycle intermediate, isocitrate dehydrogenase (IDH) (Grelli, 2013).

Oxidative Stress

Oxidative stress is defined as a rapid and excessive generation of ROS and a decrease in the detoxifying and scavenging activities of intracellular antioxidants (Halliwell and Gutteridge, 2007; Mehta, 2007). Excessive generation of ROS occurs not only during the initial insult of an ischemic event but also during the subsequent return of blood flow (reperfusion) (Rodrigo, 2013). Post-mitotic neurons are particularly susceptible to attack by ROS, which can damage macromolecular structures including proteins, lipids and nucleic acids, ultimately activating downstream signaling pathways that result in cell death (Halliwell and Gutteridge, 2007).

Under physiological conditions, cells are equipped with robust antioxidant defenses to scavenge and remove ROS, all while maintaining cellular integrity. There are numerous antioxidants, including those that are synthesized *in vivo*, such as glutathione (GSH), catalase and superoxide dismutase (SOD), and those that are supplemented by diet, such as ascorbic acid (Vitamin C) and alpha-tocopherol (Vitamin E) (Halliwell and Gutteridge, 2007). During ischemia, while ROS levels rise, antioxidant levels decrease drastically as a function of time (Mizui, 1992). For example, the most abundant cellular antioxidant, glutathione, is typically maintained at ~5 to 10 mM but can drop by up to 90% following focal ischemia (An, 2012; Maher, 2005).

The Excitotoxic Cascade

The combined effects of the energetic and oxidative stressors described above ultimately result in activation of the 'excitotoxic cascade' a term first described in 1954 by Dr. T. Hayashi (Hayashi, 1954) and later coined by Dr. J. Olney (Olney, 1969). Briefly, loss of blood supply during an ischemic event means that critical components necessary for neurons to maintain energetics (particularly ATP) within and around the stroke lesion are depleted.

Ultimately unable to maintain ion homeostasis (Doyle, 2008) cytosolic sodium (Na^+) increases and potassium (K^+) decreases resulting in depolarization of neuronal membranes (Onteniente, 2003). The loss of membrane potential triggers opening of voltage gated Ca^{2+} channels, a rapid influx of Ca^{2+} (Mehta, 2007; Onteniente, 2003) and release of the major excitatory neurotransmitter, glutamate, into the synaptic cleft (Lipton, 1999).

Synaptic glutamate is normally maintained between 1-5 μM (Doyle, 2008; Mehta, 2007). However, within minutes following an ischemic insult, glutamate levels can reach as high as 30 μM causing excessive activation of members of the ionotropic glutamate receptor family, namely *N*-methyl-D-aspartate (NMDA) and alpha-amino-3-hydroxy-5-methyl-4-isoxazolepropionic acid (AMPA) receptors (Brouns and De Deyn, 2009; Greene and Greenamyre, 1996; Lakhan, 2009).

1.3 The Mitochondria – Not Just a Powerhouse

Mitochondria are integral organelles responsible for maintaining bioenergetic reserves but are also being increasingly recognized as mediators of neuronal cell signaling and health. Intra-mitochondrial GTPases, chaperones, kinases and phosphatases, have a broad range of roles in cell mobility, architectural integrity, cell division, cell signaling and survival. Mitochondria are continuously produced by neurons and remodeled by fusion and fission events (Cagalinec, 2013). The ability to relocate within cells allows mitochondria to rapidly perform regulatory roles in response to changes in electrical stimulation, environmental cues and intracellular nutrient sensing (McBride, 2006; Niescier, 2016).

Mitochondrial Signaling in Response to Ischemia

Mitochondria continuously produce reactive oxygen species as by-products of aerobic respiration. These ROS are essential for maintaining the redox state of a cell. Any ischemic

event leads to alterations of the mitochondrial electron transport chain complexes (ETC) and decreased antioxidants (Consolini, 2017); however, the severity of the ischemic attack can result in drastically different mitochondrial responses. Ischemic insults of short duration will increase the electronegativity of the ETC complexes and result in some leakage of electrons but it is often times not significant enough of a stress to alter antioxidant systems allowing the ROS produced to be scavenged.

If however, the ischemic event is of lasting duration, neuronal mitochondria experience decreased activity of the ETC (particularly at complex I and complex IV) that ultimately impairs overall bioenergetics (Consolini, 2017). This impairment results in uncoupling of the ETC from ATP production and causes not just electron leak but also the subsequent formation of damaging oxygen radicals as antioxidant system are depleted. Other detrimental events in cases of severe ischemia include increased mitochondrial membrane permeability as calcium accumulates within the matrix, a switch to anaerobic metabolism with a subsequent buildup of lactic acid[3] and therefore a significant alteration of mitochondrial pH (Consolini, 2017; Jassem and Heaton, 2004).

Mitophagy: Separating the Good, the Bad and the Ugly

Mitochondria form a dynamic network controlled by a range of cellular mechanisms including: fission and fusion, *de novo* mitochondrial biogenesis, and the elimination of unwanted mitochondria by mitophagy, to guarantee an appropriate population of healthy mitochondria (Martinez-Vicente, 2017; Ploumi, 2017). Proper maintenance of this mitochondrial pool is necessary for cellular homeostasis, but is particularly important for post-

[3] Lactic acid is often used in the clinic as a metric of survival. However, using real-time microphysiometry, we were able to demonstrate that the greatest single predictor of neuronal survival is extracellular acidification with neurons fated to die experiencing rapid and significantly increased acid generation (McKenzie, 2012).

mitotic neurons that must maintain basal turnover to eliminate old and inefficient organelles even under physiological conditions.

In addition, mitophagy can be induced as a stress-response to eliminate selectively damaged mitochondria following depolarization, which occurs during ischemia. Mitophagic processing typically involves a receptor-mediated mechanism whereby mitochondria are physically connected to LC3-II, the major component of autophagosomes. The nature and origin of mitophagy receptors can vary depending on the type of mitophagy; some are proteins or lipids localized in the mitochondrial membrane, others are non-mitochondrial proteins that recognize and simultaneously bind ubiquitinated chains on the mitochondrial surface (Wild, 2014).

The most well studied mechanism of mitophagy is the PINK1/Parkin pathway. PTEN-induced putative kinase 1 (PINK1) is a serine-threonine kinase containing a mitochondrial targeting sequence (MTS) that is constitutively synthesized and imported into all mitochondria. In properly polarized, 'healthy' mitochondria, PINK1 is cleaved by inner mitochondrial membrane (IMM) proteases (Greene, 2012). In damaged mitochondria that fail to maintain membrane potential, PINK1 accumulates on the outer mitochondrial membrane (OMM) exposing a catalytic kinase domain that can recruit and activate the E3 ligase Parkin (Narendra, 2010). Once activated, Parkin can either phosphorylate or ubiquitinate other specific OMM proteins (Durcan and Fon, 2015). Most commonly, ubiquitination followed by proteasomal degradation of OMM proteins such as mitofusin 1 (Mfn1) and mitofusin 2 (Mfn2), for example, results in fragmentation of the mitochondria and recruitment of the mitophagic receptor, p62 (Narendra, 2010).

While removing damaged mitochondria from the cellular milieu seems like a reasonable means to support cell health, the literature regarding the role of mitophagy in response to ischemia varies (Tang, 2016). In some studies it has been shown to be

protective (Carloni, 2010; Lizama, 2018), while in others, destructive (Koike, 2008) depending on the model system used and the extent / severity of the ischemic insult.

1.4 The Preconditioning Paradox

What Doesn't Kill You Makes You Stronger

In the above sections, I described the molecular events that occur after ischemia with a slight bend towards detrimental signaling pathways and damaged cellular components. However, overall outcome following an ischemic event depends highly upon the magnitude and duration of the initial insult. In fact, there exists a phenomenon known as ischemic preconditioning (PC) in which a brief bout of ischemia results in neuroprotection from a subsequent and typically lethal exposure (Barone, 1998; Lizama, 2018; McLaughlin, 2003). Importantly, many seemingly detrimental events elicited following an ischemic attack such as the generation of ROS and caspase activation are also required for PC to be effective (McLaughlin, 2003). This means that our brains have endogenous mechanisms for responding to insults that, if understood better, may be harnessed to inform future therapeutic directives.

There are numerous *in vivo* and *in vitro* models of PC that have revealed specific windows during which neuroprotection is maximal and that have demonstrated key shared features regardless of the exact model employed. These hallmarks include: new protein synthesis, induction of heat shock proteins, activation of mitochondrial K_{ATP} channels, and spatially and temporally limited activation of caspases (McLaughlin and Gidday, 2013; McLaughlin, 2003). Researchers have increasingly come to appreciate that signaling pathways commonly associated with apoptosis and cell death can also be triggered (to some extent) during non-lethal, preconditioning events (Brown, 2010; McLaughlin, 2003).

The Connection to the Clinic[4]

In the clinic, roughly 300,000 patients present annually with a transient ischemic attack (TIA) (Zhan, 2011). By classic definition, these ischemic events involve a sudden, focal neurological deficit that lasts for less that 24 hours, and does not result in permanent damage (Albers, 2002). In 2009, the AHA refined this definition as up to 50% of TIA patients exhibited brain injury via magnetic resonance imaging (MRI) well after the event (Easton, 2009). Although TIA symptoms resolve, these events are far from benign. In fact, following a TIA, a patient's risk of stroke, myocardial infarction, and death are as high as 25% within 90 days following the initial insult (Easton, 2009). And herein lies the paradox. While the overall risk of future ischemic stroke after a TIA is increased, studies have shown that patients whom have suffered a TIA prior to a full-blown stroke have improved functional recovery and survival compared to first time stroke patients (Bejot, 2011; McLaughlin and Gidday, 2013; Wang, 2017).

1.4 Timing Is Everything

The clinical mantra for stroke, 'Time Is Brain,' underscores the importance of drug delivery, clot or stenosis disruption and reperfusion of oxygen and glucose to neuronal tissue. Indeed, the importance of timing in stroke cannot be overstated.

A Brief Look into Failed Clinical Trials

Despite a wealth of basic molecular knowledge regarding the pathology of neuronal cell death following ischemic stroke, clinical trials for drugs targeting 'excitotoxic' and

[4] Participating in the Clinical Neuroscience Scholars Program was one of the most rewarding aspects of my graduate training. Under the joint mentorship of Dr. McLaughlin and Dr. Lori Jordan, I was able to gain insights into the reality of stroke in infants, children and adolescents that not only guided, but constantly fueled my passion for my thesis work.

oxidative stress signaling pathways have been extremely disappointing. The National Institute of Neurological Disorders and Stroke (NINDS) invested more than $200 million on clinical trials from 1977-2002 (Ravina, 2004) during which time not a single therapy decreased morbidity or mortality (Doyle, 2008).

These failures may be explained by the fact that despite recognizing ischemic stroke as a heterogeneous disease, many trials focus on the role of a single molecular pathway that occurs upstream of clinical presentations. Additionally, prior trials have targeted early events such as oxidative and energetic dysfunction in neurons by attempting to block glutamate neurotransmission, calcium entry and resultant ionic imbalance. These studies were marginally successful at best mostly because therapeutics were administered much too late following target activation.

Our goals are to continue to refine the characterization of excitotoxicity, oxidative stress and proteotoxicity and evaluate molecules and proteins that act as dual stress sensors using time scales that are clinically relevant (Stankowski and Gupta, 2011). We seek to investigate molecular pathways that may be elicited early following an ischemic event but are known to continue for days and may provide more relevant sites for intervention. Our data suggests that upregulation of HSP70 blocks necrosis, apoptosis and autophagy and targets both early and late events in ischemic cell death (Beere, 2004; Beere and Green, 2001; Lizama, 2018; Stankowski and Gupta, 2011) making chaperone regulation more appealing clinically than agents that exclusively block early events in the ischemic cascade.

1.5 The Chaperone Response to Ischemic Stress

The proteotoxic accumulation of damaged, denatured, misaligned and mal-adducted proteins is an essential hallmark of a host of chronic and acute neurodegenerative conditions

including ischemia (Gestwicki and Garza, 2012; Kalmar and Greensmith, 2009; Kalmar and Greensmith, 2017; Leak, 2014; Liu, 2005; Pratt, 2010). While increased chaperone expression is a common response to injury (Liu, 2005; Magrane, 2004; McLean, 2004; Wang, 2013), important gaps exist in our understanding of which chaperone-mediated activities are most beneficial to neuronal survival and how to recapitulate the endogenous protective response mediated by chaperones when exposed to low-level stress (as in preconditioning).

HSP70

One of the major consequences of ischemic stroke is rapid modification of neuronal proteins that can result in maladaptive changes in both structure and function. Buildup of these damaged proteins can overwhelm the protein triage system spearheaded by heat shock protein (HSP) chaperone complex (Li, 2005). HSPs are a highly conserved and functionally interactive family of chaperone proteins. While some HSPs are constitutively expressed, others are inducible in response to chemical, environmental and physiological stressors. Notably, increased expression of both the inducible form of heat shock cognate proteins (HSC70), heat shock protein 70 (HSP70), and its co-chaperone, c-terminus of HSP70 interacting protein (CHIP), occur following OGD (Lizama, 2018; Palubinsky, 2015; Stankowski, 2011).

HSP70 is a cytosolic, stress-inducible chaperone that binds to multiple co-chaperones to form a protein triage complex that can disaggregate, degrade, refold, or re-nature proteins in order to avoid otherwise fatal consequences. Ultimately, whether client proteins are degraded or refolded depends on interactions with co-chaperones as well as the bioenergetic status of the cell. The “pro-folding” state of the complex involves HSP70-HSP40 binding to HSP70 interacting protein (HIP) and HSP70 organizing protein (HOP) while the “pro-degradation” state requires instead the recruitment of BCL2 associated athanogene 1 (BAG1)

and CHIP to the core HSP70-HSP40 complex (Hohfeld, 2001; Jinwal, 2009). Under degradative conditions, the co-chaperone CHIP also works as an E3 ligase, ubiquitinating the client protein to signal for proteasomal degradation.

The HSP70 complex plays a critical role in overall neuronal proteostasis and has been suggested as a potential therapeutic for multiple neurodegenerative diseases (Kalia, 2010; Pratt, 2015; Zuiderweg, 2017). While HSP70 overexpression aids in survival in many chronic disease models (Broer, 2011; Cummings, 2001; Ebrahimi-Fakhari, 2013; Hoshino, 2011; Magrane, 2004), genetically manipulating the chaperone complex is a poor long-term clinical strategy as sustained expression of chaperones is associated with both initiation and progression of precancerous and cancerous states (Murphy, 2013; Sherman and Gabai, 2015).

CHIP

CHIP is a 35kDa E3 ubiquitin ligase that can target misfolded or damaged proteins to the proteasome for degradation. CHIP appears to be unique amongst the dozen of other eukaryotic E3 ligases in brain in that it can also can also act as an autonomous molecular chaperone to block proteotoxic stress (Lee, 2013; Rosser, 2007), control HSP70 expression (Qian, 2006) and regulate cellular processes including signaling, development, DNA damage repair, immunity and aging (Joshi, 2016). This broad range of activities, as well the fact that CHIP participates in the degradation of protein inclusions and aggregates formed in common neurodegenerative diseases has made CHIP a unique target for drug discovery**.**

Overexpression of CHIP was found to compensate for failure of other ubiquitin ligases (Imai, 2002), resulting in enhanced protein turnover and survival under chronic stress conditions (Lee, 2013), yet the role of CHIP in response to acute neurological stress was not evaluated in these studies. Previous data from our lab provided the first evidence that CHIP

was indeed upregulated in postmortem human tissue from patients whom had suffered from a TIA or stroke. However, unlike chronic stress disorders, CHIP overexpression impaired neuronal survival in *in vitro* models of OGD and was associated with loss of proteasome activity in response to oxidative stress (Stankowski, 2011). Additionally, siRNA silencing of CHIP increased neuronal tolerance to oxidative injury (Stankowski, 2011). Lastly, CHIP knockout (KO) mice have severe phenotypic and behavioral dysfunction (Dai, 2003; McLaughlin, 2012; Sahara, 2005; Schisler, 2016; Shi, 2014; Wu, 2018).[5] Taken together, these data suggest an essential role for the HSP70 chaperone machinery in response to acute neurological injury.

1.6 Rationale

Ischemic stroke is the leading cause of death and disability worldwide yet we have only one FDA-approved therapeutic for patients with limited efficacy beyond ~3 hours. By leveraging the power of proteomics and drug screening and coupling them with exceptional platforms to measure biochemical responsiveness, we can identify new neuroprotective molecules and pathways.

1.7 Hypothesis

The neuronal HSP70 chaperone machinery triages proteins damaged by ischemia. HSP70 client proteins can either be degraded or refolded. We hypothesize that small molecule modulators of the chaperone complex can be used to improve neuronal survival following oxygen and glucose deprivation.

[5] For our analysis we compared wild-type (WT) to heterozygous (Het) mice because the frailty phenotype of CHIP KO mice was so severe that they could not complete routine behavioral tasks.

1.8 Thesis Specific Aims

Research Plan: The goal of this research program is to further understand of the role of the HSP70 chaperone machinery in response to ischemia. By exposing primary neuronal cultures to varying degrees of oxygen and glucose deprivation, we can monitor the activity of the chaperone machinery to determine which aspects differ between a survivable and a lethal stressor. Such experiments will allow us to identify endogenous protective pathways employed by neurons that survive an ischemic event, and allow us to target these pathways to augment neuronal survival.

Aim 1: Determine the function of the HSP70 chaperone machinery in response to varying durations of oxygen and glucose deprivation. Our preliminary data demonstrate that following mild, non-toxic OGD, there is a rapid increase in the expression levels of HSP70 and its co-chaperone, CHIP. Given that this OGD is non-toxic, we hypothesize that this upregulation is part of an adaptive survival response and that the expression patterns of the chaperone machinery and therefore overall protein environment will be altered with increased stress. In this Aim, we will utilize primary neuronal cultures under mild (15'), moderate (45') and lethal (90') durations of OGD in order to determine if fundamental components of cell stress including lipid peroxidation, protein oxidation, protein ubiquitination and protein aggregation vary based on severity of the insult. We will then examine the molecular makeup, sub-cellular localization and activity of the HSP70 chaperone complex in OGD-tolerant neurons versus those destined to die.

Aim 2: Assess the neuroprotective potential of HSP70 chaperone complex modulation in response to oxygen and glucose deprivation. Our preliminary data suggests that when compounds that promote protein refolding are administered following moderate (45') OGD

there is an increase in neuronal survival. We therefore hypothesize that OGD-tolerant neurons drive the chaperone complex towards protein refolding. In this Aim, the neuroprotective potential of allosteric modulators of the HSP70 complex will be assessed using primary neuronal cultures subject to varying durations of OGD. Critical windows of protection will be determined using cell survival assays.

CHAPTER 2

CHIP IS AN ESSENTIAL DETERMINENT OF NEURONAL MITOCHONDRIAL STRESS SIGNALING

2.1 Abstract

Aims: Determine the mechanism by which CHIP induction alters neuronal survival under conditions of mitochondrial stress induced by oxygen and glucose deprivation.

Results: We report that animals deficient in the E3 ubiquitin ligase, CHIP, have high baseline levels of CNS protein oxidation and lipid peroxidation, reduced antioxidant defenses and decreased energetic status. Stress-associated molecules typically linked to Parkinson's disease such as the mitochondrial kinase PINK1 and another E3 ligase, Parkin, are upregulated in brains from CHIP KO animals. Utilizing a novel biotin-avidin capture technique, we found that the oxidation status of Parkin and the mitochondrial fission protein, Drp1 are altered in a CHIP-dependent manner. We also found that following oxygen glucose deprivation (OGD) the expression of CHIP, PINK1 and the autophagic marker LC3 are increased and there is activation of the redox sensitive kinase $p66^{shc}$. Under conditions of OGD, CHIP relocalizes from the cytosol to mitochondria. Mitochondria from CHIP KO mice have profound impairments in stress response induced by calcium overload resulting in accelerated permeability transition activity. While CHIP deficient neurons are morphologically intact, they are more susceptible to OGD consistent with a previously unknown neuroprotective role for CHIP in maintaining mitochondrial homeostasis.

Innovation: CHIP relocalization to the mitochondria is essential for the regulation of mitochondrial integrity and neuronal survival following OGD.

Conclusions: CHIP is an essential regulator of neuronal bioenergetics and redox tone. Altering the expression of this protein has profound effects on neuronal survival when cells are exposed to OGD.

2.2 Introduction

E3 ubiquitin ligases and mitochondrial dysfunction have been increasingly implicated in neurological disease, suggesting that the CNS has a conserved group of signaling molecules that participate in mitochondrial quality control and the regulation of neural cell fate (Huang, 2011; Khandelwal, 2011). The identification of genetic mutations in the E3 ligase Parkin, which can result in inherited forms of Parkinson's disease (PD), provided compelling evidence linking neuronal mitochondrial function to protein ubiquitination (Kitada, 1998; Lücking, 2000). Members of the E3 ligase family are thought to protect cells by tagging damaged proteins for proteasomal degradation (Di Napoli and McLaughlin, 2005).

Parkin controls mitochondrial dynamics via its interaction with the mitochondrial redox sensor and serine-threonine kinase, PTEN-inducible putative kinase 1 (PINK1) (Matsuda, 2010; Matsuda and Tanaka, 2010; Narendra, 2008; Poole, 2008; Ziviani, 2010), mutations in which result in an autosomal-recessive, inherited form of PD (Valente, 2004). Although E3 ligases often interact with substrates in a redundant manner, they can also impact protein folding and transcription independent of their ubiquitinating activities, and can participate in the autophagy-dependent clearance of damaged mitochondria (mitophagy) (Fu, 2013; Lokireddy, 2012; Matsuda, 2010).

We recently reported that CHIP haploinsufficiency results in mild behavioral impairments and profound changes in motor function in young animals (McLaughlin, 2012).

These data are particularly striking given that deletion of Parkin has a benign phenotype (Perez and Palmiter, 2005) whereas loss of CHIP is catastrophic early in life resulting in the death of ~30% of animals by post-natal day (PND) 40 (Dai, 2003; Min, 2008).

In the current study, we report that CHIP relocalizes to damaged mitochondria following injury, and that CHIP positive materials are engulfed in autophagic bodies. We also report that in the absence of CHIP, young animals (PND35) have significantly increased baseline levels of protein oxidation and lipid peroxidation and undergo accelerated stress-induced mitochondrial permeability transition activity. Using a novel biochemical capture methodology, we found that Drp1, a key protein associated with mitochondrial homeostasis, and Parkin, are oxidized in WT and Het but not CHIP KO animals. Lastly, we note that while neuronal cultures generated from CHIP KO mice appear intact, they are much more vulnerable to OGD than WT control cells. Taken together, this work suggests that CHIP is a critical determinate of mitochondrial integrity, function and homeostasis in response to acute injury.

2.3 Materials and Methods

Reagents

Commercial vendors of chaperone antibodies as well as reagents and supplies used for immunoblotting, immunofluorescence and cell culture experiments are the same as previously described (Brown, 2010; Stankowski, 2011). Additional primary antibodies used for immunoblotting in this study include $p66^{shc}$ (566807, EMD), VDAC, COX IV and Parkin (4866, 4850 and 2132, respectively; Cell Signaling), PINK1, Mfn1 and Drp1 (BC100-494, NB110-58853, and NB110-55288, respectively; Novus Biologicals), polyclonal CHIP (PC711; Calbiochem), LC3 (PD014; MBL International) and Cytochrome c (556433, BD Pharmingen). For immunocytochemistry, the following secondary antibodies were used: anti-rabbit Cy2 (711-225-152), anti-mouse Cy2 (715-225-150) and anti-rabbit Cy3 (711-165-152), all

purchased from Jackson ImmunoResearch. Coverslips were mounted using ProLong Gold (P36934) from Invitrogen. Commercially available kits that were used include the D_C Protein Assay kit (500-0112, Bio-Rad), the OxyBlot™ Protein Oxidation Detection Kit (Millipore, S7150) and an ATP/ADP Ratio Assay Kit (Z5030042, BioChain). Reagents and materials required for the biotin-avidin-capture methodology were obtained from the same companies as previously described (Stankowski, 2011). All cell culture medium and supplements were purchased from Invitrogen. Unless otherwise stated, all other chemicals were purchased from Sigma-Aldrich.

Animals

The Institutional Animal Care and Use Committee at Vanderbilt University approved all animal husbandry and experiments. Parent mouse lines used in this study were previously described (Dai, 2003). All mice are maintained on a mixed background of C57BL/6 and 129SvEv as backcrossing unto a pure genetic background exacerbates the early lethality of CHIP KO animals with a less than 5% survival at birth. As CHIP KO mice are sterile, heterozygous matings are used to maintain the colony. Genotyping is performed by PCR with DNA from tail clippings using primers for the CHIP allele. Primers were purchased from XXIDT and the sequences of the reverse and forward primers used are 5' TGA CAC TCC TCC AGT TCC CTG AG 3' and 5' AAT CCA CGA GGC TCC GCC TTT 3', respectively. Unless otherwise noted, all experiments were completed and tissue samples harvested at PND35 to ensure proper age-matched controls.

OxyBlot™ Methodology

Derivatization of oxidized proteins was performed as previously described (Stankowski, 2011). Briefly, whole brains from PND35 WT, Het and CHIP KO mice were

removed and immediately treated with 50 mM DTT to prevent auto-oxidation of proteins. Samples were homogenized and then equally divided into derivatization reaction (DR) solution containing 2,4-dinitrophenylhydrazine or negative control (NC) solution. Samples were stored at 4°C and processed further within seven days. Equal protein concentrations were separated using Criterion Bis-Tris gels and processed as described in the Immunoblotting section below. The manufacturer provided antibodies specific for the detection of oxidized proteins.

Lipid Oxidation

Lipid peroxidation was assessed through quantification of F_{2t}Isoprostanes (F_{2t}-IsoPs), prostaglandin-like molecules generated from free radical-mediated, non-enzymatic peroxidation of arachidonic acid. F_{2t}IsoPs are considered the gold standard in detecting oxidative stress and are measured using gas chromatography–mass spectrometry as previously described (Milne, 2005). Briefly, whole brains of PND35 WT, Het and CHIP KO mice were removed and immediately treated with methanol containing 0.05% (v/v) butylated hydroxy-toluene to prevent auto-oxidation of lipids. F_{2t}-IsoPs esterified to phospholipids were hydrolyzed by chemical saponification, after which total isoprostanes were extracted using C-18 and silica Sep-Pak cartridges, purified by thin-layer chromatography, converted to pentaflurobenzyl ester trimethylsilyl ether derivatives, and quantified by stable isotope dilution techniques using gas chromatography/negative ion chemical ionization mass spectrometry. [$2H_4$]-8-iso-PGF2 (m/z 573) was used as an internal standard. F_{2t}-IsoPs detected at m/z 569.

Glutathione Measurement

Reduced (GSH) and oxidized (GSSG) glutathione concentrations were measured by HPLC as previously described (Stankowski, 2011). Briefly, PND35 WT, Het and CHIP KO

animals were anesthetized and cervically dislocated. Brains were quickly removed and a 1-cm2 piece of cortex was dissected. Cortical tissue then underwent extraction with 5% (v/v) perchloric acid/0.2 M boric acid. Acid soluble thiols were derivatized with iodoacetic acid and dansyl chloride and were analyzed by HPLC using a propylamine column (YMC Pack, NH2, Waters) and an automated HPLC system (Alliance 2695, Waters). GSH and GSSG concentrations were normalized to protein content.

Assessing ATP:ADP ex vivo

Intracellular ATP and ADP concentrations were assessed using a bioluminescent assay. PND35 WT, Het and CHIP KO animals were anesthetized and cervically dislocated. Brains were quickly removed, placed in LN_2 and pressed to form a fine powder. The powder was then reconstituted in assay buffer, homogenized and sonicated. Samples were incubated in ATP reagent mix in the presence of luciferase and the light generated was measured via a luminometer with the intensity representing the intracellular concentration of ATP. ADP Reagent was added and allowed to incubate during which time ADP is converted to ATP, which again reacts with *D*-luciferin and the generation of light is then measured. Luminescence from the initial ATP reading is stable over time and by subtracting the relative light units of the first read from that of the second read, we determined the intracellular concentration of ADP. The remaining lysate was used for the determination of protein concentrations.

Primary Rat Neuronal Culture

Primary neuronal forebrain cultures were prepared from embryonic day 18 Sprague-Dawley rats as previously described (Stankowski, 2011). Briefly, cortices were digested in trypsin and dissociated. Resultant cell suspensions were adjusted to 335,000 cells/mL and

plated 2 mL/well in 6-well tissue culture plates containing five 12mm or one 25mm poly-L-ornithine-coated glass coverslip(s). Cultures were maintained at 37^{o}C, 5% CO_2 in growth media composed of a volume to volume mixture of 84% (v/v) DMEM, 8% (v/v) Ham's F12-nutrients, 8% (v/v) fetal bovine serum, 24 U/mL penicillin, 24 µg/mL streptomycin, and 80 µM L-glutamine. Glial proliferation was inhibited after two days in culture via the addition of 1 µM cytosine arabinoside, after which cultures were maintained in Neurobasal medium containing 2% B27 (v/v), 2x N2 and 4% NS21 (v/v) supplements (Chen, 2008) with antibiotics for 2 weeks. One week before experiments, neurons are maintained in Neurobasal medium containing 4% (v/v) NS21 and antibiotics only. All experiments were conducted 21-25 days following dissociation.

Primary Mouse Neuronal Culture

Primary neuronal forebrain cultures were prepared from embryonic day 18 mice generated by heterozygous matings. Upon dissection, mice were decapitated and the entire brain was stored individually in 10 mL of Hibernate E Medium (Brain Bits, Springfield IL; HE-Pr) at 4^{o}C while tails were processed for genotyping. Once genotype was known, WT, Het and KO brains were pooled accordingly and dissection continued with cortical tissue digestion in 0.025% trypsin for 20 min at room temperature followed by dissociation. Resultant cell suspensions were adjusted to 700,000 cells/mL and plated 2 mL/well in 6-well tissue culture plates containing five 12 mm or one 25 mm poly-L-ornithine-coated glass coverslip(s). Cultures were maintained at 37^{o}C, 5% CO_2 in growth media composed of a volume to volume mixture of 84% (v/v) DMEM, 8% (v/v) Ham's F12-nutrients, 8% (v/v) fetal bovine serum, 24 U/mL penicillin, 24 µg/mL streptomycin, 80 µM L-glutamine, 2x N2 and 4% NS21 (v/v) supplements. Glial proliferation was inhibited after two days in culture via the addition of 1 µM cytosine arabinoside, after which cultures were maintained in Neurobasal

medium containing 2% B27 (v/v), 2x N2 and 4% NS21 (v/v) supplements (Chen, 2008) with antibiotics for 2 weeks. One week before experiments, neurons are maintained in Neurobasal medium containing 4% (v/v) NS21 and antibiotics only. All experiments were conducted 21-25 days following dissociation.

Oxygen Glucose Deprivation

Oxygen glucose deprivation (OGD) experiments were performed between day *in vitro* (DIV) 21 through DIV25, at which time neurons represent at least 95% of the population as assessed by NeuN and GFAP staining (McLaughlin, 2001). OGD was performed as previously described (Stankowski, 2011) by complete exchange of media with deoxygenated, glucose-free Earle's balanced salt solution (150 mM NaCl, 2.8 mM KCl, 1 mM $CaCl_2$ and 10 mM HEPES; pH 7.3), bubbled with 10% H_2/85% N_2/5% CO_2. Cultures were exposed to OGD in an anaerobic chamber (Billups-Rothberg) for 90 min at 37°C. Upon OGD termination, cells were washed with MEM/BSA/HEPES (0.01% (w/v) BSA and 25 mM HEPES) and then maintained in MEM/BSA/HEPES/N2 (0.01% (w/v) BSA, 25 mM HEPES and 2X N2 supplement) for various recovery times at the completion of which protein extracts were prepared for immunoblotting, or cells were fixed for immunofluorescence.

Lactate Dehydrogenase Assays

Neuronal viability was determined 24 hr following OGD exposure by measuring lactate dehydrogenase (LDH) release with the LDH *in vitro* toxicology assay kit (Sigma Aldrich, Tox7). Forty microliter samples of medium were assayed spectrophotometrically (490 nm absorbance) in triplicate according to the manufacturer's protocol to obtain a measure of cytoplasmic LDH released from dead and dying neurons (Hartnett, 1997). LDH results were

confirmed qualitatively by visual inspection of the cells and, in several instances, quantitatively by cell counts using our previously described method (McLaughlin, 2003).

Immunoblotting

Western blots were performed as previously described (Brown, 2010; McLaughlin, 2001; Stankowski, 2011). For *in vivo* lysates, the tissue of interest was dissected and immediately placed into ice-cold TNEB lysis buffer (50 mM Tris-Cl, pH 7.8, 2 mM EDTA, 150 mM NaCl, 8 mM β-glycerophosphate, 100 μM sodium orthovanadate 1% (v/v) Triton X-100, and protease inhibitor diluted 1:1000) followed by homogenization (on ice) in a 7 mL glass dounce and sonication. For *in vitro* lysates, all cell lysis and harvesting steps took place on ice. Cells were washed twice with ice-cold 1x PBS and following the second wash, 250–500 μL of TNEB was added.

Approximately 100-200 μL of lysate was saved for the determination of protein concentrations and the remaining lysate was re-suspended in an equal volume of Laemmle buffer with β-mercaptoethanol (1:20). Protein samples were heated to 95°C for 10 min, and stored at -20°C. Protein concentrations were determined via the Dc Protein Assay Kit II and equal protein concentrations were separated using 4-12% Bis-Tris gels followed by transfer onto PVDF membranes and then blocked in methanol for 5min. Once dry, the membranes were incubated at 4°C overnight in primary antibody prepared in 5% (w/v) nonfat dry milk in a Tris-buffered saline solution containing 0.1% Tween 20 (TBS-Tween). All primary antibodies were diluted 1:1000 (v/v). Following incubation in primary antibodies, membranes were washed and incubated for 1 hr at room temperature in a 1:5000 (v/v) dilution of horseradish peroxidase–conjugated secondary antibodies prepared in 5% (w/v) nonfat dry milk in TBS-Tween. After additional washes in, protein bands were visualized using a chemiluminescent substrate and exposed to autoradiography film.

MitoTracker™ Labeling and Immunofluorescence

MitoTracker™ Orange was added 45 min before termination of recovery using a final concentration of 790 nM. Following this incubation, neuronal coverslips were washed with 1x PBS and fixed with 4% (v/v) formaldehyde. Cells were permeabilized with 0.1% Triton X-100, washed with 1x PBS, and blocked with 8% (w/v) BSA diluted in 1x PBS. After 25 min of blocking, coverslips were incubated in either anti-CHIP (1:500) or anti-PINK1 (1:500) primary antibodies diluted in 1% (w/v) BSA overnight at 4°C. Following primary antibody incubation, cells were washed in 1x PBS for a total of 30 min and incubated in Cy2 secondary antibody (1:500) in 1% BSA for 1 hr. Cells were next washed for a total of 30min in 1x PBS and incubated in 1.4 μM DAPI for 10 min. After 30min of additional washing, coverslips were mounted via Prolong Gold.

For immunofluorescence experiments done without MitoTracker™, neurons were prepared as described above starting with fixation. In these cases, anti-LC3 and anti-CHIP primaries (both diluted 1:500) were added simultaneously and incubated overnight at 4°C. Incubation in appropriate fluorescent secondary antibodies (1:500) was also done simultaneously.

Fluorescence was visualized using a Zeiss Axioplan microscope equipped with an Apotome (63X). Nine fields of view were imaged from 4 separate neuronal preps and subsequent experiments, totaling 36 imaged fields. The fluorescent images within the manuscript are representative of these fields.

Subcellular Fractionation

Neuronal cultures were exposed to 90 min OGD and cell lysates were prepared 6 hrs later. Subcellular fractionation via differential centrifugation was used to isolate nuclear, mitochondrial and cytosolic compartments. Briefly, neurons were washed with ice cold 1X

PBS. Following PBS wash, sucrose buffer (10 mM HEPES, 1.5 mM MgCl2, 10 mM KCl, 1 mM EGTA, 1 mM EDTA, 1 mM DTT, 250 mM sucrose, protease inhibitor, pH 7.5) was added and neurons were collected on ice via scraping and placed into a pre-cooled Sorval tube that was centrifuged at 3000 x *g* for 15 min at 4^{o}C. Pellets were re-suspended in fresh HB and incubated in ice for 30 min. Cells were then transferred to a homogenizer and dounced for roughly 40 strokes followed by centrifugation at 50 x *g* for 10 min at 4^{o}C. Following this spin, the supernatant was transferred to a new tube and centrifuged at 800 x *g* for 10 min at 4^{o}C. The supernatant was transferred to a new tube and the resultant nuclear pellet re-suspended in TNEB lysis buffer. The remaining supernatant is centrifuged at 13,000 x *g* for 10 min at 4^{o}C. The resultant mitochondrial pellet is re-suspended in TNEB lysis buffer. A second centrifugation of the initial supernatant at 13,000 x *g* for 10 min at 4^{o}C is carried out to pull down any remaining mitochondria. Following this spin, the supernatant is transferred to a new tube and the mitochondrial pellet is re-suspended in the same TNEB containing the mitochondria from the first spin. The remaining supernatant from the previous spin is then centrifuged at 100,000 x *g* for 1 hr at 4^{o}C. This cytosolic pellet is then re-suspended in TNEB lysis buffer. To test for fraction purity, following a protein assay, all three fractions were equally loaded and analyzed for Ku70 (nucleus), Cytochrome c (mitochondria) and β-tubulin (cytosol) via Western blot (Data not shown).

Mitochondrial Isolation for Swelling Assay

Mitochondrial homogenates were generated from PND40 WT, Het and CHIP KO mice. Briefly, the liver was removed, washed in ice-cold 1x PBS and weighed. The liver was then homogenized in ice-cold isolation media (250 mM sucrose, 10 mM Tris and 2 mM EGTA at pH 7.4) using a 7 mL glass dounce homogenizer at 10 mL/g of tissue. Homogenates were spun at 500 x *g* for 10 min at 4°C and the supernatant was removed and placed into a new

tube. Supernatants were then spun at 9,500 x *g* for 10 min. The pellet was washed with 10 mL of isolation media (without EGTA) and spun again at 9,500 x *g* for 10 min. The remaining pellets were either re-suspended in 1 mL of TNEB lysis buffer with protease inhibitors (1:1000), subjected to protein assay and further processed for immunoblotting or biotin-avidin-capture methodology (described below) or re-suspended in 1 mL of EGTA free isolation media, subjected to protein assay and analyzed for mitochondrial permeability transition activities (described below).

Mitochondrial Permeability Transition Assay

Briefly, isolated mitochondria were re-suspended in 1 mL of assay buffer (40 mM HEPES, 195 mM mannitol, 25 mM sucrose, 5 mM succinate and 1 μM rotenone at pH 7.2). Following a 2 min equilibration period, either 50 μM or 100 μM Ca^{2+} was added and the absorbance was measured at 535 nm over a 20 min period at 37°C. Lag time before the onset of mitochondrial swelling was measured by determining the time when the maximal rate of change in absorbance was evident following Ca^{2+} addition (Landar, 2006). Time to mitochondrial swelling was normalized to that of WT animals. Statistical significance was determined by two-tailed t test assuming unequal variances.

Biotin-Avidin-Capture Methodology

Derivatization of specific protein targets of oxidative stress was performed using the biotin-avidin-capture methodology as previously described (Stankowski, 2011). Briefly, liver mitochondrial extracts from PND35-40 WT, Het and CHIP KO animals were prepared as described in the mitochondrial preparation section. Equal protein concentrations (2 mg/mL) were incubated with biotin hydrazide (5 mM) while rotating in the dark for 2 hrs at RT after which samples were incubated with sodium borohydride (50 mM) for 30 min at RT. Samples

were then transferred into Amicon Ultra Centrifuge Filter Devices (UFC 801024, Millipore), and washed three times via addition of 1x PBS followed by centrifugation for 30 min at 2,500 x *g*. Following the last wash, a 100 µl aliquot was removed to prepare an input sample (In) via addition of DTT (50 mM) and NuPage Sample buffer (4x; NP0007, Invitrogen). The remainder of the sample was added to Streptavidin Sepharose High Performance Beads (17-5113-01, GE Healthcare) and incubated while rotating overnight at 4°C. The next day, samples were centrifuged briefly at 2,500 x *g*. The supernatant of the first spin was saved and a 100 µl aliquot of this sample was used to prepare a flow through sample (FT) via addition of DTT and sample buffer. Sample elution was initiated by treating twice with each of the following reagents: SDS (1% w/v), urea (4 M), NaCl (1 M) and 1x PBS. Eluate samples (E) were then prepared in sample buffer with DTT, heated for 10 min at 95°C and stored at -20°C. Equal protein concentrations were separated on SDS-PAGE gels as described in the immunoblotting section above and probed with antibodies specific to Mfn1, VDAC, Cytochrome c, Drp1, Parkin and COX IV.

Analysis and Statistics

Except where otherwise noted, data were summarized and are represented as mean ± SEM. The statistical significance of differences between means was assessed using one-way analysis of variance (ANOVA) at the 95% confidence interval, followed by Bonferroni multiple comparison *post hoc* testing using GraphPad Prism software. Semi-quantitative analyses of immunoblot results were generated to determine the mean relative densities of each protein band in comparison to control conditions or WT genotype (NIH Image, Scion Image J).

2.4 Results

CHIP Deficient Animals have Increased Protein Oxidation and Lipid Peroxidation, Impaired Antioxidant Defenses and Experience Energetic Stress in the CNS Early in Development

We previously reported that CHIP expression is increased in post-mortem human tissue samples in patients following ischemic stroke as well as in an *in vitro* model of neuronal ischemia (Stankowski, 2011). In contrast to the benefits associated with transiently increased CHIP expression in blocking cell death induced by PD mutant genes (Tetzlaff, 2008), prolonged overexpression of CHIP worsens outcome following acute injury and causes proteasomal uncoupling (Stankowski, 2011), suggesting that a fine balance exists in the temporal expression of CHIP that affords protection.

To identify the mechanisms by which CHIP alters neuronal responsiveness to stress, we compared baseline levels of total oxidized proteins in CNS samples from post-natal day 35 (PND35) WT, Het and CHIP KO mice. A robust increase in total protein oxidation was evident in CHIP KO animals compared to age-matched WT and Het littermates (**Figure 1A**). In addition, comparing F_{2t}-Isoprostanes (F_{2t}-IsoPs), the gold standard for assessing oxidative injury (Kadiiska, 2005), across genotypes, we found that CHIP KO animals exhibit significant increases in the non-enzymatic oxidation of arachidonic acid (**Figure 1B**) and depletion of antioxidants reflected by the ratio of reduced GSH to oxidized GSSG being decreased in CHIP KO animals (**Figure 1C**). This decrease in the reduced form of GSH that occurs when CHIP is absent could either be attributed to antioxidant depletion as cells attempt to clear the large number of oxidized substrates or due to an inherent energetic deficit in the animals, as the synthesis of GSH requires both ATP and NADPH.

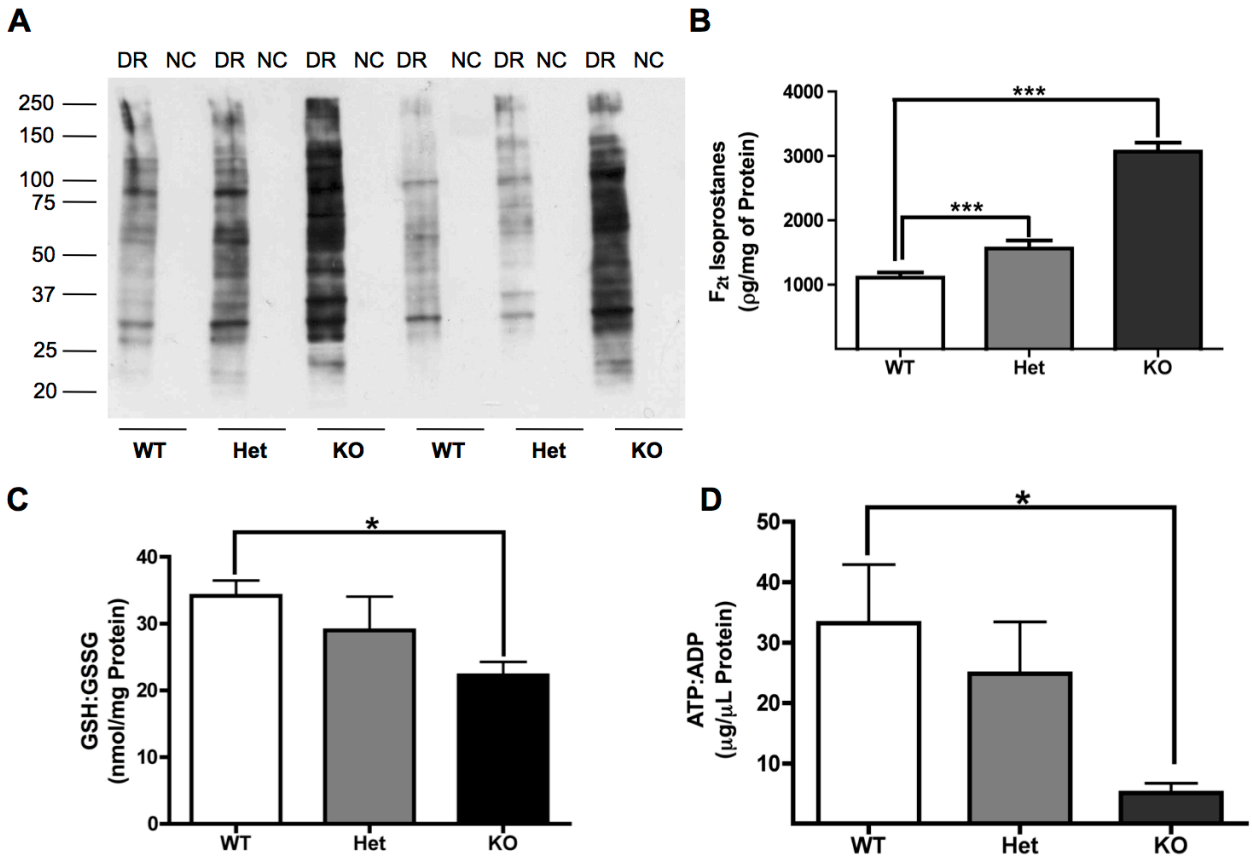

Figure 1. CHIP Deficient Animals have Increased Protein Oxidation and Lipid Peroxidation, Impaired Antioxidant Defenses and Energetic Stress Early in Development. (A) Whole brain lysates from PND35 CHIP KO animals exhibit higher levels of total oxidized proteins in comparison to WT and Het littermates. Immunoblots are representative of results from four independent OxyBlot™ experiments where "DR" denotes Derivatization Reactions and "NC" denotes Negative Controls. **(B)** PND35 CHIP KO animals have higher baseline levels of lipid peroxidation in comparison to WT and Het littermates. MS data were normalized to protein (µg/mg) and represent the mean ± SEM from three independent experiments where *** denotes $p < 0.001$. **(C)** Cortical tissue samples from PND35 CHIP KO animals demonstrate decreased amounts of the major antioxidant, glutathione, compared to WT and Het counterparts. HPLC data were normalized to protein (nmol/mg) and represent the mean ± SEM from six independent experiments where * denotes $p < 0.05$. **(D)** PND35 cortical tissue samples demonstrate (via a bioluminescent reporter assay) that CHIP KO animals have a significantly lower ATP:ADP. Data were normalized to protein (µg/µL) and represent the mean ± SEM from four independent experiments where * denotes $p < 0.05$.

To determine if variations in energetic status may account for the decreased levels of GSH in CHIP KO mice, the ratio of ATP to ADP was determined via a bioluminescent assay. There is significantly lower ATP in CHIP KO animals and a trend towards decreased ATP in Het animals while no changes in the absolute levels of ADP were noted between or within

any groups. The resulting decreased ATP to ADP ratio **(Figure 1D**) suggests that CHIP deficiency results in impaired brain energetic status.

A

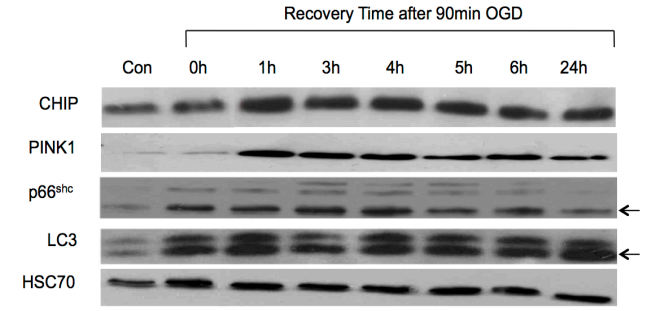

B

Fold Change Normalized to Control Neurons							
	0h	1h	3h	4h	5h	6h	24h
CHIP (n=3)	1.6 ± 0.2	1.6 ± 0.3	1.4 ± 0.3	1.4 ± 0.3	1.3 ± 0.3	1.3 ± 0.3	1.4 ± 0.3
PINK1 (n=3)	1.1 ± 0.5	7.3 ± 1.2 ***	6.9 ± 1.4 ***	6.8 ± 1.3 ***	5.6 ± 1.7 **	5.6 ± 0.6 ***	4.5 ± 1.5 *
p66shc (n=3)	2.2 ± 0.2	2.7 ± 0.2 **	3.6 ± 0.6 ***	3.5 ± 0.5 ***	2.7 ± 0.7 **	2.7 ± 0.8 **	1.5 ± 0.2
LC3-I (n=3)	3.8 ± 0.4 ***	4.4 ± 0.4 ***	3.6 ± 0.4 ***	4.1 ± 0.2 ***	4.1 ± 0.6 ***	4.6 ± 0.3 ***	4.1 ± 0.8 ***
LC3-II (n=3)	2.9 ± 0.2 ***	4.2 ± 0.1 ***	3.9 ± 0.2 ***	4.0 ± 0.3 ***	4.2 ± 0.4 ***	3.9 ± 0.3 ***	4.5 ± 0.7 ***
HSC70 (n=3)	0.9 ± 0.2	1.0 ± 0.3	0.9 ± 0.3	0.9 ± 0.4	0.9 ± 0.5	0.9 ± 0.3	1.0 ± 0.1

Figure 2. CHIP Deficiency Results in the Increased Expression of Mitochondrial Stress-Associated Proteins. (A) Whole brain lysate from PND35 CHIP KO animals exhibit increased expression of the stress-associated kinase PINK1 as well as the E3 ligase, Parkin. HSC70 was used as a loading control. **(B)** Western blots were analyzed using NIH Image (Scion Image J) to determine the mean relative densities of each protein band and fold changes were calculated using WT littermates as controls. Data represent results from four independent experiments. Statistical significance is noted within the table where * denotes $p < 0.05$, ** denotes $p < 0.01$ and *** denotes $p < 0.001$.

CHIP Deficiency Increases the Expression of Mitochondrial Proteins Associated with PD

The increase in oxidized proteins and lipids in in the absence of an exogenous stressor observed in Het and CHIP KO animals suggests that either more reactive oxygen species (ROS) are generated, that ROS are poorly converted to nonreactive species by antioxidants, or a combination of these two events. A growing body of evidence in the Parkinson's disease literature suggests a role for two genes associated with familial PD, PINK1 and Parkin, in mitochondrial stress handling. Expression of the redox sensor, PINK1, and the E3 ligase Parkin were both increased in brain extracts from CHIP KO animals (**Figure 2A & B**).

A

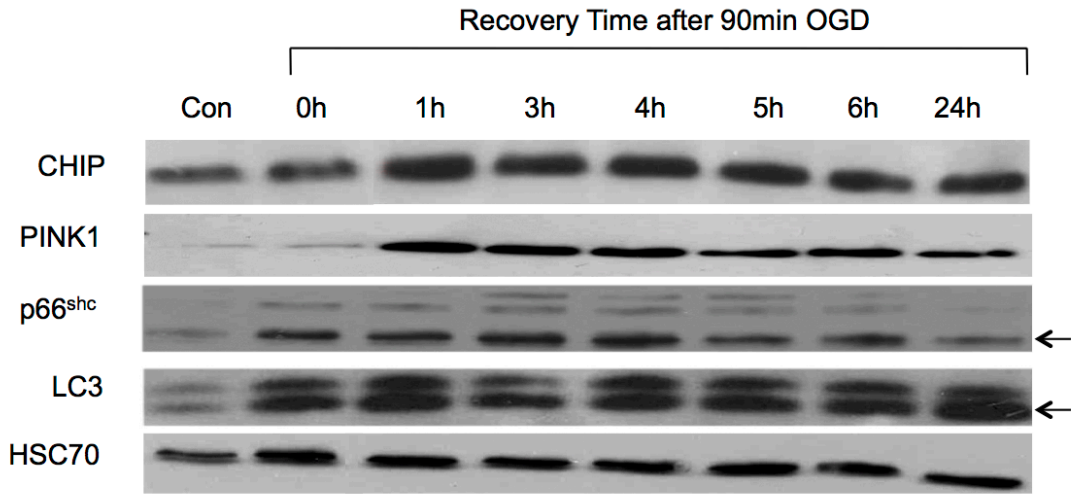

B

Fold Change Normalized to Control Neurons							
	0h	1h	3h	4h	5h	6h	24h
CHIP (n=3)	1.6 ± 0.2	1.6 ± 0.3	1.4 ± 0.3	1.4 ± 0.3	1.3 ± 0.3	1.3 ± 0.3	1.4 ± 0.3
PINK1 (n=3)	1.1 ± 0.5	7.3 ± 1.2 ***	6.9 ± 1.4 ***	6.8 ± 1.3 ***	5.6 ± 1.7 **	5.6 ± 0.6 ***	4.5 ± 1.5 *
p66shc (n=3)	2.2 ± 0.2	2.7 ± 0.2 **	3.6 ± 0.6 ***	3.5 ± 0.5 ***	2.7 ± 0.7 **	2.7 ± 0.8 **	1.5 ± 0.2
LC3-I (n=3)	3.8 ± 0.4 ***	4.4 ± 0.4 ***	3.6 ± 0.4 ***	4.1 ± 0.2 ***	4.1 ± 0.6 ***	4.6 ± 0.3 ***	4.1 ± 0.8 ***
LC3-II (n=3)	2.9 ± 0.2 ***	4.2 ± 0.1 ***	3.9 ± 0.2 ***	4.0 ± 0.3 ***	4.2 ± 0.4 ***	3.9 ± 0.3 ***	4.5 ± 0.7 ***
HSC70 (n=3)	0.9 ± 0.2	1.0 ± 0.3	0.9 ± 0.3	0.9 ± 0.4	0.9 ± 0.5	0.9 ± 0.3	1.0 ± 0.1

Figure 3. Oxygen Glucose Deprivation Increases the Expression of CHIP and Markers of Autophagy. Whole cell extracts of neuronal rat cultures (DIV 21-25) were harvested immediately (0hr), 1hr, 3hr, 4hr, 5hr, 6hr or 24hr following exposure to OGD. Equal protein concentrations were separated on SDS-PAGE gels and probed with antibodies specific to CHIP, PINK1, p66^{shc}, LC3 and the loading control, HSC70. **(A)** While p66^{shc} and LC3 expressions levels are increased immediately following the insult, CHIP and PINK1 expression increase more robustly starting 1hr following the stress. Arrows denote the p66^{shc} isoform and the lipidated form of LC3. **(B)** Alterations in protein expression were analyzed via NIH Image (Scion Image J) and fold changes were calculated using untreated neuronal cultures as controls. Immunoblots are representative of results from three independent experiments. Statistical significance is noted within the table where * denotes $p < 0.05$, ** denotes $p < 0.01$ and *** denotes $p < 0.001$.

OGD Increases Mitochondrial Stress-Associated Protein Expression

We next used an OGD model in neurons to determine if convergent signaling molecules between OGD and CHIP deficiency could be identified. We have previously shown that 90 min OGD results in membrane rupture and greater than 80% cell death evidenced as

LDH release commencing 10 hrs after the onset of stress (Zeiger, 2010). Neuron-enriched cultures from rats were exposed to 90 min OGD to analyze levels and trafficking of redox sensitive molecules including CHIP. PINK1 and CHIP expression increase as early as 1 hr following the insult and remain elevated for 24 hrs. Increased expression of the redox-sensitive kinase $p66^{shc}$, as well as the unlipidated (LC3-I) and lipidated (LC3-II, noted with an arrow) forms of the autophagic marker, LC3 were also observed from 2-6 hrs after OGD (**Figure 3A & B**).

The early redox sensors upregulated by OGD, $p66^{shc}$ and PINK1, associate with mitochondria in response to stress (Brown, 2010; Matsuda, 2010). Prior studies have only evaluated CHIP distribution in cytosolic and nuclear fractions, the latter of which likely contained mitochondria as the centrifugation speeds noted in the methods are not sufficient enough to efficiently separate these organelles (Anderson, 2010; Sengupta, 2011). Our immunocytochemical analysis revealed a very different pattern of distribution following OGD where CHIP relocates from cytosolic and perinuclear sites to mitochondria. After 90 min OGD, mitochondria (shown in red) underwent morphological reorganization and CHIP became more punctate, increasingly co-localizing with these organelles (**Figure 4, Left vs Right**). Subcellular fractionation experiments 6 hrs following 90 min OGD revealed that there was no nuclear CHIP signal with all CHIP associated with mitochondria in response to 90 min OGD. Control blots were run for KU70, β-Tubulin and cytochrome oxidase to confirm the purity and integrity of the organelles and showed no cross contamination (data not shown). Stabilization of PINK1 (green) at MitoTracker labeled organelles (red) was also detected 6 hrs following OGD whereas in control cells, PINK1 levels were barely detectable in keeping with immunoblot data (**Figure 4C Left vs. Right**).

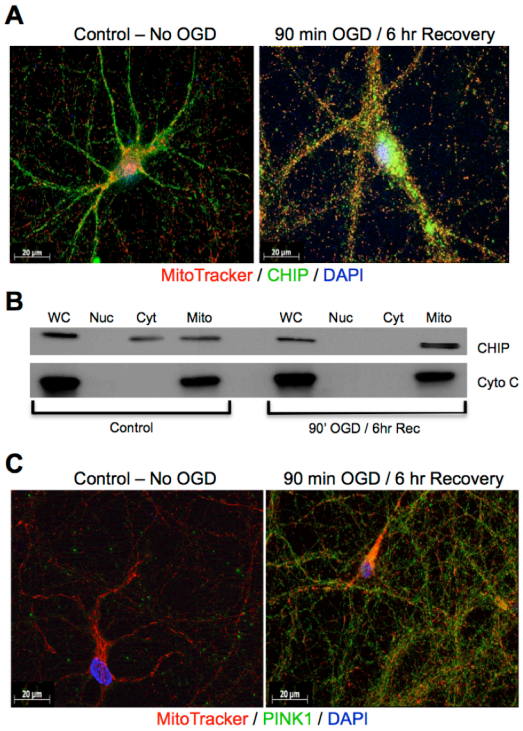

Figure 4. Oxygen Glucose Deprivation Results in the Association of CHIP and PINK1 with Mitochondria. Neuron-enriched primary rat cultures (DIV 21-25) were exposed to OGD for 90min and allowed to recover for 6hrs at which time cells were fixed and further processed for immunocytochemistry. **(A)** In control neurons, CHIP (green) is primarily cytosolic, however, 6hrs following OGD exposure, CHIP (green) becomes punctate and is found to colocalize with MitoTracker Orange (red). **(B)** Subcellular fractionation of cultures revealed that CHIP is both mitochondrial and cytosolic, but that 6hrs after OGD, almost all CHIP associates with the mitochondrial fraction. CHIP is not present in nuclear fractions in either control or stressed conditions. Cytochrome c was used to demonstrate that the mitochondria are still structurally and biochemically intact 6hrs after OGD as well as to show fraction purity. KU70 and β-Tubulin were also used to verify purity of the nuclear and cytosolic fractions, respectively (data not shown). **(C)** In control neurons, PINK1 (green) levels are extremely low, however 6hrs following exposure to OGD, PINK1 (green) is increased and exhibits colocalization with MitoTracker Orange (red). Fluorescence was visualized using a Zeiss Axioplan microscope equipped with an Apotome (63X). Nine fields of view were imaged from 4 separate neuronal preps and subsequent experiments, totaling 36 imaged fields. The fluorescent images within the manuscript are representative of these fields.

Mitochondrial accumulation of PINK1 leads to the recruitment of the E3 ligase Parkin and subsequent autophagic degradation of mitochondria via mitophagy (Geisler, 2010; Geisler, 2010; Narendra and Youle, 2011). We detected no change in Parkin or VDAC

expression in response to OGD *in vitro,* which is in keeping with results from other labs which

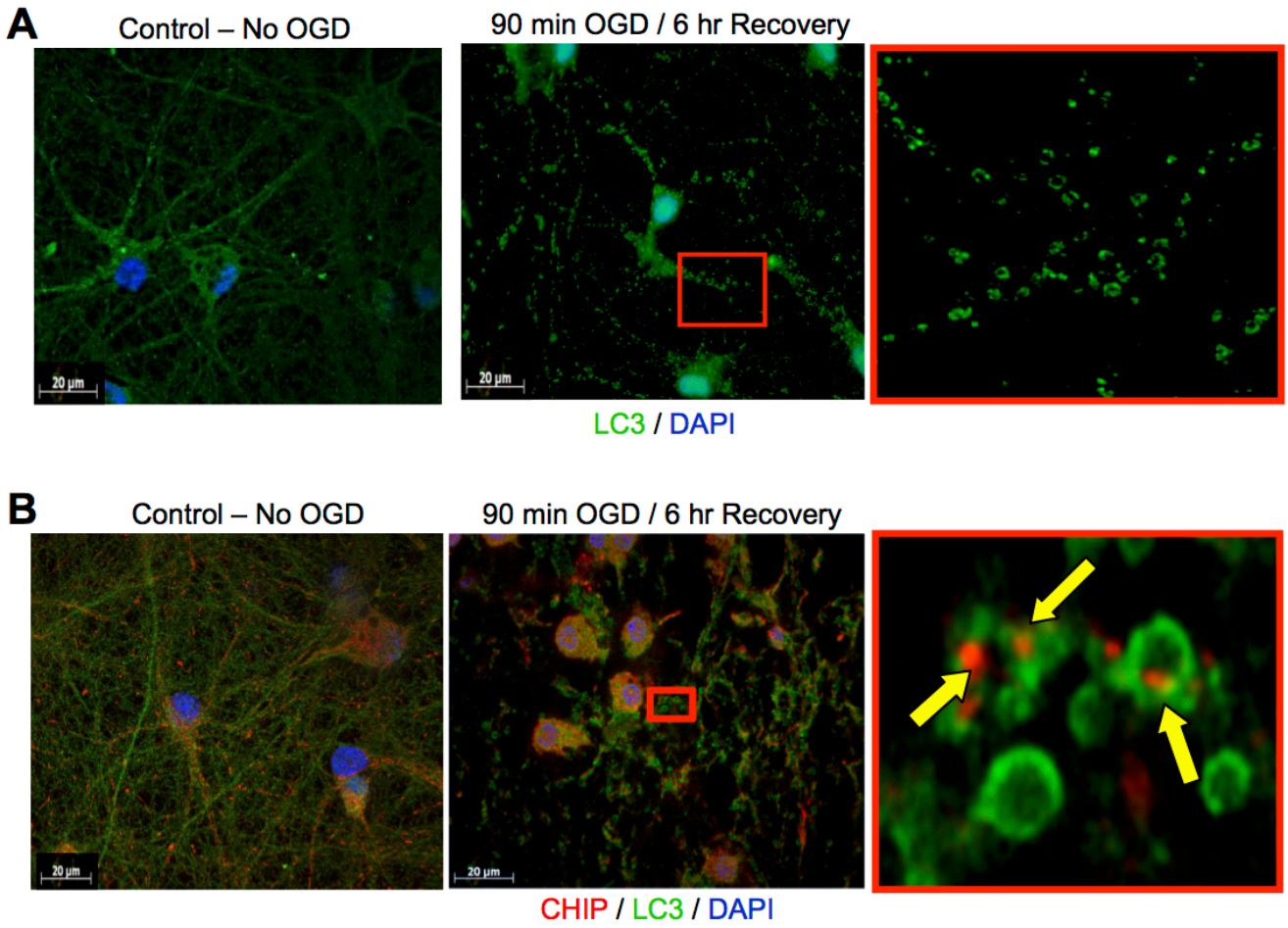

Figure 5. CHIP Positive Organelles are Degraded by Autophagy Following OGD. (A) Primary rat neuronal cultures were exposed to 90min of OGD and fixed 6hrs later for immunofluorescent staining of LC3. Control cultures had low levels of well-dispersed LC3 staining (green) throughout the soma and processes. Neuronal nuclei were stained with DAPi (blue). Staining was uniform with no signs of nuclear condensation or chromatin reassembly. Six hours following OGD, LC3 staining was much more pronounced (Second panel; top), particularly in the soma. Small, vacuolar structures were present in the parenchyma (red highlighted box) that is magnified in the top right box. This staining revealed highly regular circular structures. **(B)** Cultures stained with LC3 (green) and CHIP (red) reinforce the morphological dysfunction caused by severe OGD exposure (middle panel) as evidence by poorly defined neuronal soma and discontinuous processes. Again, small circular patterns were observed in processes that were magnified in the red box shown in the far right panel. This staining revealed that CHIP (red) is present in LC3 positive vacuoles. Nine fields of view were imaged from 4 separate neuronal preps and subsequent experiments, totaling 36 imaged fields. The fluorescent images within the manuscript are representative of these fields.

demonstrate that Parkin is poorly inducible in cortical neuronal cultures exposed to endoplasmic reticulum stress (Mengesdorf, 2002). We did, however, observe increases in LC3-I and LC3-II, the major component of autophagosomes (**Figure 3A & B**; **Figure 5A & B**). These data could reflect the induction of autophagy, reduction in autophagosome turnover, or the inability of turnover to keep pace with increased autophagic processing (Klionsky, 2008).

Immunofluorescent staining of cultures 6hrs after exposure to 90 min OGD revealed many fields of small, circular LC3 positive structures (**Figure 5**). Upon closer inspection of the fields (shown in red boxes magnified in the bottom panels), these structures were morphologically consistent with autophagosomes. Subsequent immunofluorescent staining revealed that many of the structures had CHIP engulfed within these autophagic bodies (**Figure 5; Bottom Right**).

CHIP Deficient Cultures Appear Morphologically Intact and Exhibit Extensive Neuronal Processes and Mitochondrial Networks

Given the relocalization of CHIP to the mitochondria and the stress associated with CHIP deficiency *in vivo*, we sought to generate primary cultures from transgenic animals to determine if neurons develop and respond normally to stress in the absence of CHIP. Live cell micrographs (20X) of WT, Het and CHIP KO cultures demonstrate that regardless of the genotype, neurons are viable, with phase bright somas and extensive neuronal processes after three weeks in culture (**Figure 6A**). Immunocytochemical analyses using the neuronal marker, MAP2 (green), the glial marker, GFAP (red) and the nuclear marker, DAPI (blue) revealed that genotype has no effect on neuronal survival as these cells constituted 85% of the culture in every genotype (**Figure 6B**). Using the live cell dye, MitoTracker Orange, which

is taken up into healthy mitochondria based on their membrane potential, no changes in the mitochondrial morphology or networks were evident across genotype (**Figure 6C**).

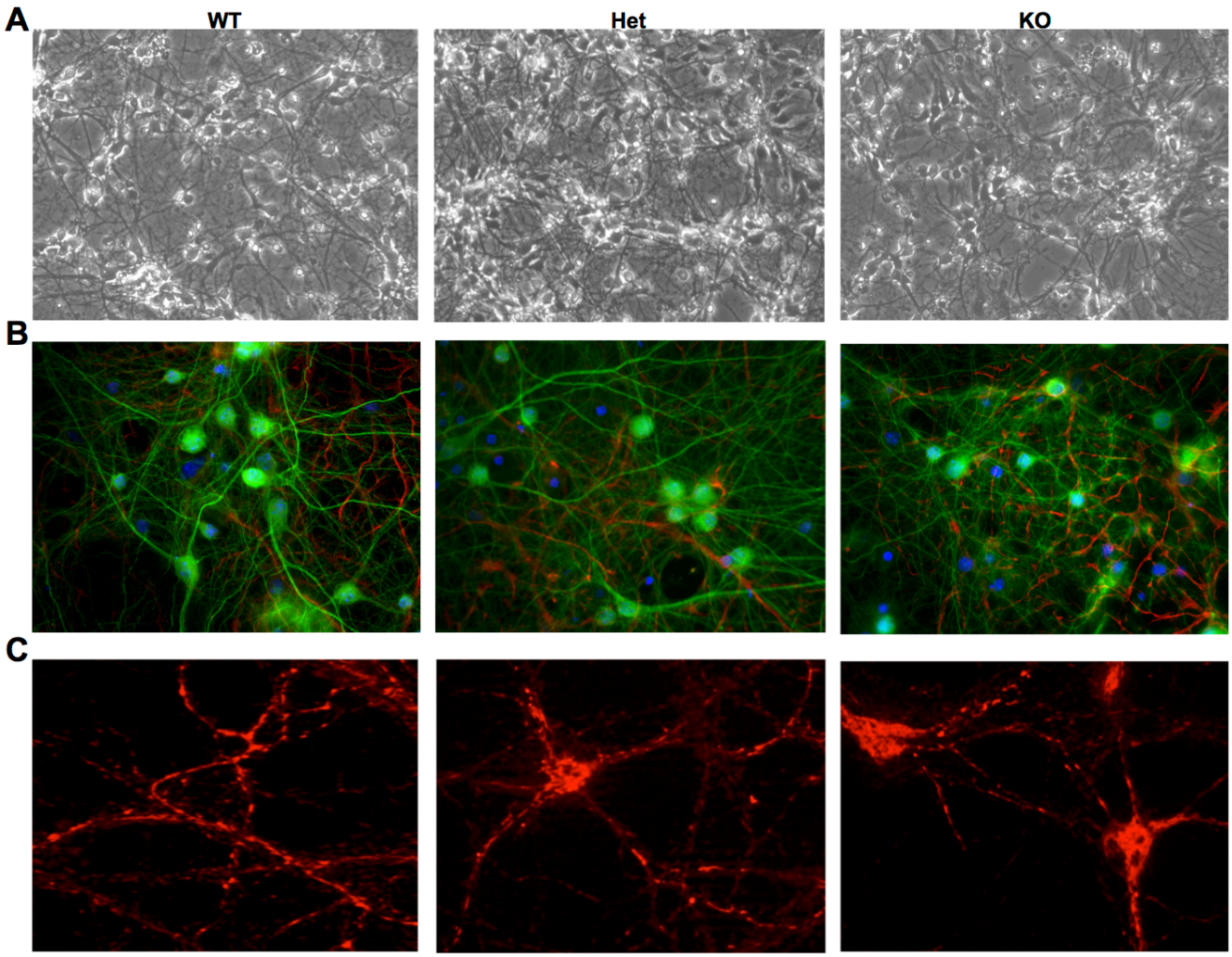

Figure 6. Visual Characterization of Primary Neuronal Cultures Generated from CHIP Deficient Mice Demonstrate no Apparent Deviations from WT or Het Sister Cultures. (A) Phase bright (20X), live cell images of WT, Het and CHIP KO mouse cultures at DIV20 demonstrate no obvious differences in overall neuronal morphology between genotypes at baseline. **(B)** Cultures fixed at DIV20 were probed with antibodies for the neuronal marker MAP2 (green), the glial marker GFAP (red) and the nuclear marker DAPI (blue). Cell counts revealed that these cultures are roughly 85% neuronal and 15% glial. **(C)** MitoTracker Orange labeling (red) demonstrates extensive and continuous mitochondrial networks at baseline across all three genotypes. Nine fields of view were imaged from 4 separate neuronal preps and subsequent experiments, totaling 36 imaged fields. The fluorescent images within the manuscript are representative of these fields.

Taken together, these data suggest that while CHIP deficiency has profound effects on baseline protein oxidation, lipid peroxidation, antioxidants and energetics, neurons derived from CHIP KO animals are morphologically indistinguishable from WT and Het sister cultures.

CHIP Deficiency Affects the Oxidation of Mitochondrially-Associated Proteins and Mitochondrial Transition Activity

Given the changes in redox and energetic status associated with CHIP deficiency *in vivo*, we sought to determine if proteins involved in mitochondrial homeostasis are altered as a result of CHIP deficiency. Expression of VDAC and COX IV, proteins associated with mitochondrial integrity and function, remained unchanged in brains from CHIP KO animals (**Figure 7A & B**) but there were high levels of both LC3-I and LC3-II (**Figure 7A & B)**. Analyses of further proteins essential for maintaining mitochondrial dynamics and homeostasis (**Figure 7A & B**) revealed that CHIP KO animals have increased expression of the fission protein, dynamin related protein 1 (Drp1), with no change in the mitochondrial fusion protein Mitofusin 1 (Mfn1). As increased fission and subsequent formation of fragmented mitochondria has been linked to the induction of mitophagy (Twig, 2008), this may contribute to the pattern of LC3 expression observed in these animals.

Novel biotin-avidin-capture methodology on freshly isolated mitochondria was used to determine if the baseline redox stress in CHIP deficient animals causes specific oxidative modifications of proteins involved in mitochondrial integrity, function and homeostasis. Given that CHIP KO animals had high levels of total protein oxidation (Figure 1A), we anticipated that many essential regulators of mitochondrial function would be oxidized. We were surprised to find that both Drp1 and Parkin were subject to carbonyl adduction in WT and Het animals (the presence of a band in the eluate (E) fraction lane), but not in CHIP KO mice (**Figure 7C**).

Protein oxidation, energetic status and production of free radicals have all been linked to altered stress-induced calcium buffering and mitochondrial permeability transition. Using isolated mitochondria, we found that the lag time of Ca^{2+}-induced mitochondrial swelling (**Figure 8A & B**) was much more rapid and profound in CHIP KO animals, indicative of poor

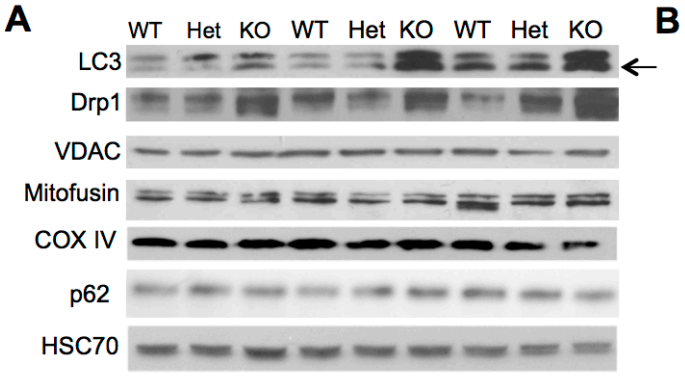

B

Fold Change Normalized to WT Animals			
		Het	KO
LC3-I	(n=3)	1.3 ± 0.3	3.3 ± 0.1 ***
LC3-II	(n=3)	1.0 ± 0.3	1.8 ± 0.1 *
Drp1	(n=3)	1.4 ± 0.4	2.6 ± 0.3 **
VDAC	(n=3)	0.8 ± 0.2	0.9 ± 0.1
Mfn	(n=3)	0.8 ± 0.2	0.9 ± 0.2
COX IV	(n=3)	0.8 ± 0.2	0.9 ± 0.3
p62	(n=3)	0.9 ± 0.05	0.9 ± 0.3
HSC70	(n=3)	1.0 ± 0.2	0.9 ± 0.4

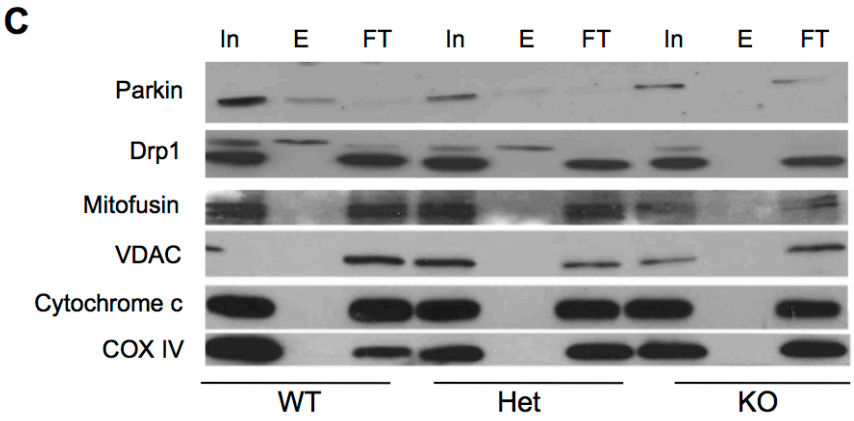

Figure 7. CHIP Deficiency Causes Changes in the Expression of Proteins Key to Maintaining Mitochondrial Dynamics. (**A)** Whole brain lysates from PND35 CHIP KO animals demonstrate increased expression of the autophagic marker, as well as increases in the mitochondrial fission protein, Drp1. Arrow denotes the lipidated form of LC3. **(B)** Western blots were analyzed using NIH Image (Scion Image J) to determine the mean relative densities of each protein band and fold changes were calculated using WT littermates as controls. Statistical significance is noted within the table where * denotes $p < 0.05$, ** denotes $p < 0.01$ and *** denotes $p < 0.001$. **(C)** Purified mitochondrial extracts were prepared from PND35 WT, Het or CHIP KO mice and further subjected to biotin-avidin-capture methodology. Protein extracts of whole cell "inputs" (denoted as In), proteins in the "eluate" fraction that have undergone oxidative modifications followed by chemical isolation and pull down (denoted as E) and oxidatively modified proteins that were able to "flow through" and escape isolation (denoted as FT) were separated on SDS-PAGE. WT and Het mice express high levels of oxidized Drp1, as well as oxidation of the E3 ligase, Parkin while CHIP KO animals do not. Immunoblots are representative of results from three independent experiments.

ion buffering capability. Taken together, these data suggest that CHIP is a regulator of mitochondrial integrity under conditions of stress and that CHIP deficiency is associated with altered stress induced mitophagy.

CHIP Deficiency Results in Increased Neuronal Death Following OGD

In order to test the hypothesis that CHIP deficient neurons have impaired stress responsiveness, neuronal cultures were exposed to varying durations of OGD and cell viability was assessed. OGD is a well-appreciated mitochondrial stress mediated by NMDA receptors and cell death can be observed after neuron enriched cultures are exposed to > 30 min of deprivation (Zeiger, 2010). In these experiments, OGD caused an increase in cell death in all genotypes in a time dependent manner (one-tailed ANOVA $p<0.01$; Note: time dependence of this effect is not shown with asterisks so as to highlight gene vs. time effects). Post hoc analysis of time points across genotypes reveled that primary cultures derived from CHIP KO animals faired worse following either 60 or 90 min of OGD when cell death was assessed 24 hr later ($p<0.05$; Bonferroni post-hoc testing). These data suggest that loss of CHIP is detrimental to neuronal survival following an ischemic event (**Figure 8C**).

2.5 Discussion

Biochemically and energetically intact mitochondria are essential determinants of cell viability in response to stress. These organelles play a critical role in ion homeostasis, metal sequestration and oxidative stress signaling. It has become increasingly evident that mitochondrial dysfunction is associated with a multitude of CNS diseases. In turn, neurons have evolved powerful mechanisms to remove injured organelles from the cell including mitophagy, a process that is an essential regulator of mitochondrial quality control and neuronal survival (Brown, 2010; Krebiehl, 2010; Michiorri, 2010; Twig, 2008). The role of

mitophagy has come under particular scrutiny lately as an increasing number of proteins have linked neurodegeneration with aberrant mitophagy (Chakrabarti, 2009; Chen and Dorn, 2013; Su and Qi, 2013; Yang, 2013). Acute overexpression of CHIP is neuroprotective against a number of acute and chronic stressors and we recently reported that CHIP KO mice

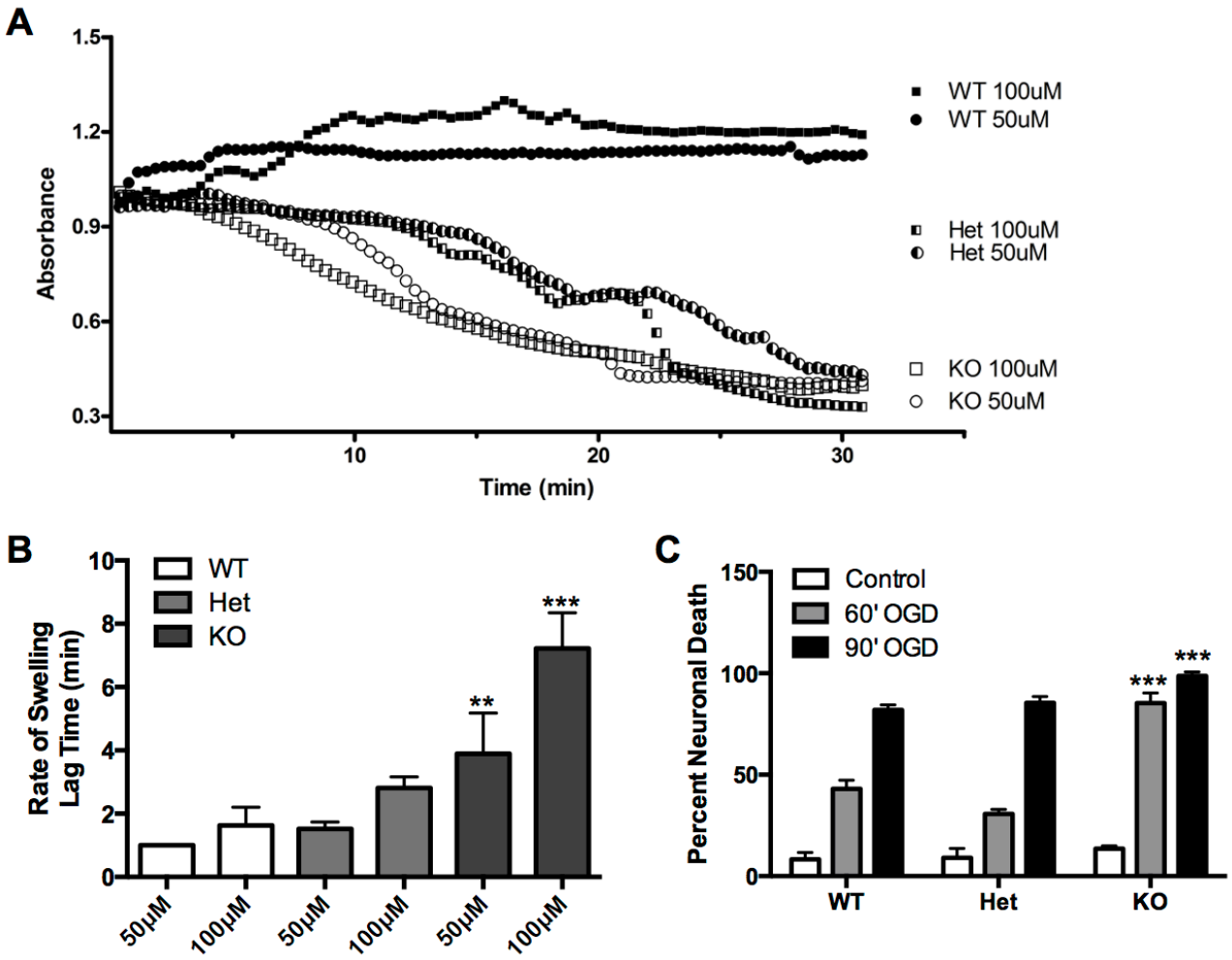

Figure 8. CHIP Deficiency Increases Mitochondrial Permeability Transition Activity and Increases Neuronal Death Following OGD. (**A**) Purified mitochondria from PND40 WT, Het or CHIP KO mice were incubated in the presence of increasing concentrations of Ca^{2+} (50μM or 100μM) while mitochondrial permeability transition activity was assessed. CHIP KO animals were found to undergo changes in mitochondrial permeability much faster than WT animals. **(B)** The rate of mitochondrial swelling was determined by assessing the maximal change in absorbance over time and was normalized to the corresponding WT mitochondria. Data represent the maximal rate of change in absorbance ± SEM from four independent experiments. Statistical significance was determined by two-tailed t test assuming unequal variances where ** denotes $p < 0.01$ and *** denotes $p < 0.001$ when compared to WT mitochondria treated with corresponding Ca^{2+} concentrations. Data were collected from four independent experiments. **(C)** CHIP KO neuronal cultures exhibit significantly greater amounts of cell death following exposure to both 60min and 90min OGD as assessed by lactate dehydrogenase release in comparison to WT cultures. Data represent the mean ± SEM from four independent experiments where *** denotes $p < 0.001$.

are uniquely impaired by the loss of this ligase, which dramatically decreases life span (Dai, 2003), impairs motor skills (McLaughlin, 2012; Min, 2008) and alters anxiety responses (McLaughlin, 2012). We show in the current work that these mice also present with atypical CNS protein oxidation and lipid peroxidation, decreased antioxidant responses and impaired bioenergetic status at baseline. Additionally, loss of CHIP results in changes in redox tone, energetic status and stress handling as well as increased vulnerability to acute stress. Taken together, these findings suggest that CHIP plays a non-redundant and previously unrecognized role in governing mitochondrial signaling in response to stress.

The observation that prompted these studies was the dramatically shortened life span and neurological impairments that are unique to CHIP deficiency. Other E3 ligase deficient animals, such as Parkin KO mice, are neurologically intact. Surprisingly, even triple transgenic KO of PINK1, Parkin and DJ1 fails to produce an overt phenotype (Dai, 2003; Dawson, 2010; Kitada, 2009; Min, 2008; Varcin, 2012). The motor phenotype and oxidative stress we observed in CHIP KO animals occur in the CNS of relatively young animals (PND35) suggesting that CHIP deficiency has a major impact early in life. We now demonstrate that these changes in physiology are accompanied by high levels of CNS protein oxidation and lipid peroxidation and decreased antioxidant responses which are far more profound than those observed in PINK1, DJ1 or Parkin deficient animals (Palacino, 2004; Varcin, 2012).

Previous studies suggest that the neuroprotective potential of CHIP lies in its role in protein triage, refolding, transcription of stress response genes and degradation of a growing list of proteins associated with cystic fibrosis, Alzheimer's disease and other disorders (Ballinger, 1999; McDonough and Patterson, 2003; Meacham, 2001; Miller, 2005; Sahara, 2005). CHIP is both cytoprotective (Zhang, 2011) and can inhibit apoptosis by increasing ubiquitination and degradation of pro-apoptotic proteins (Woo, 2010). Our data are the first to

demonstrate that CHIP is a direct regulator of mitochondrial homeostasis and cellular energetic status. These data are particularly intriguing given that CHIP appears to be one of only a handful of the approximately 500 mammalian E3 ligases in the CNS that responds to ischemia (Lackovic, 2012; Mengesdorf, 2002).

Support for a role of CHIP in response to ischemia comes from proteomic analysis of human post-mortem CNS samples from patients who suffered transient ischemic attacks (TIA) or ischemic strokes where increased levels of CHIP and loss of VDAC were noted (Stankowski, 2011). The close association of CHIP with stressed mitochondria would suggest that the upregulation of CHIP during stroke acts as a negative regulator of mitochondrial permeability transition activity, maintaining organelle homeostasis until mitophagy can be initiated. Future experiments will allow us to determine if this is a conserved stress signaling mechanism or one that is unique to Ca^{2+} overload following ischemia.

In this work, we demonstrate that the increased expression of CHIP observed in post-mortem human samples following ischemic events (Stankowski, 2011) can be recapitulated in an *in vitro* model of stroke. This allowed us to demonstrate that CHIP relocalization to mitochondria is an early event in response to OGD much like PINK1 stabilization and $p66^{shc}$ relocalization (Brown, 2010). Parkin's concerted action with PINK1 to promote mitophagy is a novel function of E3 ligases (Geisler, 2010; Geisler, 2010; Matsuda, 2010; Narendra, 2008; Narendra and Youle, 2011; Poole, 2008) and our data support the importance of these molecules in mitochondrial homeostasis as both CHIP and PINK1 colocalize with mitochondria following OGD, a feature not associated with PD. These data suggest that signaling pathways similar to those observed in PD may also mediate responses to ischemia. Conservation of mitochondrial stress signaling has also recently been noted in a mouse model of Alzheimer's disease where Parkin overexpression decreases both amyloid-beta (Aβ) accumulation and the number of damaged mitochondria (Khandelwal, 2011), as well as

in cardiomyocyte ischemic preconditioning studies where Parkin translocation to mitochondria precedes the removal of damaged organelles (Huang, 2011).

We have previously shown that phosphorylation and relocalization of the redox-sensitive kinase $p66^{shc}$ occurs within 30 min of OGD and is essential to evoke mitophagy (Brown, 2010). The importance of redox signaling in autophagic processes is underscored by the role of ROS' in autophagosome formation where redox modifications of specific cysteine residues in autophagy-related genes can regulate their bioactivity (Scherz-Shouval, 2007). Given that we observed increases in the ROS sensor PINK1 1 hr after a lethal OGD, we hypothesize that PINK1 may promote CHIP relocalization to damaged mitochondria in a manner similar to that of PINK1 recruitment of Parkin in PD. This is supported by our observation that mitochondria from CHIP KO animals have increased PINK1 stabilization, which may, in turn, recruit the E3 ligase, Parkin in the absence of CHIP.

Using a novel and powerful biotin-avidin-capture methodology, we demonstrate that Drp1 is specifically oxidized in both WT and Het animals but not CHIP KO animals. Our data support a model in which the balance between mitochondrial fission, fusion and mitophagy are impaired in CHIP deficient animals as there is a substantial increase in the baseline expression of the fission protein Drp1 yet no change in the fusion protein Mfn1. Overexpression of a Drp1-K38A which blocks mitochondrial fission was recently shown to restore mitochondrial morphology and dopamine release defects in PINK1 mutant mice (Rappold, 2014), supporting a model in which the observed increase in Drp1 in CHIP KO animals is indicative of stress.

Post-translational modifications of Drp1 are thought to play an essential role in regulation of mitochondrial fission (Otera and Mihara, 2011). Twig and colleagues have recently shown that in cells deficient in mitochondrial fission, there is an increase in oxidatively modified proteins (Twig, 2008), which is supported by our OxyBlot™ and F_{2t}-IsoP

data. If oxidation promotes degradation of Drp1, the lack of oxidation in KO animals would be predicted to promote Drp1 accumulation and potentially uncontrolled fission to the point of metabolite and mitochondrial DNA depletion - a scenario supported by our data demonstrating impaired energetics, altered autophagy, and increased Parkin and PINK1 in the brains of very young CHIP deficient animals.

We also found that the high molecular weight Parkin complex (Van Humbeeck, 2008) was oxidized in a gene dose-dependent manner. WT and Het animals express an oxidized form of Parkin whereas CHIP KO animals do not. The fusion promoting protein, Mfn1, is a substrate of Parkin, yet even increased Parkin expression was insufficient to alter baseline expression of Mfn1 across the genotypes examined (Poole, 2010). This suggests that oxidative modification of Parkin may be important for promoting its E3 ligases activity. These data are supported by reports of both S-nitrosylation and oxidation of Parkin leading to impairment in Parkin bioactivity (Chung, 2004; Meng, 2011; Yao, 2004). Taken together these data support a unique and non-recoverable role for the E3 ligase CHIP in the CNS response to stress.

In conclusion, we demonstrate that CHIP deficiency results in dramatic motor impairments and an early lethal phenotype which we show are associated with increased levels of protein and lipid oxidation, decreases in antioxidants, significant declines in CNS ATP, upregulation of a number of redox and stress-associated mitochondrial proteins and alterations in specific protein oxidation events. Moreover, acute ischemic stress reveals a unique mechanism whereby CHIP is an essential regulator of redox tone that, when absent, results in increased neuronal death in response to stroke-like insults. In combination with our previous data demonstrating that chronic CHIP overexpression is associated with decreased neuronal survival (Stankowski, 2011), these results underscore the importance of maintaining an exquisite balance of CHIP as a means of efficiently responding to acute injury.

CHAPTER 3

CHAPERONE MEDIATED PROTEIN REFOLDING FOLLOWING ACUTE ISCHEMIC STRESS INCREASES NEURONAL SURVIVAL

3.1 Abstract

Neuronal protein refolding and degradation in response to stress is largely mediated by the HSP70 chaperone complex and is critical for maintaining cell function. While some components of the triage machinery have been identified, we lack both a fundamental understanding of protein triage mechanisms evoked by neurons in response to stress and an ability to leverage this response to improve survival. In this work, we analyzed tissue from male rats given a transient middle cerebral artery occlusion (tMCAO) to identify changes in known and novel molecules that are part of the chaperone machinery and may represent essential regulators of chaperone function and expression. Luciferase-based reporter assays reveal that immediately following a short period of non-lethal oxygen and glucose deprivation (OGD), neurons attempt to refold proteins. Using an allosteric modulator of the HSP70 complex, 115-7c, we were able to improve neuronal protein and lipid integrity. Additionally, cholesterol biosynthesis, bioenergetic status and membrane integrity were all improved by 115-7c and levels of oxidized and ubiquitinated proteins were decreased. Priming naive neurons with 115-7c, mimicked the endogenous response to low-level stress and the neuroprotective effects of ischemic preconditioning (PC) in the absence of new protein synthesis. Taken together with our proteomic and metabolic data, we propose a model in which the endogenous response to acute injury is to promote protein refolding and that pharmacological augmentation of this response allows neurons to better maintain

proteostasis, decrease cell injury and maximize energetic capacity in order to survive subsequent stressors.

3.2 Introduction

Proteotoxicity is widely considered to mediate neuronal vulnerability in both chronic conditions such as Parkinson's and Alzheimer's disease and in acute injuries, such as ischemia (Gestwicki and Garza, 2012; Kalmar and Greensmith, 2009; Kalmar and Greensmith, 2017; Leak, 2014; Liu, 2005; Pratt, 2010). HSP70 binds to damaged proteins and is a critical determinant of cell fate in response to stress. While increased chaperone expression is a common response to injury (Liu, 2005; Magrane, 2004; McLean, 2004; Wang, 2013), important gaps exist in our understanding of which chaperone-mediated activities are most beneficial to neuronal survival and how to recapitulate the endogenous protective response mediated by chaperones when exposed to low-level stress.

The core components of the chaperone machinery, HSP70 and HSP40, work jointly to mediate folding, refolding, degradation and trafficking of proteins. The substrate-binding domain of HSP70, comprised of a beta sheet and a distal alpha helix that acts as a gate, allows for the binding and release of damaged proteins. This mechanism of action requires switching between a low-affinity/ATP bound state and a high-affinity/ADP bound state (Zuiderweg, 2017). Aside from bioenergetics, the clamping and release of substrates is also highly dependent upon chaperone interactions at multiple sites. This interaction include associations with HSP40, ubiquitin ligases, nucleotide-exchange factors, and other co-chaperones and has been shown *in silico* to alter binding kinetics and substrate triage (Kampinga and Craig, 2010; Radons, 2016).

The ability to leverage these interactions in a clinically meaningful way to develop treatments for bioenergetic crises such as stroke and ischemia has been limited (Kim, 2018; Stankowski and Gupta, 2011). While HSP70 over-expression aids in survival in many chronic

disease models (Cummings, 2001) (Broer, 2011) (Magrane, 2004) (Hoshino, 2011) (Ebrahimi-Fakhari, 2013), genetically manipulating the chaperone complex is a poor long-term clinical strategy to treat diseases associated with abnormal protein triage. Sustained expression of many of the protein chaperone proteins is associated with both initiation and progression of precancerous and cancerous states (Murphy, 2013; Sherman and Gabai, 2015). Pharmacological modulators targeting the chaperone complex have increasingly been recognized as a potentially valuable strategy for acute and chronic neurodegenerative diseases (Assimon, 2013; Kim, 2018; Pratt, 2015).

Allosteric modulators of the HSP70 complex have been developed which specifically target the HSP40/HSP70 interacting site as well as the ATP/ADP substrate-binding domain of HSP70 (Wisen, 2010; Wisen and Gestwicki, 2008). HSP70 activators bind to the IIA subdomain of the nucleotide-binding domain (NBD), promoting formation and stabilization of the HSP40/70 complex. This interaction results in the constant clamping and release of HSP70 bound substrates, ultimately increasing client protein refolding. HSP70 inhibitors interact at the NBD, blocking ATP turnover and driving the complex to release denatured proteins for subsequent ubiquitination and proteasomal degradation (Pratt, 2015).

In the context of chronic neurodegenerative diseases, promoting substrate degradation, as opposed to refolding, has proven effective in diminishing cytotoxicity and neuropathology (Abisambra, 2013; Chafekar, 2012; Fontaine, 2015; Guzhova, 2011; Howarth, 2009; Jinwal, 2013; Jinwal, 2009; Miyata, 2013; Wang, 2013). Until now, however, the specific pharmacological promotion of protein degradation or refolding, has not been studied with regards to acute ischemic injury. Given the rapid changes in bioenergetic status associated with oxygen and glucose deprivation (OGD), the extent and duration of short periods of ischemia may, in fact, recruit unique chaperones and triage strategies. When faced with acute bioenergetic crises, neurons employ a chaperone dependent signaling system

known as ischemic preconditioning (PC) that may not be deployed under conditions of chronic stress (Barone, 2004; Kim, 2007; Lizama, 2018; McLaughlin, 2003).

In this work, we couple high powered proteomic screening platforms with targeted pharmacology to both identify proteins altered by acute neurological injury, and assess the efficacy of small molecule modulators of the HSP70 complex which either promote HSP70 mediated substrate degradation or refolding (Pratt, 2015; Wisen and Gestwicki, 2008). In doing so, we sought to: 1) Identify critical chaperone substrates damaged as a result of transient ischemia 2) Identify factors that limit protein triage in response to OGD 3) Leverage allosteric modulators of the chaperone complex to improve neuronal survival in response to OGD and 4) Determine if profolding drugs can mimic the endogenous neuroprotective response known as ischemic preconditioning.

3.3 Materials and Methods

Reagents

Commercial vendors of chaperone antibodies as well as reagents and supplies used for immunoblotting, immunofluorescence and cell culture experiments are the same as previously described (Lizama, 2018; Palubinsky, 2015). Additional primary antibodies used for immunoblotting in this study include: CHIP (PC711; Calbiochem) ubiquitin - clone Fk2 (BML-PW8810-0500, Enzo), HSC70 (ADI-SPA-816, Enzo), HSP70 (ADI-SPA-811, Enzo), HSP40 (ADI-SPA-400, Enzo), BAG1 (ADI-AAM-400, Enzo), HOP (ADI-SRA-1500, Enzo), and HIP (ADI-SPA-766, Enzo). For immunocytochemistry, the following secondary antibodies were used: anti-rabbit Cy2 (711-225-152), anti-mouse Cy2 (715-225-150) and anti-rabbit Cy3 (711-165-152), all purchased from Jackson ImmunoResearch. Coverslips were mounted using ProLong Gold (P36934) from Invitrogen. Commercially available kits that were used include the D_C Protein Assay kit (500-0112, Bio-Rad), the OxyBlot™ Protein Oxidation

Detection Kit (Millipore, S7150) and an ATP Assay Kit (Z5030042, BioChain). Reagents and materials required for biotin-avidin-capture methodology were obtained from the same companies as previously described (Stankowski, 2011). All cell culture medium and supplements were purchased from Invitrogen. Unless otherwise stated, all other chemicals were purchased from Sigma-Aldrich.

Animals

The Institutional Animal Care and Use Committee at Vanderbilt University approved all animal husbandry and experiments.

Transient Middle Cerebral Artery Occlusion (tMCAO)

Spontaneously hypertensive male Sprague Dawley rats were obtained from Charles River at 18 weeks of age and housed for 2 weeks prior to surgery with unlimited access to food and water prior to and after surgery. Rats were weighed (250-300 g in weight) and randomly assigned to 1 of 3 groups: Sham controls (surgery but no MCAO - 2 animals for proteomic analysis), tMCAO group 1 (10 minute MCAO followed by 2 days of recovery - 10 animals: 2 for proteomic analysis, 8 for WB) or tMCAO group 2 (10 minute MCAO followed by 14 days of recovery - 10 animals: 2 for proteomic analysis, 8 for WB). tMCAO surgery was conducted as previously described (Barone, 1998; Khan, 2016). Body temperature was maintained at 37°C using a heating pad throughout the surgical procedure. Briefly, once deeply anesthetized (2% Isoflurane), the right-sided common, internal, and external carotid arteries were exposed and their tributaries cauterized. An intraluminal suture (Doccol Corp.) was routed into the internal carotid artery (ICA) via the external carotid artery and pushed through to occlude the MCA. After 10 minutes of occlusion, the suture was removed and animals were allowed to re-equilibrate. For the tMCAO groups, only rats with left-sided

weakness on upright tests were included in the remainder of this study. For the sham group, the dura was opened over the right carotid artery but the artery was not occluded.

Proteomics

Sample Preparation:

Brains were removed from untreated control and 2 day post-tMCAO animals and immediately placed onto dry ice. Hemispheres were separated and motor cortex was removed from the ipsilateral side for tMCAO samples and sham-treated controls. Samples were then placed into a glass dounce containing 1 ml of ice-cold TNEB lysis buffer. Brains were homogenized on ice (35 strokes), sonicated at 6 watts for 10 seconds and passed through a 40-micron cell strainer then through a 0.2-micron filter affixed to a 10 mL syringe. Samples were precipitated by adding 3 mL of ice-cold ethanol, vortexing and incubating on ice for 3 minutes. Following incubation, samples were spun at 3000 x rpm (1819 g) for 10 minutes at 4°C. Upon removal of the supernatant, lysates were incubated in a 2:1 mixture of chloroform and ice-cold methanol for 3 minutes and centrifuged at 3000 x rpm (1819 g) for 10 minutes. Following the spin, lysates were washed 3 times in 1 ml of ice-cold methanol. After the third wash, lysates were re-suspended in 1 ml of 0.5% SDS and sonicated at 6 watts for 10 pulses. Following sonication, 10 µl of sample was added to 8 µl of 4X sample buffer and 2 µl of 1 M DTT. This portion of the sample was heat denatured at 95°C for 10 minutes while the rest of the sample was used for protein assay.

Peptide Preparation:

Equal protein concentrations of each sample were loaded onto a 10% Bis-Tris gel with empty lanes in between samples and separated at 180V for 30 minutes. Simply Blue Safe Stain was used to visualize all protein bands and allow for each sample to be cut horizontally

into ~13 fractions. Each horizontal fraction was then cut vertically into ~1 mm cubes and placed in a microcentrifuge tube. One hundred µl of 100 mM ammonium bicarbonate (AmBic) was added to each fraction tube.

Samples were reduced with 5 mM DTT in AmBic for 30 minutes at 60°C with shaking. Samples were then alkylated with 10 mM iodoacetamide in AmBic for 20 minutes in the dark at RT. Any remaining Safe Stain dye was removed with additional 100 µl washes in 50 mM AmBic /acetonitrile (1:1, v/v). Once clear of all dye, gel pieces were dehydrated in 100% acetonitrile. Next, samples were rehydrated in 200 µl of 25 mM AmBic containing 300 ng of trypsin gold (Promega) and incubated at 37oC overnight. Following trypsinization, peptides were extracted from the gel via 3, 20 minute washed in 200 µl of 60% aqueous acetonitrile containing 1% formic acid and evaporated to dryness *in vacuo*. Lastly, peptides were re-suspended in 30% aqueous acetonitrile containing 0.1% formic acid and stored at -80^{o}C.

Proteomics Database search and assembly:

Data from shotgun LC-MS/MS runs were converted to mzml format using Proteowizard version 3.0.5211 (Kessner, 2008). The mzml files were searched using MyriMatch version 2.1.132 (Tabb, 2007) against the human Refseq database. A semi-tryptic search was employed with a maximum of four missed cleavages allowed. A target-decoy search was employed using a reverse sequence database to allow calculation of FDR for peptide-spectrum matches (Elias and Gygi, 2007). Protein-level FDR was calculated by dividing the number of reverse sequence proteins identified by the total number of proteins identified, multiplying by two and converting to a percent. All search result files were parsimoniously assembled in IDPicker version 3.1.643.0 (Ma, 2009). p values were calculated based on unequal variance in a two-tailed Student's t-test with alpha set to 0.05.

Immunoblotting

Western blots were performed as previously described (Lizama, 2018; Palubinsky, 2015). Briefly, neuronal cultures were placed on ice and washed twice with ice-cold 1X PBS. Following the second wash, 500µL of TNEB lysis buffer (50 mM Tris-Cl, pH 7.8, 2 mM EDTA, 150 mM NaCl, 8mM β-glycerophosphate, 100µM sodium orthovanadate 1% Triton X-100, and protease inhibitor diluted 1:1000) was added.

Approximately 100µL of lysate was saved for the determination of protein concentrations and the remaining lysate was re-suspended in an equal volume of Laemmli buffer with β-mercaptoethanol (1:20). Protein samples were heated to 95°C for 10 minutes, and stored at -20°C. Protein concentrations were determined via the Dc Protein Assay Kit II and equal protein concentrations were separated using 4-12% Bis-Tris gels followed by transfer onto PVDF membranes and then blocked in methanol for 5 minutes.

Once dry, the membranes were incubated at 4°C overnight in primary antibody prepared in 5% nonfat dry milk in a Tris-buffered saline solution containing 0.1% Tween 20 (TBS-Tween). All primary antibodies were diluted 1:1000. Following incubation in primary antibodies, membranes were washed and incubated for 1hr at room temperature in a 1:5000 dilution of horseradish peroxidase–conjugated secondary antibodies prepared in 5% nonfat dry milk in TBS-Tween. After additional washes in, protein bands were visualized using a chemiluminescent substrate and exposed to autoradiography film. All experiments were performed using cultures from at least four independent dissections.

Primary Rat Neuronal Culture

Primary neuronal forebrain cultures were prepared from embryonic day 18 Sprague-Dawley rats similar to as previously described (Palubinsky, 2015). Briefly, cortices were digested in trypsin and dissociated. Resultant cell suspensions were adjusted to 750,000

cells/mL and plated 2 mL/well in 6-well tissue culture plates containing five 12mm or one 25mm poly-L-ornithine-coated glass coverslip(s). Cultures were maintained at 37^{o}C, 5% CO_2in growth media composed of a volume to volume mixture of 84% DMEM, 8% Ham's F12-nutrients, 8% fetal bovine serum, 24U/mL penicillin, 24µg/mL streptomycin, and 80µM l-glutamine.

Glial proliferation was inhibited after two days in culture via the addition of 1µM cytosine arabinoside, after which cultures were maintained in Neurobasal medium containing 2% B27, 2x N2 and 4% NS21 supplements (Chen, 2008) with antibiotics for 2 weeks. One week before experiments, neurons are maintained in Neurobasal medium containing 4% NS21 and antibiotics only. All experiments were conducted 21-25 days following dissociation.

Oxygen Glucose Deprivation

Oxygen glucose deprivation (OGD) experiments were performed between day *in vitro* (DIV) 21 through DIV 25, at which time neurons represent at least 95% of the population as assessed by NeuN and GFAP staining. OGD was performed as previously described (Lizama, 2018) complete exchange of media with deoxygenated, glucose-free Earle's balanced salt solution (150mM NaCl, 2.8mM KCl, 1 mM $CaCl_2$ and 10 mM HEPES; pH 7.3), bubbled with 10% H_2/85% N_2/5% CO_2. Cultures were exposed to OGD in an anaerobic chamber (Billups-Rothberg) at 37°C. Upon OGD termination, cells were washed with MEM/BSA/HEPES (0.01% BSA and 25mM HEPES) and then maintained in MEM/BSA/HEPES/N2 (0.01% BSA, 25mM HEPES and 2X N2 supplement) for various recovery times at the completion of which neurons were prepared for immunoblotting, biochemical assessments or fixed for immunofluorescence.

Lactate Dehydrogenase Toxicity Assay

Twenty-four hours following the final OGD, 40 µl of culture media was removed in triplicate from each well, placed in a 96 well plate and incubated in assay buffer for 20 minutes at room temperature. During this time, NAD is reduced to NADH by lactate dehydrogenase (LDH) during the stoichiometric conversion of a tetrazolium dye present in the buffer. Following the incubation, absorbance is read at 490 nm as a measure of the amount of LDH released by dead and dying neurons. In order to account for variation in total LDH content, raw LDH values were normalized to the toxicity caused by exposure to a lethal, 90 minute OGD insult. All experiments were performed using cultures from at least four independent dissections. In addition, LDH results were confirmed qualitatively by visual inspection and live cell imaging of the cells and, in several instances, quantitatively by cell counts.

Sterol Analysis

Folch solution was added to 30 µg of protein from neuronal cells to extract lipids followed by the addition of an equal volume of 0.9% NaCl. Folch solution (2:1 chloroform: methanol) contained 0.25 mg/mL TPP, 0.005% BHT, and the internal standards d_7-7-DHC (118 ng), $^{13}C_3$-Des (116 ng), d_7-Chol (1.18 µg). Note: all natural and isotopically labeled sterols are available from Kerafast, Inc. The resulting mixture was vortexed and centrifuged. The lower organic phase was recovered and dried under vacuum. To increase sensitivity, the lipid extract was derivatized with 4-phenyl-1,2,4-triazoline-3,5-dione (PTAD). 100 µL of freshly prepared 2 mg/mL PTAD solution in MeOH was added to each sample and incubated for 30 minutes at room temperature with occasional shaking then transferred into sample vials. The sterol samples (10 µL injection) were analyzed on an UPLC C18 column (Acquity UPLC BEH C18, 1.7 µm, 2.1 mm × 50 mm) with 100% MeOH (0.1% v/v acetic acid) mobile phase at a

flow rate of 500 µL/min and runtime of 1.2 min. A TSQ Quantum Ultra tandem mass spectrometer (ThermoFisher) was used for MS detections, and data were acquired with Finnigan Xcalibur software. Selected reaction monitoring (SRM) of the PTAD derivatives was acquired in the positive ion mode using atmospheric pressure chemical ionization (APCI). MS parameters were optimized for the 7-DHC-PTAD adduct and were as follows: auxiliary nitrogen gas pressure at 55 psi and sheath gas pressure at 60 psi; discharge current at 22 µA and vaporizer temperature at 342°C. Collision induced dissociation (CID) was optimized at 12 eV under 1.0 mTorr of argon. The monitored transitions included: Chol 369→369, d_7-Chol 376→376, 7-DHC 560→365, d_7-7-DHC 567→372, Des 592→365, and $^{13}C_3$-Des 595→368. Data was then normalized to protein.

Primary Neuronal Transfection and Assessment of Protein Folding

Primary neuronal cultures in a 6 well plate were transfected via LipoJet (SL100468, SignaGen) with a plasmid containing both *Firefly* and *Renilla* luciferase reporters (E1910, Promega) according to manufacturer's protocols. Briefly, cultures underwent a 100% media change to fresh growth media 1 hour prior to the addition of lipid-based transfection reagents including 5µg of plasmid. After a 6-hour incubation, culture media was aspirated, fresh growth media was returned and cultures were used for subsequent OGD experiments at 48 hours post transfection and folding assays at 72 hours post-transfection.

Protein folding was assessed using a dual luciferase reporter assay. Cultures were washed twice with 1X PBS then placed in 500µL of passive lysis buffer with gentle shaking for 15 minutes at room temperature. Following lysis, 100µL of lysate was collected for protein assay determination and the remaining lysate was divided into triplicate wells (20µL each) of a 96 well plate. One hundred microliters of luciferase assay reagent was added to the samples, mixed well and luminescence was immediately read over a 10 second period to

obtain a *Firefly* luciferase reading. Following this first reading, 100µL of Stop & Glo reagent was added to each sample, mixed well and luminescence was again read to obtain a *Renilla* luciferase reading.

Firefly luciferase is rapidly denatured and refolded via the HSP70 complex and is subject to CHIP-mediated ubiquitination *Renilla* luciferase is appreciably smaller, more stable (in its commercialized form) and resistant to denaturation. As such, the *Firefly* luciferase signal (a measure of protein refolding) can be normalized to the total *Renilla* luciferase activity.

OxyBlot™ Methodology

Derivatization of oxidized proteins was performed as previously described (Palubinsky, 2015; Stankowski, 2011). Briefly, whole cell lysates were harvested and immediately treated with 50mM DTT to prevent auto-oxidation of proteins. Samples were homogenized and then equally divided into derivatization reaction (DR) solution containing 2,4-dinitrophenylhydrazine or negative control (NC) solution. Samples were stored at 4°C and processed further within seven days. Equal protein concentrations were separated using Criterion Bis-Tris gels and processed as described in the Immunoblotting section below. The manufacturer provided antibodies specific for the detection of oxidized proteins. All experiments were performed using cultures from at least four independent dissections.

Immunofluorescence

Briefly, neuronal coverslips were washed with 1X PBS and fixed for 10 minutes in 4% formaldehyde. Cells were permeabilized for 5 minutes with 0.1% Triton X-100, washed with 1X PBS, and blocked with 8% BSA diluted in 1X PBS. After 25 minutes of blocking, coverslips were incubated in anti-MAP2 (1:500) and anti-Fk2 (1:500) primary antibodies

diluted in 1% BSA overnight at 4°C. Following primary antibody incubation, cells were washed in 1X PBS for a total of 30 minutes and incubated in Cy2 and Cy3 secondary antibodies (1:500) in 1% BSA for 1 hour. Cells were next washed for a total of 30 minutes in 1X PBS and mounted with Prolong Gold + DAPi. Fluorescence was visualized using a Zeiss Axioplan microscope equipped with an Apotome optical sectioning slider. Nine fields of view were imaged from 4 separate neuronal preps and subsequent experiments, totaling 36 imaged fields per condition. The fluorescent images within the manuscript are representative of these fields.

ATP Measurement

The concentration of intracellular ATP was assessed using bioluminescence. Neuronal cultures were washed twice with 1X PBS then incubated in ATP reagent mix in the presence of luciferase. The light generated was measured via a luminometer with the intensity representing the intracellular concentration of ATP. Sister cultures undergoing the same treatments were used for the determination of protein concentrations. All experiments were performed using cultures from at least four independent dissections.

Analysis and Statistics

Unless otherwise noted, data were summarized and are represented as mean ± SEM. The statistical significance of differences between means was assessed using one-way analysis of variance (ANOVA) at the 95% confidence interval, followed by the specified post hoc testing using GraphPad Prism software.

3.4 Results

The protein triage complex rapidly and robustly responds to short periods of oxygen and glucose deprivation: An in vivo model of ischemic preconditioning

Adult male rats were given a brief, 10-minute period of ischemia induced by transient middle cerebral artery occlusion (tMCAO), which is equivalent to a transient ischemic attack (TIA). The ipsilateral and contralateral motor cortices were harvested 24 hours later for next generation global proteomic profiling. One hundred and seventy eight proteins were significantly altered (greater than 2 fold) by tMCAO. Eighty-three demonstrate increased expression and 95 exhibit decreased expression profiles. Moreover, 10.8% of the proteins with increased expression (9 of 83) and 7.4% of the proteins with significant decreases in expression (7 of 95) were identified as chaperone-related molecules. A subset of these proteins are listed in **Figure 9A**.

To confirm these proteomic hits, the ipsilateral and contralateral motor cortices from animals subjected to tMCAO were collected at 2 or 14 days post-ischemia. Tissue harvested at 2 days is considered to be within a preconditioned (PC) window where neurons are protected from subsequent lethal ischemic events, while those harvested at two weeks are no longer within the protected window. Western blot analysis corroborates results from our proteomics screen within the PC (2 day) samples (**Fig. 9B**). Increased HSP70 expression, a hallmark of the PC effect, is evident only in samples harvested during the protected window (2 day). Many of the identified chaperone components are key in either the degradation (CHIP, HIP, DJ1) or refolding of ischemia-damaged proteins (HSP90, HOP, HSP60).

Protein refolding increases neuronal survival in response to OGD

Mild to moderate OGD increases reactive oxygen species (ROS) to form oxidized proteins and lipids, while limiting the capacity of mitochondrial respiration for sustained ATP

A

Proteomics Changes of Chaperone Machinery		
Decreased in PC	**Increased in PC**	**Unchanged**
CHIP ($p = 0.00002$)	HSP70 ($p = 0.0255$)	HSC70 ($p = 0.25$)
HSP60 ($p = 0.0053$)	HSP90 ($p = 0.0054$)	HSP40 ($p = 0.2595$)
DJ1 ($p = 0.0323$)	HSP27 ($p = 0.0226$)	HOP ($p = 0.4888$)

B

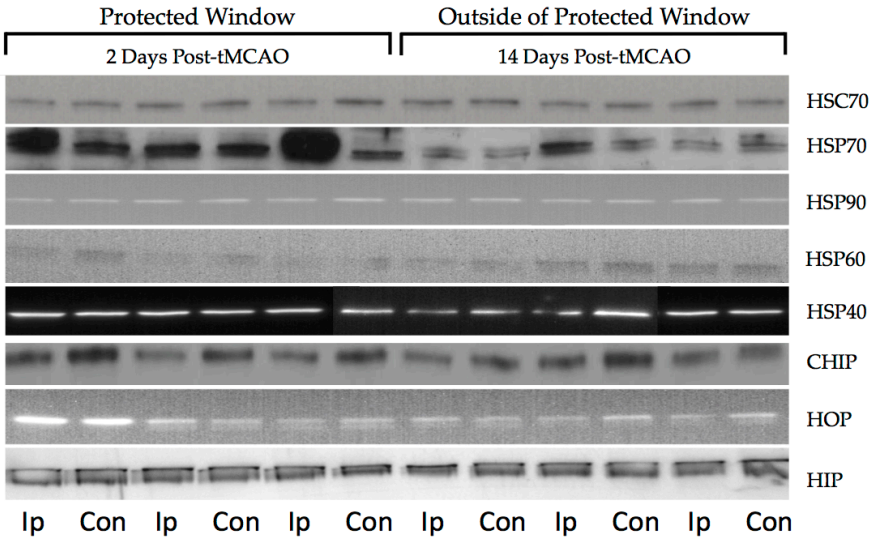

Figure 9: Integral components of the HSP70 molecular chaperone complex are altered in an *in vivo* model of ischemia. Next generation proteomic analysis (**A**) identified molecules closely associated with the chaperone machinery that undergo expression changes (at least 2 fold) 48hr following a 10 minute tMCAO in comparison to control rat brains. **(B)** Western blot analysis confirms several essential signaling changes observed in the proteomic data set. (Con = Contralateral hemisphere, Ip = Ipsilateral hemisphere).

synthesis during stress (Brown, 2010; Ravati, 2000; Zeiger, 2010). To determine whether promoting protein degradation or refolding could afford neuroprotection, primary neuronal cultures were exposed to various durations of OGD in the presence or absence of allosteric modulators of the HSP70 complex during recovery (**Fig. 10A**). The HSP70 inhibitor, MKT-077, binds to the nucleotide binding domain of HSP70, blocking ATP turnover and driving the complex to release denatured proteins for subsequent ubiquitination (Pratt, 2015; Rousaki, 2011). MKT-077 (10 μM) is non-toxic to control cultures but offers no beneficial effects on

neuronal survival when assessed 24 hours following various durations of OGD via lactate dehydrogenase (LDH) assays (**Fig. 10B**). The HSP70 activator, 115-7c, promotes substrate refolding by acting as an HSP40 mimetic and increasing the ATPase activity of the HSP70 complex, resulting in the constant clamping and release of HSP70 substrates required for refolding (Jinwal, 2009). Addition of 115-7c (25μM) following OGD significantly improved neuronal viability, with 21.5% increased survival following 30 minute OGD and 29.2% following 60 minute OGD (**Fig. 10C**).

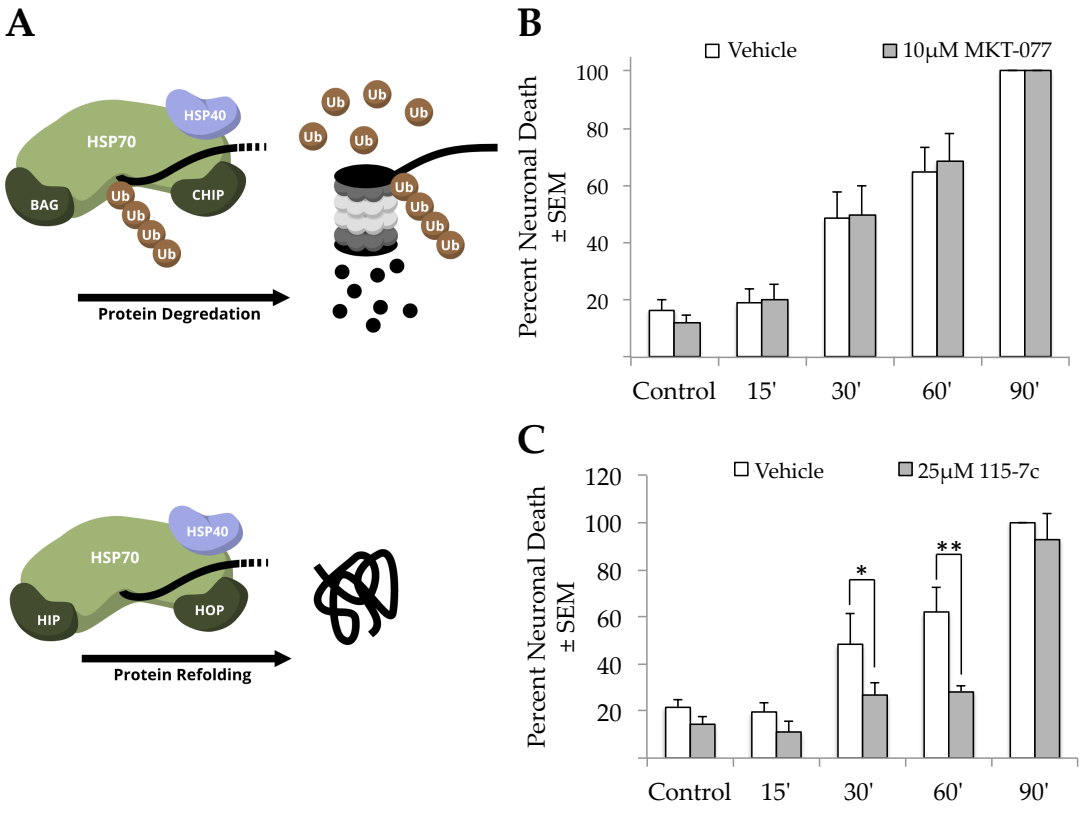

Figure 10: Promoting protein refolding improves cell survival in response to OGD. Novel allosteric modulators of the HSP70 complex can direct HSP70 chaperone activity towards degradation or refolding of ischemia-damaged proteins (**A**). Treatment with the pro-degradation compound, MKT-077, while not detrimental has no benefit on neuronal survival following various durations of OGD when analyzed via lactate dehydrogenase toxicity assay (**B**). Immediate administration of the pro-folding compound, 115-7c following varying durations of OGD increases neuronal survival (**C**). Data were compiled from five independent cultures and analyzed via one-way ANOVA using Tukey's *post-hoc* testing where $p < 0.05$ = * and $p < 0.01$ = **.

Promoting protein folding improves cell membrane and lipid integrity

Any number of processes can be affected by an ischemic event, including damage to DNA, lipids and proteins within different cellular compartments. Given that our measurement of lactate dehydrogenase released into culture media requires leaky cell membranes and that we saw remarkable decreases in this release with 115-7c treatment, we sought to examine whether 115-7c could play a role in preserving neuronal membranes. As the essential biomolecule, cholesterol, plays numerous roles in cellular homeostasis including maintenance of membrane integrity (Costello, 2016; Fuller and Futerman, 2018; Zhang and Liu, 2015), we sought to determine whether cholesterol biosynthetic pathways were affected.

Our data show that neurons subjected to OGD have an increase in the desmosterol:cholesterol ratio (**Fig. 11C**) suggesting weakened membrane integrity. However, when the neuroprotective agent 115-7c is added immediately following OGD, the ratio of desmosterol:cholesterol returns to baseline (**Fig. 11C**) which may be a biological response to ultimately re-stabilize membranes potentially through refolding of key players in cholesterol biosynthesis. This hypothesis is supported by data demonstrating that in the presence of 115-7c (with or without OGD), neurons have increased overall levels of cholesterol (**Fig. 11A**). We also observe increases in 7DHC levels upon 115-7c administration, but only with a concomitant OGD stress (**Fig. 11D**). This finding is interesting in that not only is 7DHC a precursor to cholesterol, but also a precursor to vitamin D (Annweiler, 2010; Mark, 2016). Vitamin D is neuroprotective and in some studies argued to activate the cellular stress response, so the observation that 7DHC increases in OGD-treated neurons with 115-7c may represent a more responsive population of cells to the ischemic stress. Even though this increase of 7DHC may be beneficial, it is also known that 7DHC is highly oxidizable and is associated with neurodevelopmental diseases like SLOS suggesting the inverse. However,

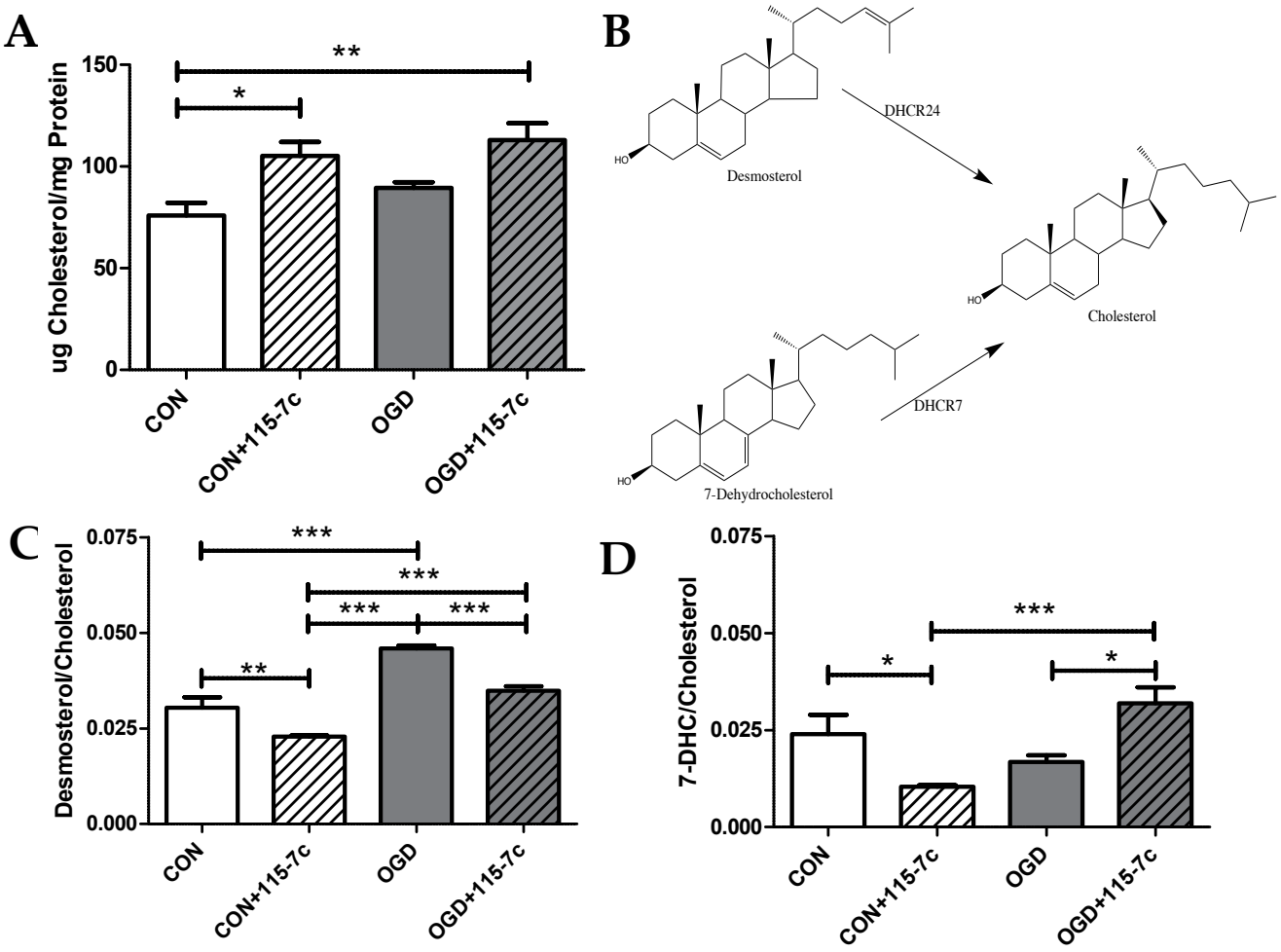

Figure 11: Treatment with 115-7c improves lipid biosynthetic pathway profiles. In the presence of 115-7c (with or without OGD), neurons have increased overall levels of cholesterol (**A**). When subjected to OGD neurons exhibit an increase in the desmosterol:cholesterol ratio that returns to baseline levels when 115-7c is administered immediately following OGD (**C**). Increases in 7DHC levels upon 115-7c administration are noted, but only with a concomitant OGD stress (**D**). Data were compiled from eight independent cultures and analyzed via one-way ANOVA using Tukey's *post-hoc* testing where $p < 0.05$ = * and $p < 0.01$ = **.

this data in conjunction with the previous findings support the former, that 7DHC is possibly neuroprotective in this specific scenario by serving as an increased pool of precursor to synthesize vitamin D.

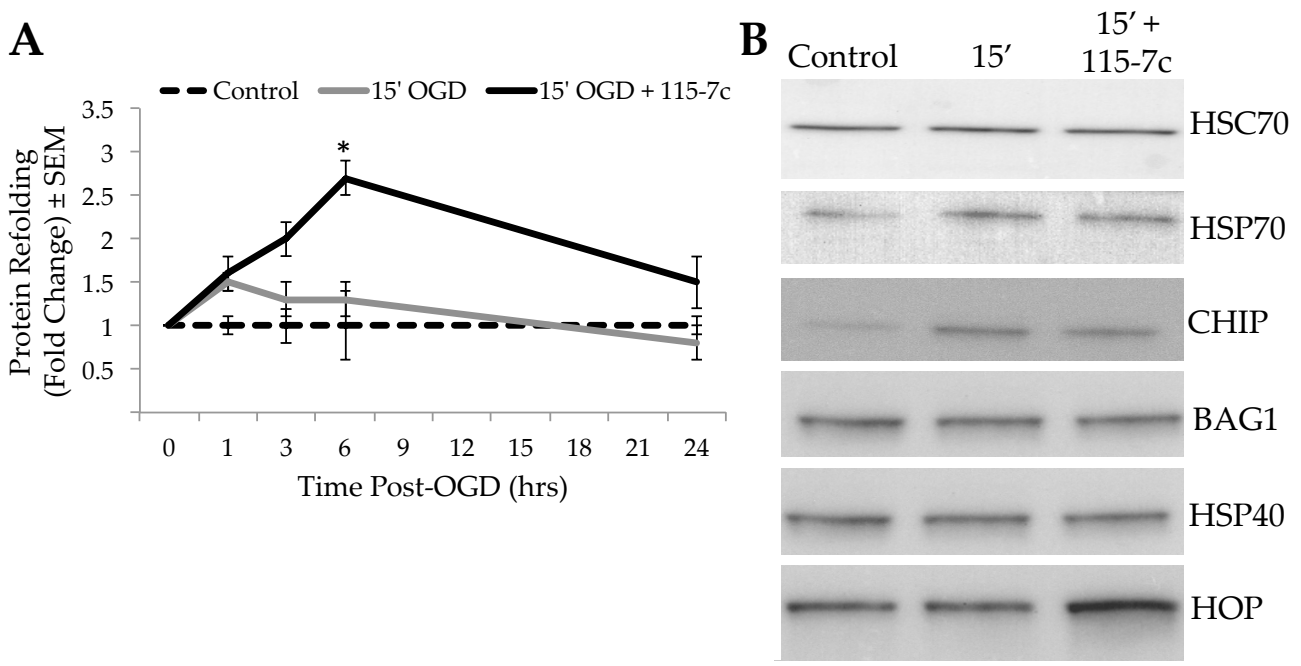

Figure 12: 115-7c allows neurons to maintain increased levels of folding activity for a longer duration than PC alone. (**A**) One hour following 15' (PC) OGD, neuronal cultures exhibit a roughly 1.5 fold increase in protein folding whether untreated (gray line) or in the presence of 115-7c (solid, black line) when normalized to control cultures (black, hashed line). At later time points (3hr and 6hr) following PC OGD, untreated and treated cultures diverge where untreated cultures begin to lose their ability to refold (slowly returning to near baseline levels) while 115-7c treated cultures continue an upward trend in folding, peaking at 6hr with a nearly 3 fold increase in protein folding. Twenty-four hours following PC OGD, folding rates in untreated cultures return to baseline while those treated with 115-7c maintain at least a 0.5 fold increase. Data were conducted in neurons from four independent cultures and analyzed via one-way ANOVA with Tukey's post hoc testing where $p < 0.05$ = *. Western blot analysis (**B**) of major components of the HSP70 chaperone complex demonstrate that HOP expression is unchanged with 15' PC OGD alone, but increases in the presence of 115-7c. Representative data shown is based on analysis from 5 independent cultures.

Protein refolding rates are maximized by treatment with 115-7c

Based on these data, we hypothesized that a protein refolding failure may limit survival following OGD. To test this, we transfected a bi-cistronic *Firefly*/*Renilla* dual luciferase reporter into primary neurons 24 hours prior to 15 minutes of OGD. *Firefly* luciferase is rapidly denatured and refolded via the HSP70 complex as a result of OGD (Bonomo, 2010; Wisen and Gestwicki, 2008) while *Renilla* luciferase remains resistant to denaturation and can be used as an internal control. Endogenous folding activity increases slightly above control by 1

hour (1.5 fold) following OGD but is not maintained thereafter (**Fig. 12A** - dark gray line) falling below untreated control levels (dashed black line) by 24 hours. Administration of 115-7c immediately following 15 minute OGD results in increased folding (1.6 fold at 1 hour, 2 fold by 3 hours and 2.7 fold by 6 hours) that remains elevated above untreated control and 15 minute OGD levels, even at 24 hours (1.5 fold, solid black line). Taken together, these data demonstrate that neurons subjected to OGD in the presence, or absence, of 115-7c begin folding on the same trajectory (within 1 hour), but only cultures treated with 115-7c are able to sustain and maximize this folding capacity.

To determine which chaperone components are limiting in the cellular milieu that would explain diminished endogenous folding capabilities, primary neuronal cultures were subject to 15 minute OGD in the presence or absence of 115-7c, harvested for Western blot 24 hours later and probed for chaperone components known to shift the complex towards degradation or refolding. Expression of the pro-folding protein and HSP70 co-chaperone, HOP (HSP70 Organizing Protein), is increased by 186% [ImageJ densitometry measurements (*n* of 5)] in the presence of 115-7c but not with OGD alone (**Fig. 12B**). Treatment with 115-7c can therefore increase luciferase refolding and drive expression of a key-folding molecule, HOP, while untreated neurons are unable to maximize endogenous folding capabilities.

Protein oxidation and poly-ubiquitination decrease following mild bioenergetic stress when protein folding is promoted

Mild OGD alone increases the amount of proteins with carbonyl adducts that could benefit from refolding and levels of these endogenous substrates decrease with 115-7c treatment (**Fig. 13A**). While the mono-ubiquitin pool remains steady across conditions, poly-ubiquitinated proteins increase 24 hours following 15 minute OGD. Treatment with 115-7c

returns the poly-ubiquitinated protein pool back to baseline levels, comparable to untreated control (**Fig. 13B**). These data are also confirmed using immunocytochemistry. The intensity and localization of poly-ubiquitinated proteins appear similar between untreated controls (**Fig. 13C**) and 15 minute OGD neurons treated with 115-7c when neurons are stained for Fk2 (magenta), MAP2 (green) and DAPi (blue) (**Fig. 13E**). In neurons treated with 15 minute OGD alone, increased Fk2 staining can be visualized within the soma and in neuronal processes (**Fig. 13D**). Taken together, these data show that protein oxidation and subsequent ubiquitination of endogenous protein substrates resulting from mild stress can be restored to baseline levels by augmenting protein refolding capabilities using 115-7c.

115-7c promotes the refolding of key Krebs cycle intermediates to maintain neuronal bioenergetic profiles

Proteomics data of our *in vivo* tMCAO model revealed a high level of changes associated with neuronal bioenergetic proteins. That is, 16 of the 83 proteins that decreased greater than 2 fold and seven of 95 of the proteins with significantly increased expression have key roles in maintaining neuronal energetics. Based on these proteomic 'hits' in **Figure 14A**, we hypothesized that Krebs cycle enzymes that are decreased with ischemia would be first-line indicators of damage and may be preferentially refolded in the presence of 115-7c. We therefore examined the protein expression profiles of IDH3α and αKGDH in our *in vitro* neuronal model in the absence and presence of 115-7c (25μM) and the protein synthesis inhibitor, cycloheximide (CHX, 1 μM). We found that the expression of both enzymes were decreased 24 hours following 15 minute OGD, as predicted by our proteomics but were replenished by 115-7c treatment, even in the absence of new protein synthesis (**Fig. 14B**). At the 1 hour time point we observed no significant change in neuronal bioenergetics between control cultures, cultures subjected to OGD or those subjected to OGD followed by immediate

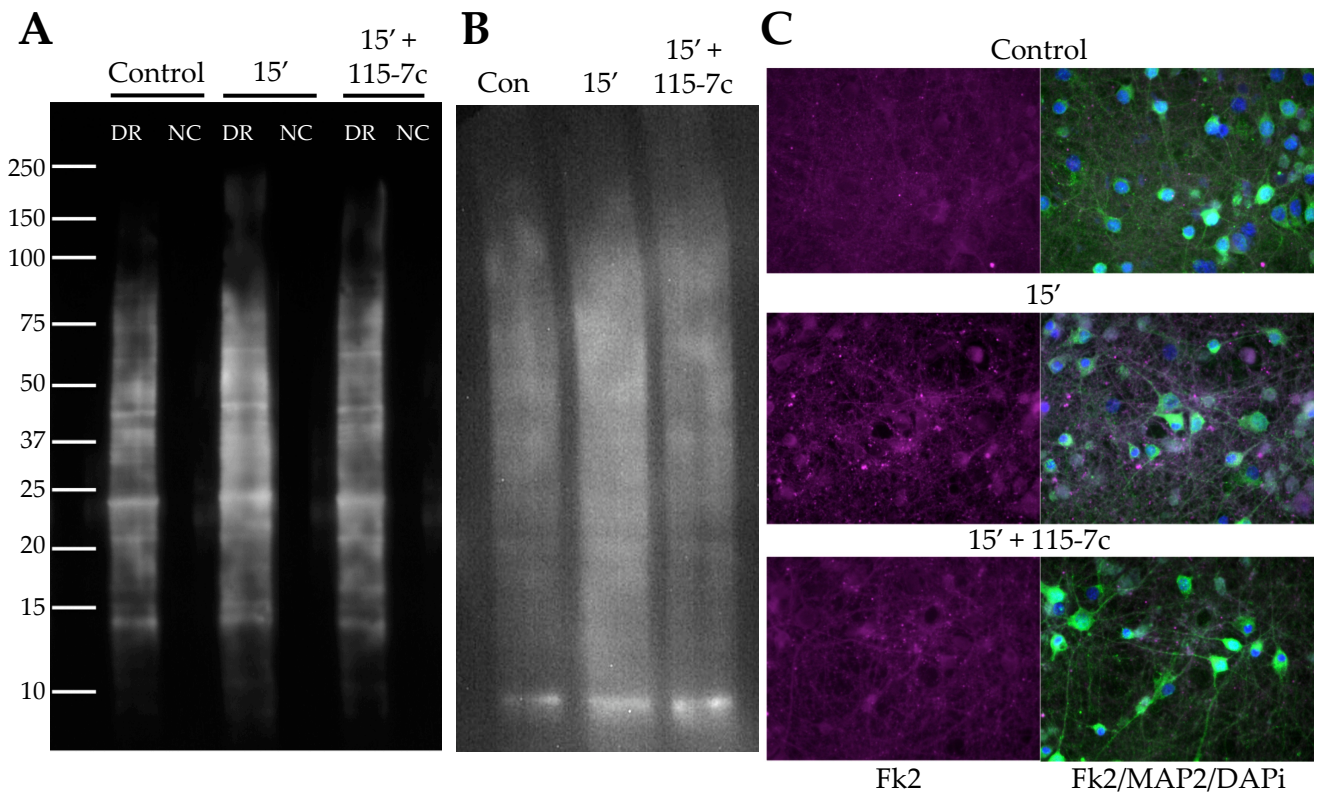

Figure 13: 115-7c decreases protein oxidation and ubiquitination *in vitro* after 15' OGD. Analysis of protein oxidation status via OxyBlot™ technology (**A**) reveals an increase in total carbonyl formation above control levels with 15' OGD that is alleviated when 115-7c is on board. Fifteen minute OGD also causes an increase in poly-ubiquitinated proteins as measured via WB for ubiquitin (**B**) that decreases to near control levels with 115-7c treatment. Notably, the mono-ubiquitin pool is not depleted in any case (band at ~8 kDa). Immunocytochemical analysis (40X) for ubiquitin (Fk2 - magenta) and DAPi (blue) reveals little to no poly-ubiquitin aggregates in control neurons (**C**) 15' OGD cultures demonstrate an increase in ubiquitin staining that can be seen near the nucleus and spreading within neuronal processes. Fifteen minute OGD neurons immediately treated with 115-7c (**E**) demonstrate decreased protein aggregation compared to 15' OGD alone. All samples were harvested or fixed 24hrs following the OGD stress and representative data comes from four independent cultures. For ICC, images, 9 fields of view were imaged from 4 separate neuronal preps and subsequent experiments, totaling 36 imaged fields per condition.

administration of 115-7c (white bars) (**Fig. 14C**). By 3 hours post-OGD (light gray bars) neurons undergo a 0.7-fold decrease in ATP while those treated with 115-7c experience a 1.7-fold increase and at 24 hours (dark gray bars) ATP levels in untreated OGD cultures rebound above controls (1.6-fold) as do those treated with 115-7c, but to a much greater extent (3.0-fold). These data suggest that essential, early components of the Krebs cycle

undergo a rapid decrease in expression that can be overcome by addition of 115-7c and that this rescue allows neurons to better maintain their bioenergetics status in response to a mild ischemic event.

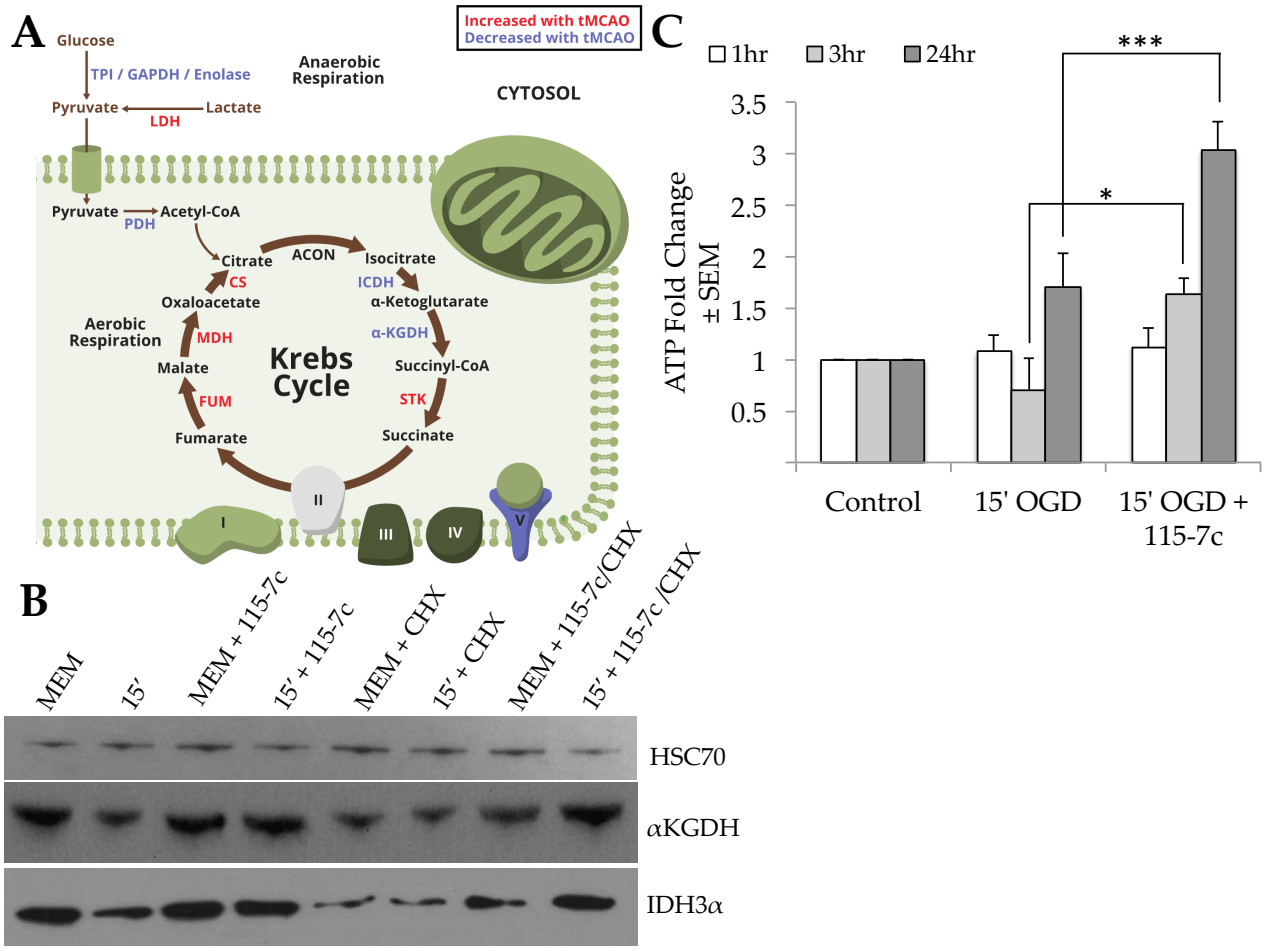

Figure 14: 115-7c promotes the refolding of IDH3α and αKGDH, positively impacting neuronal bioenergetics following 15' OGD. A schematic diagram depicting proteomic hits (**A**) identifies novel molecules closely related to neuronal energetics that undergo expression changes (at least 2 fold) 48hrs following a 10 minute tMCAO in comparison to control rat brains. Decreases in key Krebs cycle intermediates (IDH3α and αKGDH) identified by our proteomics screen were corroborated via WB analysis in our *in vitro* model of 15' OGD (**B**). Expression of these proteins is rescued when 115-7c is onboard in the presence of cycloheximide (CHX) demonstrating that increased expression is the result of protein refolding as opposed to new protein synthesis. Bioluminescent reporter assays of intracellular ATP levels (**C**) reveal no significant change between control cultures, cultures subjected to OGD or those subjected to OGD followed by administration of 115-7c 1hr following the neuronal stress (white). 3hrs following OGD (light gray), neurons subjected to OGD without treatment undergo a roughly 0.5 fold decrease in ATP, while those treated with 115-7c experience a 0.5 fold increase in ATP levels. At 24hrs (dark gray), ATP levels in untreated OGD cultures rebound above controls (1 fold) as do those treated with 115-7c, but to a much greater extent (3 fold). All data was compiled from four independent cultures and subsequent assays and was analyzed via one-way ANOVA with Tukey's *post hoc* testing where $p < 0.05$ = * and $p < 0.001$ = ***.

Preconditioning neuroprotection increases in the absence of new protein synthesis when protein folding is promoted

We hypothesized that the sustained bioenergetics profile afforded by 115-7c treatment following OGD would augment the neuroprotective effects of PC by alleviating the typical early decrease in ATP levels (Brown, 2010; Zeiger, 2010). For these experiments, 115-7c and/or CHX was added to primary neuronal cultures immediately following a 15 minute OGD, followed 24 hours later by a lethal, 90 minute OGD. Live cell images, cell counts and LDH assays were then performed 24 hours later. Control neurons (**Fig. 15A**) and neurons subjected to 15 minute OGD (**Fig. 15B**) are virtually indistinguishable with phase bright soma and extensive neuronal networks that were completely abolished in neurons subject to 90 minute OGD (**Fig. 15C**). Preconditioned neurons demonstrate some phase bright soma and intact neuronal processes as well as some somal shrinkage and blebbing (**Fig. 15D**) which are alleviated when 115-7c is present as neuronal processes again appear to be indistinguishable from untreated controls (**Fig. 15E**). A 21.2% increase in cell survival resulted when neurons were preconditioned and 115-7c was administered (**Fig. 15H –** diagonal hash versus horizontal hash) as assessed by LDH assay. As expected, the PC effect was lost when neurons were treated with CHX (**Fig. 15F & H**) but concomitant treatment of 115-7c and CHX alleviates the need for new protein synthesis and neurons are again able to undergo preconditioning (**Fig. 15G & H**). Taken together, we have developed a model (**Fig. 16**) in which protein refolding is an endogenous response to mild OGD that can be augmented by the addition of HSP70 modulators that further promote the folding activities of the complex. Driving this expression allows neurons to refold ischemia-damaged proteins, particularly and perhaps preferentially, those important for maintaining energetics such as IDH3α and αKGDH, key players in the Krebs cycle. All of these actions together result in increased neuroprotection from OGD in the presence of a pro-folding compound that is

administered after an ischemic event. These data speak to the clinical relevance of this type of therapeutic and the need for further studies.

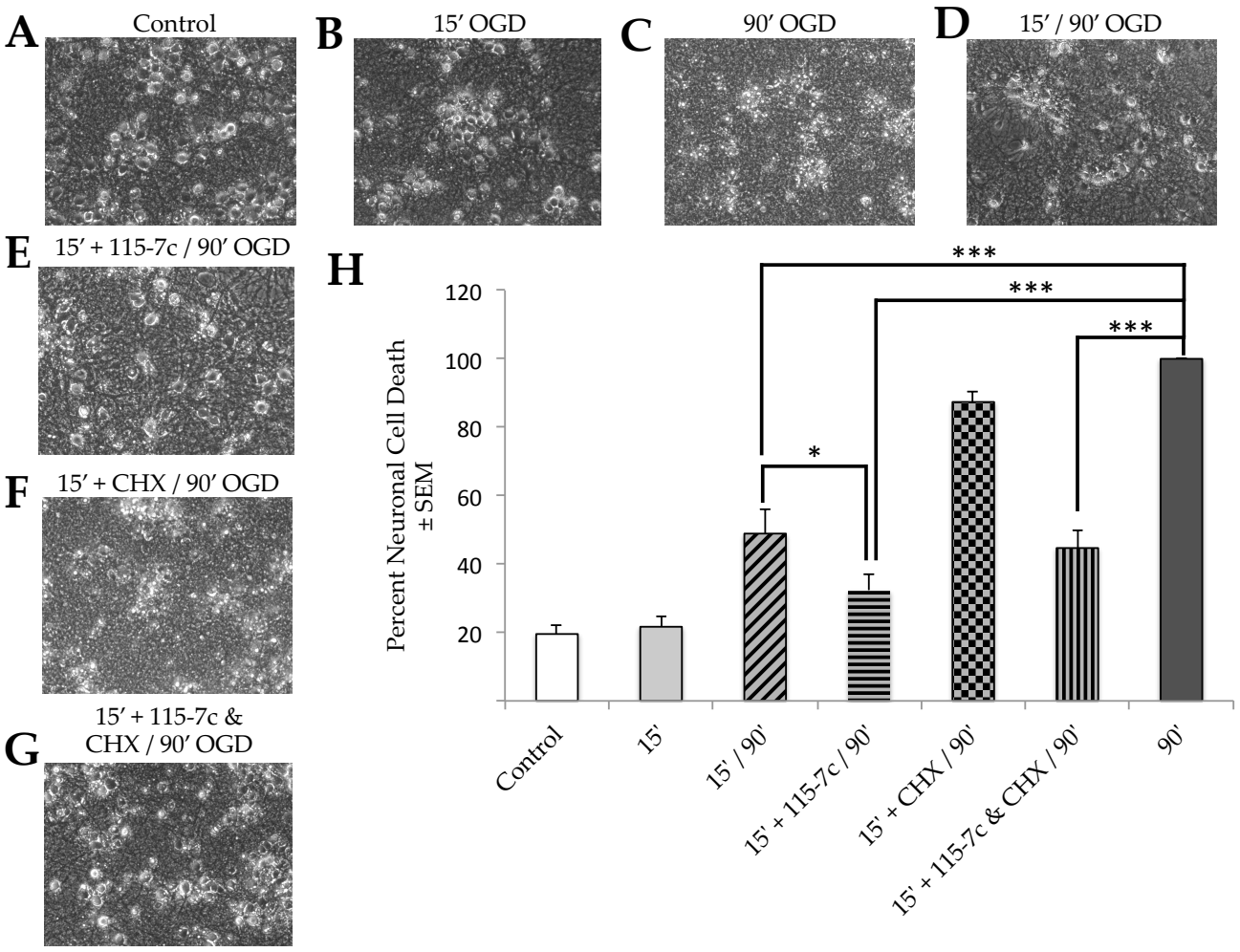

Figure 15: The pro-folding compound 115-7c augments neuroprotection in an *in vitro* model of PC independent of new protein synthesis. Control (**A**) and 15' OGD (PC) neurons (**B**) are virtually indistinguishable, demonstrating phase bright somas and extensive neuronal processes in comparison to 90' (lethal) OGD neurons (**C**) which exhibit somal shrinkage and devastation of the neuronal network. Live cell images of cultures exposed to 15' PC OGD 24hr prior to 90' OGD in the absence (**D**) or presence (**E**) of 115-7c reveal a population of surviving neurons with phase bright somas and intact neuronal connections. Treatment with CHX results in somal shrinkage and a discontinuous neuronal network (**F**) while co-treatment with 115-7c and CHX (**G)** results in cultures indistinguishable from controls. Lactate dehydrogenase assays (**H**) demonstrate that 15' PC OGD is non-toxic, 90' OGD alone is lethal and PC prior to 90' OGD decreases neuronal cell death by roughly 50%. PC neuroprotection is augmented an additional ~20% by treatment with 115-7c. The protein synthesis inhibitor, cycloheximide (CHX) blocks the neuroprotection typically seen with PC but concomitant treatment with 115-7c is able to overcome this loss of protection. Data were compiled from 5 independent cultures and experiments and subjected to one-way ANOVA analysis with Tukey's post hoc testing where $p < 0.05$ = * and $p < 0.001$ = ***.

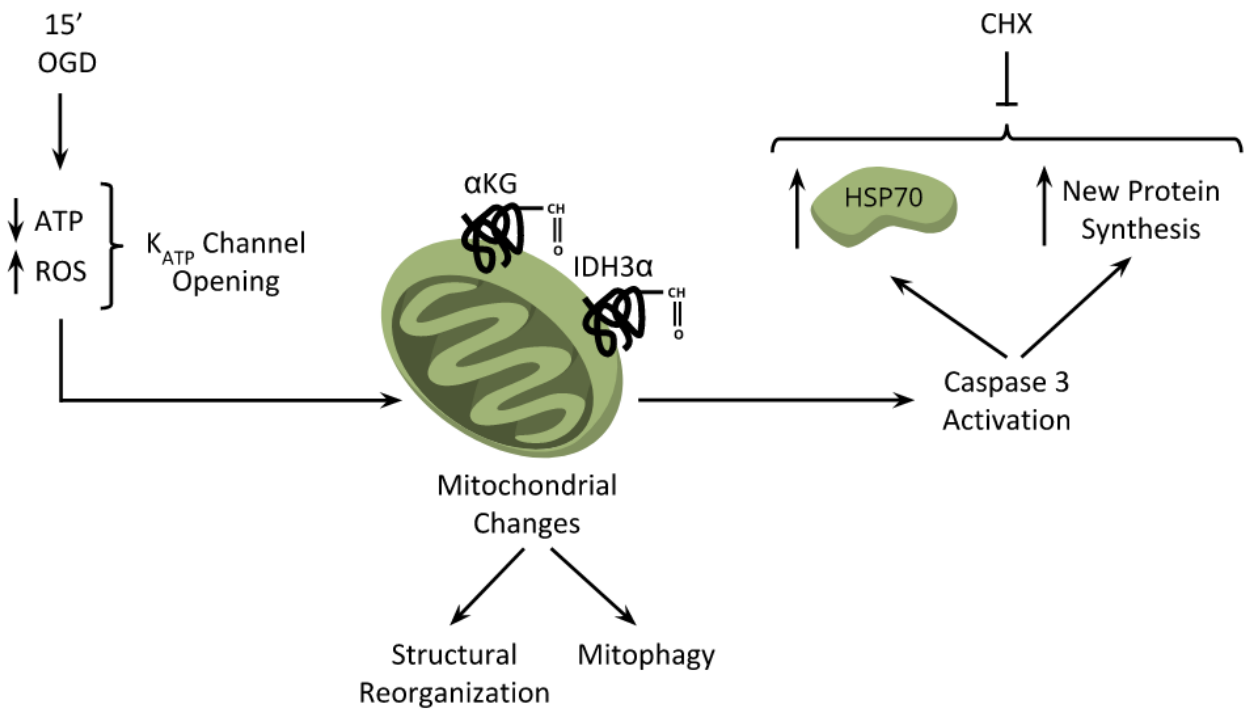

Figure 16: Overall Schematic. The protein refolding compound, 115-7c increases neuronal survival following OGD by rescuing damaged mitochondrial proteins which affords maintenance of neuronal bioenergetic status. In addition, 115-7c can overcome the loss of the preconditioning hallmark of increased new protein synthesis perhaps by instead fueling neurons with properly refolded proteins put on hold during times of stress.

3.5 Discussion

The protective effect of preconditioning has historically been thought to require increased HSP70 expression (Barone, 2004; Barone, 1998; Tirapelli, 2010), K_{ATP} channel opening (Cohen, 2000; Tani, 2001; Teshima, 2003), caspase 3 activation (McLaughlin, 2003), ROS formation (Ravati, 2000) and new protein synthesis (Burda, 2003; Matsuyama, 2000; Rowland, 1997). Our ability to leverage these pathways to evoke well-tolerated protection in the context of hypoxia and ischemia has been limited by a lack of understanding of the primary role of chaperone proteins in PC as well as a dearth of reagents that can specifically modulate chaperone activity.

Here we show that driving chaperone-mediated protein refolding augments PC neuroprotection in the absence of new protein synthesis. The HSP70 complex can either degrade or refold client proteins dependent upon cellular bioenergetics and the co-chaperones with which HSP70 interacts (Hohfeld, 2001; Zuiderweg, 2017). HSP70 itself forms the backbone of this triage complex, interacting with a number of co-chaperones to dictate protein fate. For example, when bound to the co-chaperones CHIP and BAG1, the HSP70 chaperone machinery targets client proteins for proteasomal degradation. When interacting with HIP and HOP, client proteins instead undergo refolding. The fate of HSP70 client proteins also depends upon ATP binding, duration of substrate interaction and strength of substrate affinity (Zuiderweg, 2017).

In this study, we find that endogenous protein refolding increases rapidly in response to OGD, but drops precipitously after 3 hours. We have previously reported that the 3-hour time point is also that of maximal ATP/ADP depletion in response to ischemic preconditioning. These data are consistent with the decrease we observe in the rate-limiting enzymes of the Krebs cycle, IDH3a and aKGDH. Other factors that might limit refolding, such as diminished HOP expression were not observed in either the *in vitro* or *in vivo* PC models.

By driving the refolding activity of the chaperone complex with the pro-folding agent, 115-7c, we observe decreased protein oxidation and poly-ubiquitination and increases in neuronal survival even in the absence of new protein synthesis. These data support the importance of developing short acting pharmacological tools to improve neuronal survival in response to acute CNS injuries.

These data are interesting in that other HSP70 modulators have been shown to compete with co-chaperones. For example, YM-01 outcompetes HIP for binding to the complex (Abisambra, 2013; Fontaine, 2015) while 115-7c appears to work cooperatively with HOP allowing more protein substrates to undergo refolding following OGD. These data are

further supported by previous work by Howarth and colleagues who demonstrated that overexpression of HIP alleviated inclusion formation in *in vitro* models of Spinal Bulbar Muscular Atrophy and polyQ expansion disease by facilitating the refolding cycle of the HSP70 complex (Howarth, 2009). In these studies, it is important to note that the beneficial effects of refolding are not observed unless there is also an increase in HSP70, again suggesting that temporal expression of the chaperone is key.

Because refolding is heavily dependent upon energetics, we examined ATP levels in the presence or absence of 115-7c and found that preconditioned neurons do not undergo the previously described early drop in ATP levels (Brown, 2010; Kalogeris, 2012; Zeiger, 2010), but instead maintain ATP at levels higher than baseline even at 24 hours. We sought to understand the ATP levels by referencing proteomic data of rats that were exposed to tMCAO. Validation of our proteomic data via WB analysis demonstrates that in the presence of 115-7c, the expression of proteins essential to energetic status are increased, suggesting that they may be preferentially refolded during ischemia in order to maintain energetics. Reports of mitochondrial IDH (Yoshida 2014) and α-KGDH (Humphries, 2006; Shi, 2011) undergoing oxidative or nitrative modifications and subsequent inactivation, combined with studies demonstrating target-focused refolding of proteins with oxidation events on cysteine residues (Sardiu, 2007), further support this hypothesis. In this case, ischemia-damaged proteins are refolded as opposed to having to be generated *de novo,* utilizing neuronal energetics and resources. Importantly, the neuroprotective effect of 115-7c was observed in the presence of cycloheximide, a protein synthesis inhibitor supporting a model whereby promoting protein recycling evokes both immediate and long-lasting changes in chaperone complex activity. These data support a model whereby preferential refolding of ischemia-damaged mitochondrial client proteins essential for maintaining neuronal energetics results in increased survival.

The literature robustly demonstrates the benefits of promoting client protein degradation in chronic models of neurodegeneration (Abisambra, 2013; Fontaine, 2015; Howarth, 2009; Jinwal, 2013; Jinwal, 2009; Kilpatrick, 2013; Wang, 2013). Yet until now, these compounds have been untested in the context of an acute event such as an ischemic stroke. In chronic model systems, increases in protein aggregates, whether of a-synuclein, Tau, or HTT, may result in a preference for protein degradation in these environments where persistent aggregation renders proteins insoluble and no longer viable substrates for refolding. While an acute ischemic event also results in protein aggregation (Hu, 2001) [29], these aggregates may still be salvageable and therefore protein refolding still an option.

A pharmacological modulator that can enhance neuroprotection following a mild ischemic event is especially exciting in regards to treating patients who experience a TIA. While transient ischemic attacks are known to result in the upregulation of endogenous protective pathways, this protection is short-lived and a TIA often precedes a large-scale stroke (Wu, 2007). There are currently no neuroprotective therapeutics offered to high-risk stroke patients who have suffered a TIA. The data presented here suggest that introducing a profolding compound following an acute ischemic event may improve outcome for this patient cohort. In addition, and of particular interest when thinking of these compounds as therapeutics, is our finding that administration of 115-7c as late as 6 hours following a moderate (30 minute) ischemic insult still provides significant neuroprotection for up to at least 72 hours (**Fig. 17A & B**). More studies of this nature are essential since there is only one FDA approved drug (tissue plasminogen activator: tPA) currently available for ischemic stroke. Of the patients eligible to receive tPA, less than 5% do (Adeoye, 2011) mainly as a result of the small window of effectiveness, with administration within 3 to 4.5 hours of stroke onset (Cheng and Kim, 2015).

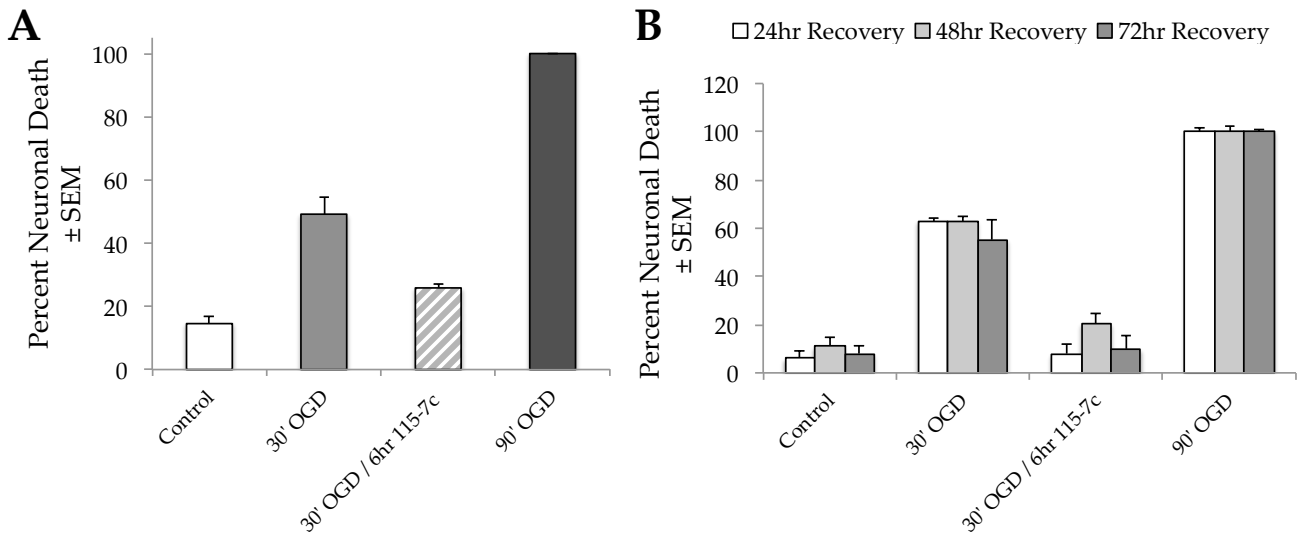

Figure 17: Administration of 115-7c exceeds the current standard of IV tPA. 115-7c can be administered 6hrs following OGD and still result in increased viability as measured by LDH release 24hrs post-treatment (**A**). The beneficial effect of administering 115-7c 6hrs following OGD can still be seen as far out as 72hrs in terms of neuronal viability (**B**).

CHAPTER 4

SUMMARY

Increased HSP70 expression in response to OGD has been well established, yet the role of the chaperone machinery and the precise activities employed by this complex to ensure neuronal survival following an ischemic event remain unknown and were the main goals of this thesis work.

4.1 CHIP Relocalizes to Damaged Mitochondria

HSP70 and CHIP expression are increased in human post-mortem samples from patients whom had suffered from a TIA or stroke (Stankowski, 2011). These increased expression profiles can be recapitulated in a highly reproducible *in vitro* model system. Using primary forebrain neuronal cultures subjected to OGD, we found that indeed both HSP70 and CHIP are increased in a time-dependent fashion following a lethal ischemic event (Palubinsky, 2015). Using immunocytochemistry we also discovered, for the first time, that CHIP relocates from the cytosol to damaged mitochondria following acute stress where it acts as an essential mediator of redox tone and energetics (Palubinsky, 2015).

Once at the mitochondria, CHIP associates with LC3-II labeled mitochondria providing the first data that it may be essential for the removal of damaged mitochondria from the cellular milieu via mitophagy. Further studies in the McLaughlin lab by Dr. Britney Lizama revealed that in the context of ischemic preconditioning, loss of CHIP not only prevents mitophagy but also negates the neuroprotective responses of PC all together (Lizama, 2018).

The literature provides a strong connection between mitochondrial dysfunction and neurodegeneration (Beal, 2003; Burchell, 2010; Burchell, 2010; Cozzolino, 2013; Cui, 2006; Johri and Beal, 2012; Khandelwal, 2011). As such, we continued to focus on the link between

CHIP and the mitochondria. Utilizing whole brains from WT, Het and CHIP KO mice, we were able to show that loss of CHIP results in severe mitochondrial deficits including: energetic scarcity (decreased ATP:ADP), insufficient antioxidant response (decreased GSH:GSSG), an inability to properly respond to calcium challenge and homeostatic imbalance of key mitochondrial proteins (example: increased expression and subsequent oxidation of Drp1) (Palubinsky, 2015).

4.2 Loss of CHIP is Detrimental to a Host of Cellular Processes

In addition to severe gross physiological and motor impairments, cardiovascular abnormalities, stress sensitivity and early lethality observed in CHIP deficient animals (McLaughlin, 2012; Min and Patterson, 2011; Palubinsky, 2015), our data provides molecular evidence for increased protein oxidation and lipid peroxidation in brain, deficits in bioenergetics and antioxidant response mechanisms and mitochondrial failure (Palubinsky, 2015). To further uncover the relationship between loss of CHIP and these molecular insufficiencies, we have established 3 proteomic libraries (**Figure 18 & Table 1**).

The first encompasses all proteins that are differentially expressed based on the presence or absence of CHIP (WT vs CHIP KO mouse brain), many of which are involved in bioenergetics and mitochondrial quality control (Lizama, 2018; Lizama, 2018). The second library contains brain proteins that are oxidatively modified in a CHIP dependent manner. And the third is a library specifically composed of mitochondrial proteins that are oxidatively modified in a CHIP dependent manner and thus provide a further link between CHIP and overall mitochondrial homeostasis (Lizama, 2018). We have also interrogated the ultrastructure of mitochondria obtained from WT versus CHIP KO mice and found that loss of CHIP increases mitochondrial number and significantly alters mitochondrial morphology (Lizama, 2018). These data correlate well with the increased expression of the pro-fission protein, Drp1, we have found in CHIP KO brain (Palubinsky, 2015).

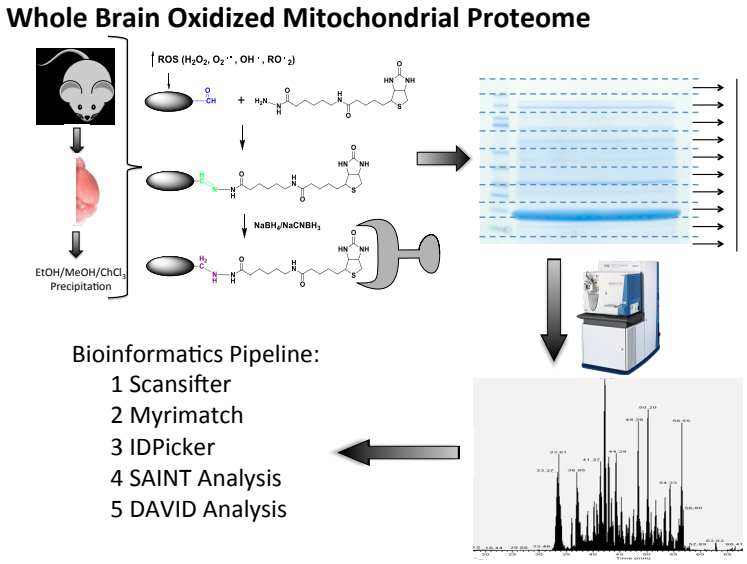

Figure 18: Generation of Whole Brain & Oxidized Mitochondrial Proteomes. Brains from PND35 WT and CHIP KO mice underwent lipid extraction followed by mitochondrial isolation. Mitochondrial lysates were then subjected to biotin avidin capture of oxidized species. Following pull-down, oxidized proteins were separated via gel electrophoresis. Peptides were extracted from the gel, tryptically digested and analyzed by MS.

Table 1

Oxidized Proteins	
Neurodegenerative Diseases: Parkinson's/Huntington's/Alzheimer's/ALS	
ATP-Synthase	Voltage Dependent Anion Channel 1 *
ADP/ATP Translocase	Voltage Dependent Anion Channel 2
Ubiquinol-Cytochrome C Reductase	Voltage Dependent Anion Channel 3 *
NADH Dehydrogenase	Fused in Sarcoma *
Succinate Dehydrogenase	Dynamin Related Protein 1
Hydroxysteroid Dehydrogenase	Parkin
Clathrin	Superoxide Dismutase 1 *
Adenine Nucleotide Translocator *	Superoxide Dismutase 2
Metabolism and Energetics: Krebs Cycle/Oxidative Phosphorylation/Glycolysis	
Aconitase	Alpha Ketoglutarate Dehydrogenase
Citrate Synthase	Isocitrate Dehydrogenase 1 *
Fumarate Dehydrogenase	Isocitrate Dehydrogenase 2 *
Malate Dehydrogenase	Isocitrate Dehydrogenase 3
Succinate Dehydrogenase	Pyruvate Dehydrogenase
Aldehyde Dehydrogenase	Pyruvate Carboxylase
Lactate Dehydrogenase	Glucose-6-phosphate Isomerase
Fumarate Hydratase *	Hexokinase 2 *
Cytochrome c Oxidase IV	Fatty acid synthase *
Glycerol-3-phosphate Dehydrogenase	
Antioxidants: Production and Degradation	
Glutamate Dehydrogenase	Glutathione S-transferase

Acetyl-coA Acyltransferase	Glutathione peroxidase 1
Carbamyl-phosphate Synthetase	Peroxiredoxin (1 through 6)
Glutamate Oxaloacetate Transaminase	Thioredoxin *
Aminobutyrate Aminotransferase	All-trans-retinol 13,14-reductase
Alanine-Glycoxylate Aminotranferase	Glutamic Pyruvate Transaminase
Arginosuccinate Synthetase	
Oxidized Proteins Continued	
Chaperone Response / Ubiquitin Proteasome System	
Protein Disulfide Isomerase	Chaperonin *
Peptidylprolyl Isomerase	Cullin 3 *
Hypoxia Upregulated Protein	Heat Shock Protein 5
Leucine Aminopeptidase	Heat Shock Protein 8
Ubiquitin	Heat Shock Protein 27
Ubiquitin Specific Peptidase *	Heat Shock Protein 10 *
Ubiquitin-conjugating enzyme E2L	Heat Shock Protein 40
Ubiquitin-conjugating enzyme E2N	Heat Shock Protein 60
Ubiquitin-like activating enzyme 1 *	Heat Shock Protein 70 *
Proteasome Subunit alpha 6 *	Heat Shock Protein 75 *
Proteasome Subunit beta (5-7) *	Heat Shock Protein 90 alpha
Proteasome 26S subunit (1,2,3,5 and 6) *	Heat Shock Protein 105/110 *
Microtubule-associated Protein 1A	Microtubule-associated Protein 1B
Calcium Signaling	
Neurocalcin *	ATPase, Ca^{++} Transporting Protein *
Ca^{++}/calmodulin-Dependent Protein Kinase	Calmodulin 1 Phosphorylase Kinase
Calbindin 2	Calnexin *
S100 Calcium Binding Protein *	Solute Carrier 8 (Na^{++} /Ca^{++} Exchanger)
Ca++-dependent Secretion Activator	
Synaptic Proteins and Neurotransmission	
Neural Cell Adhesion Molecule 1 *	Syntaxin
Synaptotagmin	Synaptophysin
Other Proteins of Interest	
Programmed Cell Death Interacting Protein	Translocase of Outer Mito Membrane 70
Neural Cell Adhesion Molecule 2	Optic Atrophy 1 *
Doublecortin-like Kinase 1 *	Glia Maturation Factor
Estradiol Dehydrogenase	Protein Kinase C

4.3 To Fold or Not to Fold

While increased chaperone expression is a common response to injury (Liu, 2005; Magrane, 2004; McLean, 2004; Wang, 2013), important gaps remain in our understanding of which chaperone-mediated activities would be most beneficial to neuronal survival following

an ischemic event. By monitoring protein dynamics following an ischemic stress, we find that the endogenous neuronal response is to refold ischemia-damaged proteins.

These findings were particularly interesting to us in that our previous data demonstrating increased CHIP expression would support a model in which protein degradation is favored. However, if we take into account the extremely broad range of activities that CHIP has the potential to participate in (Joshi, 2016) and the fact that following stress CHIP relocalizes to the mitochondria (Lizama, 2018; Palubinsky, 2015), it may be that upregulation of this vital protein has more to do with maintaining mitochondria than participating in chaperone duties, particularly in an environment of acute stress.

By utilizing newly developed small molecule modulators of HSP70 for the first time in the setting of an acute neuronal stress, we were able to determine that promoting the refolding of ischemia-damaged proteins significantly increases neuronal survival. Additionally, by analyzing the expression profiles of the chaperone machinery in response to treatment with a profolding drug, we were also able to identify new potential targets for therapeutic intervention, which is the focus of the following chapter.

CHAPTER 5

FUTURE DIRECTIONS

1) Specific Aims

A major consequence of ischemia is neuronal protein damage that can overwhelm the essential protein triage unit, the HSP70 molecular chaperone complex. The aim of this proposal is to further understand the role of protein refolding in response to ischemia.

Specific Aim I: Determine a treatment paradigm that results in maximal neuroprotection and the corresponding protein profile of the HSP70 chaperone machinery. Proteasomal inhibition has been shown to be beneficial in the context of ischemia. Our preliminary data are in agreement, demonstrating that the addition of the pro-folding compound (115-7c) following OGD increases neuronal survival (**Figure 10C**). We hypothesize that co-treatment with the proteasomal inhibitor (lactacystin) and 115-7c will further augment neuronal survival and that the expression profiles of the major HSP70 chaperone complex components will be altered to reflect an adaptive survival response.

Aim 1A: Assess neuronal survival following OGD in the presence of a proteasomal inhibitor and a pro-folding compound. In this aim we will subject mature, primary neuronal cultures to mild OGD followed by the administration of the proteasomal inhibitor, lactacystin, the pro-folding compound, 115-7c or both. Lactate dehydrogenase (LDH) released from dead and dying neurons will be measured to assess neuronal survival in the absence versus presence of compound(s).

Aim 1B: Determine changes in the expression of the HSP70 molecular chaperone complex in response to OGD in the presence of lactacystin and/or 115-7c. Primary neuronal cultures will be subjected to mild OGD followed by the administration of lactacystin, 115-7c or both during a 24hr recovery period. Western blot samples will be harvested and proteomics run to determine changes in the protein profiles of the major components of the HSP70 chaperone complex including, HSP70, HSC70, HSP90, HSP40, CHIP, BAG1, HIP and HOP.

Specific Aim 2: Determine the real-time metabolic and folding profiles of neurons following OGD in a pro-folding environment. OGD results in significant changes in neuronal energetics that, in turn, can affect the co-chaperones with which the HSP70 complex interacts. Our preliminary data demonstrate that post-OGD treatment with 115-7c allows neurons to better maintain ATP levels (**Figure 14C**). We hypothesize that in response to OGD, neurons preferentially attempt to refold, as opposed to degrade, damaged proteins because folding is more energetically advantageous.

Aim 2A: Determine the energetic profile of neurons in the presence of 115-7c. For this aim, primary neuronal cultures will be subjected to OGD in the presence or absence of 115-7c during recovery and metabolic profiles will be assessed via the Seahorse XF-24 analyzer.

Aim 2B: Determine the rate of neuronal protein refolding following oxygen and glucose deprivation. In this aim we will utilize mature, primary neurons transfected with a dual *Firefly / Renilla* luciferase reporter and subjected to mild OGD +/- 115-7c and +/-

proteasome inhibitors during recovery to track, in real time, the refolding of *Firefly* luciferase.

Specific Aim 3: Assess the neuroprotective potential and localization of HSP70 Organizing Protein (HOP). Our preliminary data demonstrate that post-OGD treatment with 115-7c results in a significant increase in the expression of the co-chaperone, HSP70 Organizing Protein (HOP) (**Figure 12B**). We hypothesize that in response to OGD, the expression of HOP is limiting for neurons that do not survive ischemic stress.

Aim 3A: Determine if overexpression of HOP is sufficient to support neuronal survival following ischemia. Neural cell lines as well as primary neuronal cultures will be transfected with a HOP overexpression plasmid prior to OGD. LDH survival assays will be completed to determine whether this overexpression results in levels of neuronal survival similar to those noted with 115-7c treatment.

Aim 3B: Assess the levels and localization of HOP in the presence or absence of 115-7c following ischemia. Neurons will be subjected to mild ischemia in the presence or absence of 115-7c during recovery. Quantum Dot labeled HOP will be visualized in order to determine changes in expression as well as localization patterns in response to ischemia.

2) Background & Significance

There is a critical need to develop better therapies to protect the brain following an ischemic event. Currently, there is only one FDA-approved treatment for ischemic stroke,

thrombolysis via administration of tissue plasminogen activator (tPA) within a very short temporal window (~3.5 hours following stroke onset). Additionally, the use of tPA is often associated with the risk of life-threatening bleeding in the brain. As such, less than 3% of ischemic stroke patients in the US are eligible to receive tPA as a treatment (Adeoye, 2011).

A major consequence of ischemic stroke is protein damage that persists well after blood flow has been restored (Stankowski and Gupta, 2011). To combat this damage, neurons rely heavily upon the Heat Shock Protein 70 (HSP70) molecular chaperone complex, which acts as a triage system influencing the fate of damaged proteins by either initiating proteasomal degradation or refolding. While depletion of HSP70 increases vulnerability to physical and environmental stressors and decreases lifespan (Daugaard, 2007; Lee, 2004), overexpression has routinely been found to provide neuroprotection (Kalia, 2010; Pratt, 2015; Shiber and Ravid, 2014). However, while overexpression can protect neurons from stroke-like injuries *in vitro*, this chronic strategy is not clinically feasible, and our lab and others have shown that long-term overexpression of HSP70 family members and co-chaperones can be cytotoxic (Shimshek, 2010; Stankowski, 2011; Tanaka, 2014; Yaglom, 2007). Therefore, to be beneficial as a therapeutic, modulation of the chaperone complex must be more refined. Our lab and others have shown that the expression of HSP70 is upregulated in human and rodent models of ischemic stroke as well as in neuronal cultures in response to oxygen and glucose deprivation (OGD) (Stankowski, 2011; Tirapelli, 2010; Turturici, 2011).

There is a large body of literature demonstrating that the activity of the proteasome is impaired during ischemia as a result of decreased energy availability (Ge, 2007; Keller, 2000; Stankowski, 2011). These data together with the fact that proteasomal inhibition is beneficial in ischemic model systems (Kandilis, 2014; van Leyen, 2005) support a hypothesis whereby

increased HSP70 expression following OGD may play an important role in the refolding of damaged proteins and suggests that refolding may be more energetically favorable than proteasomal degradation during times of limited ATP. Our colleague, Dr. Jason Gestwicki, has recently developed specific allosteric modulators of the HSP70 complex that can either promote protein refolding or degradation (Jinwal, 2013; Li, 2013; Miyata, 2013). Utilizing these compounds alone or in combination with proteasomal inhibitors already available and in use in the clinic for other disorders (Kandilis, 2014), we aim to uncover the mechanisms of this substantial neuroprotection and leverage these findings to develop more efficient and practical therapies for stroke.

To define the neuroprotective potential of the chaperone complex we will leverage the power of highly-reproducible models of OGD that have been used extensively by our lab and others to demonstrate an essential role of chaperones in stroke biology. Briefly, primary cortical neurons will be grown in culture until they express the proper complement of NMDA receptor subunits necessary for ischemic excitotoxicity (DIV20-25). Once mature, these neurons will be subjected to OGD in the presence or absence of the HSP70 modulator and profolding compound, 115-7c during recovery and then used for biochemical analyses. Our lab has used these cultures for roughly 20 years to model chaperone dysfunction, excitotoxicity, oxidative stress and developmental changes in vulnerability to environmental and genetic dysfunction. This rigorous and reproducible model maximizes future success in moving from *in vitro* to *in vivo* testing.

3) Preliminary Studies

The overall goal of this research program is to further understand role of the HSP70 chaperone complex in mediating protein refolding in response to ischemia in order to

determine whether targeting this chaperone activity via neurotherapeutics is a potential new avenue for stroke treatment. Preliminary data demonstrate that neurons exposed to varying durations of OGD have increased survival when the HSP70 modulator/profolding compound, 115-7c, is administered following the ischemic insult (**Figure 10C**). In Aim 1, we will administer 1.) The proteasomal inhibitor lactacystin, which has also been shown to improve neuronal survival in the face of ischemia, (Kandilis, 2014) 2.) 115-7c or 3.) A combination of lactacystin and 115-7c to determine which compound or combination results in maximal neuroprotection. Additionally, we will analyze time courses of the expression of the HSP70 chaperone complex components via Western blot and proteomics across treatment conditions in order to correlate maximum neuroprotection with a corresponding protein expression profile. These experiments will allow us to identify the components of the chaperone machinery that change in response to OGD when a profolding environment is favored.

In addition to the increased neuronal survival observed with post-OGD administration of 115-7c, our preliminary data also suggests that when this profolding compound is on board, neuronal ATP levels are better maintained (**Figure 14C**). Depletion of ATP during OGD results in ion gradient and mitochondrial dysfunction, membrane depolarization, significant calcium influx and ultimately, excitotoxicity (Martin, 1994). Much research has focused on ways to prevent or limit ATP loss during ischemia as well as ways to enhance the recovery of ATP following ischemia (Galeffi, 2000). Given that 115-7c does just this, suggests that perhaps the profolding environment is more energetically favorable than that of degradation. In Aim 2 we propose to investigate this hypothesis further by generating complete metabolic profiles of neurons subjected to OGD in the presence or absence of 115-

7c using a Seahorse XF-24 analyzer. Simultaneous experiments will be carried out on sister neuronal cultures transfected with a dual *Firefly / Renilla* luciferase reporter plasmid which will allow us to track protein refolding in real time. Correlations can then be made regarding the amount of refolding that is occurring and the energetic profile during those same specific time points.

While we know that some amount of protein refolding occurs following OGD, being able to identify a chaperone component(s) that is both sufficient and essential for this process and in turn the neuroprotection noted could be a paramount finding. Our preliminary data (**Figure 12B**) demonstrate that a 24hr treatment with 115-7c after a mild OGD (50% neuronal survival and 50% neuronal death) results in a significant increase in the expression of the co-chaperone, HOP. Intriguingly, levels of HOP are unchanged between control and mild OGD treatments where we also see no significant increases in folding (**Figure 12A**). These data suggest that increasing HOP may be essential for the neuroprotection afforded by refolding. To test this, in Aim 3 we plan to overexpress HOP without addition of compound and see if overexpression alone can increase neuronal survival following ischemia. This type of protection has been seen in chronic neurodegenerative models (Song, 2009; Wolfe, 2013), however it has not been assessed in models of acute stress such as ischemia. Notably, loss of HOP has also been shown to increase susceptibility to stress and decrease lifespan in *C. elegans* (Song, 2009) suggesting this protein is essential for overall survival. Lastly, we plan to determine the localization of HOP using Quantum Dot technology which will allow for 3D reconstruction of neurons and superior morphological and spatiotemporal resolution above that of typical immunocytochemistry (Tokumasu and Dvorak, 2003). These experiments are essential in that where HOP localizes intracellularly following OGD with or without 115-7c on

board can provide insight into the mechanisms of protein refolding that neurons undergo in response to ischemia. Our lab has recently found that the E3 ligase, C-terminus of HSP70 Interacting Protein (CHIP), another HSP70 co-chaperone, relocalizes to the mitochondria following OGD where it plays a role in autophagic processing of damaged organelles (Palubinsky, 2015). If CHIP is important for removing damaged mitochondria, perhaps HOP is responsible for maintaining (via refolding) mitochondrial proteins that allow for the maintenance of bioenergetics noted when HOP expression is increased.

In spite the impressive neuroprotective potential of many of the HSP70 family members, major disparities still exist in our understanding of chaperone biology that limit our ability to develop practical therapies that capitalize on this system. This program aims to gain a clearer understanding of these molecules in the context of a protein profolding environment. Given the critical balance of HSP70 and its co-chaperones in mediating protein triage, and subsequently cell survival, we hypothesize that the changes we uncover will be essential to understanding protective pathways in response to ischemia.

4) Research Design & Methods

Specific Aim I: Determine a treatment paradigm that results in maximal neuroprotection and the corresponding protein profile of the HSP70 chaperone machinery.

Rationale: Following OGD, both proteasomal inhibition and compounds that promote damaged protein refolding have been found to be neuroprotective, yet a combination therapy has not yet been assessed as specific HSP70 modulators have only recently become available. Our goal is to test if this combinatorial treatment can potentially augment the positive impact these singular compounds have on neuronal cell fate and to determine the

expression profiles of the HSP70 chaperone machinery under conditions of maximal neuroprotection.

Strategy: We will utilize neuronal cultures exposed to 30' OGD for these studies. Primary cultures will be prepared from embryonic day 18 Sprague-Dawley rats as previously described (Palubinsky, 2015). Briefly, cortices will be digested in trypsin and dissociated. Resultant cell suspensions will be adjusted to 750,000 cells/mL and plated. OGD experiments will be conducted 20-25 days following dissociation at which time neurons express the mature complement of NMDA receptors necessary for proper excitotoxicity in response to ischemia (Sinor, 1997). To induce ischemia, cultures will be moved into glucose-free Earle's balanced salt solution bubbled with nitrogen to deplete O_2 and sealed in a humid 37^{o}C anaerobic chamber. At the termination of OGD, cells will be returned to glucose replete media in the presence of the proteasomal inhibitor, lactacystin, the pro-folding compound, 115-7c or a combination of the two for the appropriate recovery periods. All experiments will be repeated from cultures prepared from *at least* four independent dissections.

Twenty-four hours following the final OGD, levels of lactate dehydrogenase (LDH) released into the culture media from dead and dying neurons will be assessed by toxicity assay. Briefly, NAD reduction to NADH via LDH results in a stoichiometric conversion of tetrazolium dye present in the buffer that can be analyzed spectrophotometrically at 490nm. In order to account for variation in total LDH content, raw LDH values will be normalized to the toxicity caused by exposure to a lethal, 90' OGD insult. Additionally, LDH results will be confirmed by visual inspection and live cell imaging of the neurons and, in several instances, quantitatively by cell counts.

Once the treatment paradigm that results in maximal neuroprotection is identified, neurons will be harvested over a time course (0, 1, 3, 6, 9, 12, 18, 24hrs) for Western blot and proteomic analysis in order to determine the expression profiles of components of the HSP70 chaperone machinery including: HSP70, HSC70, HSP90, HSP40, CHIP, BAG1, HIP and HOP. WB analysis will be carried out as previously described (Palubinsky, 2015). For proteomic analysis, we will utilize a targeted MS approach in order to quantify protein stoichiometry of the HSP70 chaperone complex (Joel D. Federspiel, 2016).

Potential Pitfalls & Alternative Strategies: We recognize that WB analysis is not quantitative, which is why we have also proposed proteomics analysis via mass spectrometry. Our lab has collaborated extensively and I have trained with Dr. Dan Liebler in order to carry out these experiments although I have not yet delved into the light and heavy labeling for PRM, I am excited to learn this powerful new technique.

Summary: Upon completion of Aim 1, we will have 1) determined a post-OGD treatment paradigm that results in maximal neuroprotection and 2) quantitatively determined the composition and expression profiles of the HSP70 chaperone machinery that correlate with maximal neuroprotection.

Specific Aim 2: Determine the real time metabolic and folding profiles of neurons following OGD in a pro-folding environment.

Rationale: OGD results in significant changes in neuronal energetics (Galeffi, 2000; Martin, 1994) that, in turn, can affect the co-chaperones with which the HSP70 complex interacts (Mayer and Bukau, 2005). Our preliminary data demonstrate that post-OGD treatment with 115-7c allows neurons to better maintain ATP levels at times concomitant with increased

folding activities (**Figure 12 A & B**). While protein degradation via the proteasome and protein refolding both require ATP, it is unclear from the current literature which of these processes is most energetically favorable during times when oxygen, glucose and ultimately ATP are limiting such as during an ischemic stroke. To address this issue, we propose to utilize the power of real time metabolic profiling via Seahorse technology. In addition, we will analyze levels of protein refolding via a dual Firefly / Renilla luciferase construct. Given that 115-7c increases neuronal survival following OGD, we hypothesize that neurons preferentially attempt to refold, as opposed to degrade, damaged proteins because folding is more energetically advantageous.

Strategy: We will again take advantage of the OGD induced vulnerability of mature neuronal primary cultures for these studies as described in Aim 1. Briefly, neurons will be plated in multi-well XF24 Analyzer plates and cultured to maturity. Cultures will undergo 30' OGD plus or minus 115-7c and the oxygen consumption rate (OCR), indicative of mitochondrial respiration and the extracellular acidification rate (ECAR), indicative of glycolysis, will be analyzed every 30 minutes over a 24hr period. At the completion of analysis, neurons will be harvested and total protein content determined in order to normalize data.

For folding analysis, neuronal cultured will undergo lipid based transfection using LipoJet (SignaGen) with a dual *Firefly / Renilla* luciferase plasmid (Addgene) and GFP. Forty-eight hours later, cultures will be subjected to OGD then recovered in media plus or minus 115-7c and harvested at various time points as per Promega's Dual Luciferase Reporter Assay System. While *Firefly* luciferase is rapidly denatured and refolded as a result of OGD via the HSP70 complex (Kudo, 2008; Wisen and Gestwicki, 2008), *Renilla* luciferase remains resistant to denaturation. As such, we are able to normalize the *Firefly* luciferase activity to

the total *Renilla* luciferase present across experiments and within conditions to determine a refolding rate.

Potential Pitfalls & Alternative Strategies: We are confident that the experiments in this Aim will further our understanding of the energetics consumption involved in protein refolding processes. Both Seahorse technology and luciferase reporter assays are biologically relevant and highly sensitive tools that will allow us to assess protein triage activities that impact neuronal health. We propose to utilize Seahorse, as our preliminary data regarding ATP levels is limited in that it is only one component of the overall metabolic changes that occur following ischemic events. One issue we face is recapitulating our results when growing neurons on the XF Analyzer plates, which may or may not be compatible with the substrate we currently use. However, The VICB core at Vanderbilt, which houses the XF24 analyzer, includes on site technicians adept at troubleshooting these types of problems. In addition, we may need to reduce the number of sample readings taken over the 24hr window to prevent false results based on media withdrawal. We were also initially concerned about the poor efficiency and variability of primary neuronal transfections, which could limit our ability to detect a luciferase-refolding signal. However, in preliminary experiments (**Figure 12A**), we were able to overcome this obstacle using a combination of next generation lipid-based transfection reagents and we are consistently observing ~25% neuronal transfection efficiency which provides ample luciferase signal detection above background / untransfected neurons.

Summary: Upon completion of Aim 2 we will have 1) determined the metabolic profile of neurons when a pro-folding environment is promoted and 2) correlated the rate of folding that occurs with the energetics (ATP) available.

Specific Aim 3: Assess the neuroprotective potential and localization of HSP70 Organizing Protein (HOP).

Rationale: HOP deficiency results in increased susceptibility to stress and decreased lifespan(Song, 2009) suggesting its potential importance in response to ischemia. Our preliminary data demonstrate that OGD itself does not increase HOP levels but that post-OGD treatment with 115-7c results in a significant increase HOP expression (**Figure 12B**). As a major player in the HSP70 chaperone complex when protein folding activity is online, we hypothesize that overexpression of HOP itself may prove beneficial for neuronal survival following OGD and that its relocalization from the nucleus may be key in this protection.

Strategy: Primary neuronal cultures will be transfected with a plasmid in order to transiently overexpress HOP. These cultures will then be subjected to 30' OGD and the culture media will be analyzed via LDH toxicity assay (Described in detail in Aim 1) 24hrs later to determine if overexpression of HOP alone can promote neuronal survival, suggesting that its expression may be a limiting factor in neurons that do not survive the ischemic insult. Additionally, cultures will be subjected to mild OGD in the presence of absence of 115-7c and Quantum Dot labeled HOP will be assessed via immunocytochemistry to analyze its intracellular localization using a Zeiss Axioplan microscope equipped with an Apotome sectional slider (63X).

Potential Pitfalls & Alternative Strategies: Although we propose to use a Zeiss Axioplan microscope fit with an Apotome sectioning slider, should this resolution not be definitive enough we also have access to confocal microscopy as well as stochastic optical reconstruction microscopy (STORM) through the Vanderbilt Cell Imaging Shared Resource

(CISR), which can generate images with a 10-fold increase in resolution (detecting overlap within 20 nm).

Summary: Upon completion of Aim 3 we will have: 1) determined if overexpression of HOP is sufficient to produce levels of neuroprotection similar to those seen with 115-7c treatment, 2) determined the intracellular localization of HOP via 3D reconstruction of neurons in the presence or absence of OGD and plus or minus 115-7c.

REFERENCES

Abisambra J, Jinwal UK, Miyata Y, Rogers J, Blair L, Li X, et al. (2013) Allosteric Heat Shock Protein 70 Inhibitors Rapidly Rescue Synaptic Plasticity Deficits by Reducing Aberrant Tau. Biol Psychiatry.

Adeoye O, Hornung R, Khatri P, Kleindorfer D. (2011) Recombinant tissue-type plasminogen activator use for ischemic stroke in the United States: a doubling of treatment rates over the course of 5 years. STROKE. 42. 7: 1952-5.

Albers GW, Caplan LR, Easton JD, Fayad PB, Mohr JP, Saver JL, et al. (2002) Transient Ischemic Attack -- Proposal for a New Definition. N Engl J Med. 347. 21: 1713-6.

An L, Dani KA, Shen J, Warach S, Natural History of Stroke I. (2012) Pilot results of in vivo brain glutathione measurements in stroke patients. J Cereb Blood Flow Metab. 32. 12: 2118-21.

Anderson LG, Meeker RB, Poulton WE, Huang DY. (2010) Brain distribution of carboxy terminus of Hsc70-interacting protein (CHIP) and its nuclear translocation in cultured cortical neurons following heat stress or oxygen–glucose deprivation. Cell Stress and Chaperones. 15. 5: 487-95.

Annweiler C, Schott AM, Berrut G, Chauvire V, Le Gall D, Inzitari M, et al. (2010) Vitamin D and ageing: neurological issues. Neuropsychobiology. 62. 3: 139-50.

Assimon VA, Gillies AT, Rauch JN, Gestwicki JE. (2013) Hsp70 protein complexes as drug targets. Curr Pharm Des. 19. 3: 404-17.

Ballinger CA, Connell P, Wu Y, Hu Z, Thompson LJ, Yin LY, et al. (1999) Identification of CHIP, a novel tetratricopeptide repeat-containing protein that interacts with heat shock proteins and negatively regulates chaperone functions. Mol Cell Biol. 19. 6: 4535-45.

Barone FC. (2004) Endogenous brain protection - Models, gene expression, and mechanisms. Stroke Genomics: Methods And Reviews. 104. 105-84.

Barone FC, White RF, Spera PA, Ellison J, Currie RW, Wang X, et al. (1998) Ischemic preconditioning and brain tolerance: temporal histological and functional outcomes, protein synthesis requirement, and interleukin-1 receptor antagonist and early gene expression. STROKE. 29. 9: 1937-50; discussion 50-1.

Beal MF. (2003) Mitochondria, oxidative damage, and inflammation in Parkinson's disease. Annals Of The New York Academy Of Sciences. 991. 120-31.

Beere HM. (2004) The stress of dying': the role of heat shock proteins in the regulation of apoptosis. Journal Of Cell Science. 117. 13: 2641-51.

Beere HM, Green DR. (2001) Stress management - heat shock protein-70 and the regulation of apoptosis. Trends In Cell Biology. 11. 1: 6-10.

Bejot Y, Aboa-Eboule C, Marie C, Giroud M. (2011) [Neuroprotective effect of transient ischemic attack]. Presse Med. 40. 2: 167-72.

Benjamin EJ, Blaha MJ, Chiuve SE, Cushman M, Das SR, Deo R, et al. (2017) Heart Disease and Stroke Statistics-2017 Update: A Report From the American Heart Association. Circulation. 135. 10: e146-e603.

Bonomo J, Welsh JP, Manthiram K, Swartz JR. (2010) Comparing the functional properties of the Hsp70 chaperones, DnaK and BiP. Biophys Chem. 149. 1-2: 58-66.

Broer L, Ikram MA, Schuur M, DeStefano AL, Bis JC, Liu F, et al. (2011) Association of HSP70 and its co-chaperones with Alzheimer's disease. J Alzheimers Dis. 25. 1: 93-102.

Brouns R, De Deyn PP. (2009) The complexity of neurobiological processes in acute ischemic stroke. Clin Neurol Neurosurg. 111. 483.
Brown JE, Zeiger SLH, Hettinger JC, Brooks JD, Holt B, Morrow JD, et al. (2010) Essential role of the redox-sensitive kinase p66shc in determining energetic and oxidative status and cell fate in neuronal preconditioning. Journal Of Neuroscience. 30. 15: 5242-52.
Burchell VS, Gandhi S, Deas E, Wood NW, Abramov AY, Plun-Favreau H. (2010) Targeting mitochondrial dysfunction in neurodegenerative disease: Part I. Expert Opin Ther Targets. 14. 4: 369-85.
Burchell VS, Gandhi S, Deas E, Wood NW, Abramov AY, Plun-Favreau H. (2010) Targeting mitochondrial dysfunction in neurodegenerative disease: Part II. Expert Opin Ther Targets. 14. 5: 497-511.
Burda J, Hrehorovska M, Bonilla LG, Danielisova V, Cizkova D, Burda R, et al. (2003) Role of protein synthesis in the ischemic tolerance acquisition induced by transient forebrain ischemia in the rat. Neurochem Res. 28. 8: 1213-9.
Cagalinec M, Safiulina D, Liiv M, Liiv J, Choubey V, Wareski P, et al. (2013) Principles of the mitochondrial fusion and fission cycle in neurons. J Cell Sci. 126. Pt 10: 2187-97.
Carloni S, Girelli S, Scopa C, Buonocore G, Longini M, Balduini W. (2010) Activation of autophagy and Akt/CREB signaling play an equivalent role in the neuroprotective effect of rapamycin in neonatal hypoxia-ischemia. Autophagy. 6. 3: 366-77.
Chafekar SM, Wisen S, Thompson AD, Echeverria A, Walter GM, Evans CG, et al. (2012) Pharmacological tuning of heat shock protein 70 modulates polyglutamine toxicity and aggregation. ACS Chem Biol. 7. 9: 1556-64.
Chakrabarti L, Eng J, Ivanov N, Garden GA, La Spada AR. (2009) Autophagy activation and enhanced mitophagy characterize the Purkinje cells of pcd mice prior to neuronal death. Mol Brain. 2. 24.
Chen Y, Dorn GW, 2nd. (2013) PINK1-phosphorylated mitofusin 2 is a Parkin receptor for culling damaged mitochondria. Science. 340. 6131: 471-5.
Chen Y, Stevens B, Chang J, Milbrandt J, Barres BA, Hell JW. (2008) NS21: Re-defined and modified supplement B27 for neuronal cultures. Journal Of Neuroscience Methods. 171. 2: 239.
Cheng NT, Kim AS. (2015) Intravenous Thrombolysis for Acute Ischemic Stroke Within 3 Hours Versus Between 3 and 4.5 Hours of Symptom Onset. Neurohospitalist. 5. 3: 101-9.
Chung KK, Thomas B, Li X, Pletnikova O, Troncoso JC, Marsh L, et al. (2004) S-nitrosylation of parkin regulates ubiquitination and compromises parkin's protective function. Science. 304. 5675: 1328-31.
Cohen MV, Baines CP, Downey JM. (2000) Ischemic preconditioning: from adenosine receptor to KATP channel. Annu Rev Physiol. 62. 79-109.
Consolini AE, Ragone MI, Bonazzola P, Colareda GA. (2017) Mitochondrial Bioenergetics During Ischemia and Reperfusion. Adv Exp Med Biol. 982. 141-67.
Costello DA, Villareal VA, Yang PL. (2016) Desmosterol Increases Lipid Bilayer Fluidity during Hepatitis C Virus Infection. ACS Infect Dis. 2. 11: 852-62.
Cozzolino M, Ferri A, Valle C, Carri MT. (2013) Mitochondria and ALS: implications from novel genes and pathways. Mol Cell Neurosci. 55. 44-9.
Cui L, Jeong H, Borovecki F, Parkhurst CN, Tanese N, Krainc D. (2006) Transcriptional repression of PGC-1alpha by mutant huntingtin leads to mitochondrial dysfunction and neurodegeneration. CELL. 127. 1: 59-69.

Cummings CJ, Sun YL, Opal P, Antalffy B, Mestril R, Orr HT, et al. (2001) Over-expression of inducible HSP70 chaperone suppresses neuropathology and improves motor function in SCA1 mice. Human Molecular Genetics. 10. 14: 1511-8.

Dai Q, Zhang C, Wu Y, McDonough H, Whaley RA, Godfrey V, et al. (2003) CHIP activates HSF1 and confers protection against apoptosis and cellular stress. EMBO J. 22. 20: 5446-58.

Daugaard M, Rohde M, Jaattela M. (2007) The heat shock protein 70 family: Highly homologous proteins with overlapping and distinct functions. FEBS Lett. 581. 19: 3702-10.

Dawson TM, Ko HS, Dawson VL. (2010) Genetic animal models of Parkinson's disease. Neuron. 66. 5: 646-61.

Del Zoppo GJ, Saver JL, Jauch EC, Adams HP, Jr., American Heart Association Stroke C. (2009) Expansion of the time window for treatment of acute ischemic stroke with intravenous tissue plasminogen activator: a science advisory from the American Heart Association/American Stroke Association. STROKE. 40. 8: 2945-8.

Di Napoli M, McLaughlin B. (2005) The ubiquitin-proteasome system as a drug target in cerebrovascular disease: therapeutic potential of proteasome inhibitors. Curr Opin Investig Drugs. 6. 7: 686-99.

Doyle KP, Simon RP, Stenzel-Poore MP. (2008) Mechanisms of ischemic brain damage. Neuropharmacology. 55. 3: 310-8.

Durcan TM, Fon EA. (2015) The three 'P's of mitophagy: PARKIN, PINK1, and post-translational modifications. Genes Dev. 29. 10: 989-99.

Easton JD, Saver JL, Albers GW, Alberts MJ, Chaturvedi S, Feldmann E, et al. (2009) Definition and evaluation of transient ischemic attack: a scientific statement for healthcare professionals from the American Heart Association/American Stroke Association Stroke Council; Council on Cardiovascular Surgery and Anesthesia; Council on Cardiovascular Radiology and Intervention; Council on Cardiovascular Nursing; and the Interdisciplinary Council on Peripheral Vascular Disease. The American Academy of Neurology affirms the value of this statement as an educational tool for neurologists. STROKE. 40. 6: 2276-93.

Ebrahimi-Fakhari D, Saidi LJ, Wahlster L. (2013) Molecular chaperones and protein folding as therapeutic targets in Parkinson's disease and other synucleinopathies. Acta Neuropathol Commun. 1. 79.

Elias JE, Gygi SP. (2007) Target-decoy search strategy for increased confidence in large-scale protein identifications by mass spectrometry. Nat Methods. 4. 3: 207-14.

Folbergrova J, Memezawa H, Smith ML, Siesjo BK. (1992) Focal and perifocal changes in tissue energy state during middle cerebral artery occlusion in normo- and hyperglycemic rats. J Cereb Blood Flow Metab. 12. 1: 25-33.

Fontaine SN, Martin MD, Akoury E, Assimon VA, Borysov S, Nordhues BA, et al. (2015) The active Hsc70/tau complex can be exploited to enhance tau turnover without damaging microtubule dynamics. Hum Mol Genet. 24. 14: 3971-81.

Fu M, St-Pierre P, Shankar J, Wang PT, Joshi B, Nabi IR. (2013) Regulation of mitophagy by the Gp78 E3 ubiquitin ligase. Mol Biol Cell. 24. 8: 1153-62.

Fuller M, Futerman AH. (2018) The brain lipidome in neurodegenerative lysosomal storage disorders. Biochem Biophys Res Commun.

Galeffi F, Sinnar S, Schwartz-Bloom RD. (2000) Diazepam promotes ATP recovery and prevents cytochrome c release in hippocampal slices after in vitro ischemia. J Neurochem. 75. 3: 1242-9.

Ge P, Luo Y, Liu CL, Hu B. (2007) Protein aggregation and proteasome dysfunction after brain ischemia. STROKE. 38. 12: 3230-6.
Geisler S, Holmstrom KM, Skujat D, Fiesel FC, Rothfuss OC, Kahle PJ, et al. (2010) PINK1/Parkin-mediated mitophagy is dependent on VDAC1 and p62/SQSTM1. Nature Cell Biology. 12. 2: 119-31.
Geisler S, Holmstrom KM, Treis A, Skujat D, Weber SS, Fiesel FC, et al. (2010) The PINK1/Parkin-mediated mitophagy is compromised by PD-associated mutations. Autophagy. 6. 7: 871-8.
Gestwicki JE, Garza D. (2012) Protein quality control in neurodegenerative disease. Prog Mol Biol Transl Sci. 107. 327.
Greene AW, Grenier K, Aguileta MA, Muise S, Farazifard R, Haque ME, et al. (2012) Mitochondrial processing peptidase regulates PINK1 processing, import and Parkin recruitment. EMBO Rep. 13. 4: 378-85.
Greene JG, Greenamyre JT. (1996) Bioenergetics and glutamate excitotoxicity. Progress In Neurobiology. 48. 6: 613-34.
Grelli KN, Palubinsky AM, Kale AC, Lizama-Manibusan BN, Stankowski JN, Milne GL, et al. (2013) Alteration of isocitrate dehydrogenase following acute ischemic injury as a means to improve cellular energetic status in neuroadaptation. CNS Neurol Disord Drug Targets. 12. 6: 849-60.
Guzhova IV, Lazarev VF, Kaznacheeva AV, Ippolitova MV, Muronetz VI, Kinev AV, et al. (2011) Novel mechanism of Hsp70 chaperone-mediated prevention of polyglutamine aggregates in a cellular model of huntington disease. Hum Mol Genet. 20. 20: 3953-63.
Hacke W, Kaste M, Bluhmki E, Brozman M, Davalos A, Guidetti D, et al. (2008) Thrombolysis with alteplase 3 to 4.5 hours after acute ischemic stroke. N Engl J Med. 359. 13: 1317-29.
Halliwell B, Gutteridge JMC. Free Radicals in Biology and Medicine2007. 1 p.
Hartnett KA, Stout AK, Rajdev S, Rosenberg PA, Reynolds IJ, Aizenman E. (1997) NMDA receptor-mediated neurotoxicity: a paradoxical requirement for extracellular Mg2+ in Na+/Ca2+-free solutions in rat cortical neurons in vitro. J Neurochem. 68. 5: 1836-45.
Hayashi T. (1954) Effects of sodium glutamate on the nervous system. . Keio J Med. 3. 192–3.
Hess DC, Wang S, Hamilton W, Lee S, Pardue C, Waller JL, et al. (2005) REACH: clinical feasibility of a rural telestroke network. STROKE. 36. 9: 2018-20.
Hofmeijer J, van Putten MJ. (2012) Ischemic cerebral damage: an appraisal of synaptic failure. STROKE. 43. 2: 607-15.
Hohfeld J, Cyr DM, Patterson C. (2001) From the cradle to the grave: molecular chaperones that may choose between folding and degradation. EMBO Reports. 10. 2: 885-90.
Hoshino T, Murao N, Namba T, Takehara M, Adachi H, Katsuno M, et al. (2011) Suppression of Alzheimer's Disease-Related Phenotypes by Expression of Heat Shock Protein 70 in Mice. Journal Of Neuroscience. 31. 14: 5225-34.
Howarth JL, Glover CP, Uney JB. (2009) HSP70 interacting protein prevents the accumulation of inclusions in polyglutamine disease. J Neurochem. 108. 4: 945-51.
Hu BR, Janelidze S, Ginsberg MD, Busto R, Perez-Pinzon M, Sick TJ, et al. (2001) Protein aggregation after focal brain ischemia and reperfusion. J Cereb Blood Flow Metab. 21. 7: 865-75.
Huang C, Andres AM, Ratliff EP, Hernandez G, Lee P, Gottlieb RA. (2011) Preconditioning involves selective mitophagy mediated by Parkin and p62/SQSTM1. PLoS ONE. 6. 6: e20975.

Humphries KM, Szweda PA, Szweda LI. (2006) Aging: a shift from redox regulation to oxidative damage. Free Radic Res. 40. 12: 1239-43.
Imai Y, Soda M, Hatakeyama S, Akagi T, Hashikawa T, Nakayama K-I, et al. (2002) CHIP Is Associated with Parkin, a gene responsible for familial Parkinson's Disease, and enhances its ubiquitin ligase activity. Molecular Cell. 10. 1: 55-67.
Jassem W, Heaton ND. (2004) The role of mitochondria in ischemia/reperfusion injury in organ transplantation. Kidney Int. 66. 2: 514-7.
Jinwal UK, Akoury E, Abisambra JF, O'Leary JC, 3rd, Thompson AD, Blair LJ, et al. (2013) Imbalance of Hsp70 family variants fosters tau accumulation. FASEB J. 27. 4: 1450-9.
Jinwal UK, Miyata Y, Koren J, 3rd, Jones JR, Trotter JH, Chang L, et al. (2009) Chemical manipulation of hsp70 ATPase activity regulates tau stability. J Neurosci. 29. 39: 12079-88.
Joel D. Federspiel SGC, Amy M. Palubinsky, Ama J. Winland, Carlos Morales Betanzos, BethAnn McLaughlin and Daniel C. Liebler. (2016) Assembly dynamics and stoichiometry of the apoptosis signal-regulating kinase (ASK) signalosome in response to electrophile stress. Molecular and Cellular Proteomics.
Johri A, Beal MF. (2012) Mitochondrial dysfunction in neurodegenerative diseases. J Pharmacol Exp Ther. 342. 3: 619-30.
Joshi V, Amanullah A, Upadhyay A, Mishra R, Kumar A, Mishra A. (2016) A Decade of Boon or Burden: What Has the CHIP Ever Done for Cellular Protein Quality Control Mechanism Implicated in Neurodegeneration and Aging? Front Mol Neurosci. 9. 93.
Kadiiska MB, Gladen BC, Baird DD, Germolec D, Graham LB, Parker CE, et al. (2005) Biomarkers of oxidative stress study II. Are oxidation products of lipids, proteins, and DNA markers of CCl4 poisoning? Free Radical Biology And Medicine. 38. 6: 698-710.
Kalia SK, Kalia LV, McLean PJ. (2010) Molecular chaperones as rational drug targets for Parkinson's disease therapeutics. CNS Neurol Disord Drug Targets. 9. 6: 741-53.
Kalmar B, Greensmith L. (2009) Activation of the heat shock response in a primary cellular model of motoneuron neurodegeneration-evidence for neuroprotective and neurotoxic effects. Cell Mol Biol Lett. 14. 2: 319-35.
Kalmar B, Greensmith L. (2017) Cellular Chaperones As Therapeutic Targets in ALS to Restore Protein Homeostasis and Improve Cellular Function. Front Mol Neurosci. 10. 251.
Kalogeris T, Baines CP, Krenz M, Korthuis RJ. (2012) Cell biology of ischemia/reperfusion injury. Int Rev Cell Mol Biol. 298. 229-317.
Kampinga HH, Craig EA. (2010) The HSP70 chaperone machinery: J proteins as drivers of functional specificity. Nat Rev Mol Cell Biol. 11. 8: 579-92.
Kandilis AN, Karidis NP, Kouraklis G, Patsouris E, Vasileiou I, Theocharis S. (2014) Proteasome inhibitors: possible novel therapeutic strategy for ischemia-reperfusion injury? Expert Opin Investig Drugs. 23. 1: 67-80.
Keller JN, Huang FF, Zhu H, Yu J, Ho YS, Kindy TS. (2000) Oxidative stress-associated impairment of proteasome activity during ischemia-reperfusion injury. J Cereb Blood Flow Metab. 20. 10: 1467-73.
Kessner D, Chambers M, Burke R, Agus D, Mallick P. (2008) ProteoWizard: open source software for rapid proteomics tools development. Bioinformatics. 24. 21: 2534-6.
Kety SS. (1963) The circulation and energy metabolism of the brain. Clin Neurosurg. 9. 56-66.
Khan IS, Odom M, Ehtesham M, Colvin D, Quarles CC, McLaughlin B, et al. (2016) Intraarterial administration of norcantharidin attenuates ischemic stroke damage in

rodents when given at the time of reperfusion: novel uses of endovascular capabilities. J Neurosurg. 125. 1: 152-9.
Khandelwal PJ, Herman AM, Hoe HS, Rebeck GW, Moussa CE. (2011) Parkin mediates beclin-dependent autophagic clearance of defective mitochondria and ubiquitinated Abeta in AD models. Hum Mol Genet. 20. 11: 2091-102.
Kilpatrick K, Novoa JA, Hancock T, Guerriero CJ, Wipf P, Brodsky JL, et al. (2013) Chemical Induction of Hsp70 Reduces α-Synuclein Aggregation in Neuroglioma Cells. ACS Chemical Biology.
Kim E, Raval AP, DeFazio RA, Perez-Pinzon MA. (2007) Ischemic preconditioning via epsilon protein kinase C activation requires cyclooxygenase-2 activation in vitro. Neuroscience. 145. 3: 931-41.
Kim JY, Han Y, Lee JE, Yenari MA. (2018) The 70-kDa heat shock protein (Hsp70) as a therapeutic target for stroke. Expert Opin Ther Targets. 22. 3: 191-9.
Kitada T, Asakawa S, Hattori N, Matsumine H, Yamamura Y, Minoshima S, et al. (1998) Mutations in the parkin gene cause autosomal recessive juvenile parkinsonism. NATURE. 392. 605.
Kitada T, Tong Y, Gautier CA, Shen J. (2009) Absence of nigral degeneration in aged parkin/DJ-1/PINK1 triple knockout mice. J Neurochem. 111. 3: 696-702.
Klionsky DJ, Abeliovich H, Agostinis P, Agrawal DK, Aliev G, Askew DS, et al. (2008) Guidelines for the use and interpretation of assays for monitoring autophagy in higher eukaryotes. Autophagy. 4. 2: 151-75.
Koike M, Shibata M, Tadakoshi M, Gotoh K, Komatsu M, Waguri S, et al. (2008) Inhibition of autophagy prevents hippocampal pyramidal neuron death after hypoxic-ischemic injury. Am J Pathol. 172. 2: 454-69.
Krebiehl G, Ruckerbauer S, Burbulla LF, Kieper N, Maurer B, Waak J, et al. (2010) Reduced basal autophagy and impaired mitochondrial dynamics due to loss of parkinson's disease-associated protein DJ-1. PLoS ONE. 5. 2: e9367.
Kudo T, Kanemoto S, Hara H, Morimoto N, Morihara T, Kimura R, et al. (2008) A molecular chaperone inducer protects neurons from ER stress. Cell Death Differ. 15. 2: 364-75.
Lackovic J, Howitt J, Callaway JK, Silke J, Bartlett P, Tan SS. (2012) Differential regulation of Nedd4 ubiquitin ligases and their adaptor protein Ndfip1 in a rat model of ischemic stroke. Exp Neurol. 235. 1: 326-35.
Lakhan SE, Kirchgessner A, Hofer M. (2009) Inflammatory mechanisms in ischemic stroke: therapeutic approaches. J Transl Med. 7. 97.
Landar A, Shiva S, Levonen AL, Oh JY, Zaragoza C, Johnson MS, et al. (2006) Induction of the permeability transition and cytochrome c release by 15-deoxy-Delta12,14-prostaglandin J2 in mitochondria. Biochem J. 394. Pt 1: 185-95.
Leak RK. (2014) Heat shock proteins in neurodegenerative disorders and aging. J Cell Commun Signal. 8. 4: 293-310.
Lee JS, Seo TW, Yi JH, Shin KS, Yoo SJ. (2013) CHIP has a protective role against oxidative stress-induced cell death through specific regulation of endonuclease G. Cell Death Dis. 4. e666.
Lee S-H, Kwon H-M, Kim Y-J, Lee K-M, Kim M, Yoon B-W. (2004) Effects of Hsp70.1 Gene Knockout on the Mitochondrial Apoptotic Pathway After Focal Cerebral Ischemia. STROKE. 35. 9: 2195-9.
Li S, Zheng J, Carmichael ST. (2005) Increased oxidative protein and DNA damage but decreased stress response in the aged brain following experimental stroke. Neurobiol Dis. 18. 3: 432-40.

Li X, Srinivasan SR, Connarn J, Ahmad A, Young ZT, Kabza AM, et al. (2013) Analogs of the Allosteric Heat Shock Protein 70 (Hsp70) Inhibitor, MKT-077, as Anti-Cancer Agents. ACS Med Chem Lett. 4. 11:

Lipton P. (1999) Ischemic cell death in brain neurons. Physiol Rev. 79. 4: 1431-568.

Liu C, Chen S, Kamme F, Hu BR. (2005) Ischemic preconditioning prevents protein aggregation after transient cerebral ischemia. Neuroscience. 134. 1: 69-80.

Liu J, Shinobu LA, Ward CM, Young D, Cleveland DW. (2005) Elevation of the Hsp70 chaperone does not effect toxicity in mouse models of familial amyotrophic lateral sclerosis. J Neurochem. 93. 4: 875-82.

Lizama BN, Palubinsky AM, McLaughlin B. (2018) Alterations in the E3 ligases Parkin and CHIP result in unique metabolic signaling defects and mitochondrial quality control issues. Neurochem Int. 117. 139-55.

Lizama BN, Palubinsky AM, Raveendran VA, Moore AM, Federspiel JD, Codreanu SG, et al. (2018) Neuronal Preconditioning Requires the Mitophagic Activity of C-terminus of HSC70-Interacting Protein. J Neurosci.

Lokireddy S, Wijesoma IW, Teng S, Bonala S, Gluckman PD, McFarlane C, et al. (2012) The ubiquitin ligase Mul1 induces mitophagy in skeletal muscle in response to muscle-wasting stimuli. Cell Metab. 16. 5: 613-24.

Lücking CB, Dürr A, Bonifati V, Vaughan J, De Michele G, Gasser T, et al. (2000) Association between Early-Onset Parkinson's Disease and Mutations in the Parkin Gene. New England Journal Of Medicine. 342. 21: 1560-7.

Ma ZQ, Dasari S, Chambers MC, Litton MD, Sobecki SM, Zimmerman LJ, et al. (2009) IDPicker 2.0: Improved protein assembly with high discrimination peptide identification filtering. J Proteome Res. 8. 8: 3872-81.

Magrane J, Smith RC, Walsh K, Querfurth HW. (2004) Heat shock protein 70 participates in the neuroprotective response to intracellularly expressed beta-amyloid in neurons. J Neurosci. 24. 7: 1700-6.

Maher P. (2005) The effects of stress and aging on glutathione metabolism. Ageing Res Rev. 4. 2: 288-314.

Mark KA, Dumas KJ, Bhaumik D, Schilling B, Davis S, Oron TR, et al. (2016) Vitamin D Promotes Protein Homeostasis and Longevity via the Stress Response Pathway Genes skn-1, ire-1, and xbp-1. Cell Rep. 17. 5: 1227-37.

Martin RL, Lloyd HGE, Cowan AI. (1994) The early events of oxygen and glucose deprivation: setting the scene for neuronal death? Trends In Neurosciences. 17. 6: 251-7.

Martinez-Vicente M. (2017) Neuronal Mitophagy in Neurodegenerative Diseases. Front Mol Neurosci. 10. 64.

Matsuda N, Sato S, Shiba K, Okatsu K, Saisho K, Gautier CA, et al. (2010) PINK1 stabilized by mitochondrial depolarization recruits Parkin to damaged mitochondria and activates latent Parkin for mitophagy. The Journal Of Cell Biology. 189. 2: 211-21.

Matsuda N, Tanaka K. (2010) Uncovering the roles of PINK1 and parkin in mitophagy. Autophagy. 6. 7: 952-4.

Matsuyama N, Leavens JE, McKinnon D, Gaudette GR, Aksehirli TO, Krukenkamp IB. (2000) Ischemic but not pharmacological preconditioning requires protein synthesis. Circulation. 102. 19 Suppl 3: III312-8.

Mayer M, Bukau B. (2005) Hsp70 chaperones: Cellular functions and molecular mechanism. Cellular And Molecular Life Sciences. 62. 6: 670-84.

McBride HM, Neuspiel M, Wasiak S. (2006) Mitochondria: more than just a powerhouse. Curr Biol. 16. 14: R551-60.

McDonough H, Patterson C. (2003) CHIP: a link between the chaperone and proteasome systems. Cell Stress & Chaperones. 8. 4: 303-8.
McKenzie JR, Palubinsky AM, Brown JE, McLaughlin B, Cliffel DE. (2012) Metabolic multianalyte microphysiometry reveals extracellular acidosis is an essential mediator of neuronal preconditioning. ACS Chem Neurosci. 3. 7: 510-8.
McLaughlin B, Buendia MA, Saborido TP, Palubinsky AM, Stankowski JN, Stanwood GD. (2012) Haploinsufficiency of the E3 ubiquitin ligase C-terminus of heat shock cognate 70 interacting protein (CHIP) produces specific behavioral impairments. PLoS ONE. 7. 5: e36340.
McLaughlin B, Gidday JM. (2013) Poised for success: implementation of sound conditioning strategies to promote endogenous protective responses to stroke in patients. Transl Stroke Res. 4. 1: 104-13.
McLaughlin B, Hartnett KA, Erhardt JA, Legos JJ, White RF, Barone FC, et al. (2003) Caspase 3 activation is essential for neuroprotection in preconditioning. Proc Natl Acad Sci U S A. 100. 2: 715-20.
McLaughlin B, Pal S, Tran MP, Parsons AA, Barone FC, Erhardt JA, et al. (2001) p38 Activation Is Required Upstream of Potassium Current Enhancement and Caspase Cleavage in Thiol Oxidant-Induced Neuronal Apoptosis. Journal Of Neuroscience. 21. 10: 3303-11.
McLaughlin BA. Dopamine neurotoxicity and neurodegeneration. In Molecular Mechanisms of Cell Death. . In: M.F. C, editor. Molecular Mechanisms of Cell Death. Totowa, NJ: Humana Press; 2001. p. 195-231.
McLaughlin BA, Buendia MA, Saborido TP, Palubinsky AM, Stankowski JN, Stanwood GD. (2012) C-Terminus of Heat Shock Cognate 70 Interacting Protein (CHIP) Haploinsufficiency Produces Specific Behavioral Impairments. PLoS ONE. 7. 5: e36340.
McLean PJ, Klucken J, Shin Y, Hyman BT. (2004) Geldanamycin induces Hsp70 and prevents alpha-synuclein aggregation and toxicity in vitro. Biochem Biophys Res Commun. 321. 3: 665-9.
Meacham GC, Patterson C, Zhang W, Younger JM, Cyr DM. (2001) The Hsc70 co-chaperone CHIP targets immature CFTR for proteasomal degradation. Nature Cell Biology. 3. 1: 100-5.
Mehta S, Manhas N, Rahubir R. (2007) Molecular targets in cerebral ischemia for developing novel therapeutics. Brain Research Reviews. 54. 34 - 66.
Meng F, Yao D, Shi Y, Kabakoff J, Wu W, Reicher J, et al. (2011) Oxidation of the cysteine-rich regions of parkin perturbs its E3 ligase activity and contributes to protein aggregation. Molecular Neurodegeneration. 6.
Mengesdorf T, Jensen PH, Mies G, Aufenberg C, Paschen W. (2002) Down-regulation of parkin protein in transient focal cerebral ischemia: A link between stroke and degenerative disease? Proceedings of The National Academy of Sciences. 99. 23: 15042-7.
Michiorri S, Gelmetti V, Giarda E, Lombardi F, Romano F, Marongiu R, et al. (2010) The Parkinson-associated protein PINK1 interacts with Beclin1 and promotes autophagy. Cell Death Differ. 17. 6: 962-74.
Miller VM, Nelson RF, Gouvion CM, Williams A, Rodriguez-Lebron E, Harper SQ, et al. (2005) CHIP Suppresses Polyglutamine Aggregation and Toxicity In Vitro and In Vivo. Journal Of Neuroscience. 25. 40: 9152-61.
Milne GL, Musiek ES, Zanoni G, Vidari G, McLaughlin BA, Morrow JD. (2005) Development of a high performance liquid chromatography-electrospray ionization tandem mass

spectrometric (LC/ESI/MS/MS) assay to quantify highly reactive cyclopentenone eicosanoids in vivo. Free Radical Biology And Medicine. 39. S113-S.
Min JN, Patterson C. (2011) Evaluating age-associated phenotypes in a mouse model of protein dyshomeostasis. Methods. 53. 3: 187-93.
Min JN, Whaley RA, Sharpless NE, Lockyer P, Portbury AL, Patterson C. (2008) CHIP deficiency decreases longevity, with accelerated aging phenotypes accompanied by altered protein quality control. Mol Cell Biol. 28. 12: 4018-25.
Miyata Y, Li X, Lee HF, Jinwal UK, Srinivasan SR, Seguin SP, et al. (2013) Synthesis and initial evaluation of YM-08, a blood-brain barrier permeable derivative of the heat shock protein 70 (Hsp70) inhibitor MKT-077, which reduces tau levels. ACS Chem Neurosci. 4. 6: 930-9.
Mizui T, Kinouchi H, Chan PH. (1992) Depletion of brain glutathione by buthionine sulfoximine enhances cerebral ischemic injury in rats. Am J Physiol. 262. 2 Pt 2: H313-7.
Murphy ME. (2013) The HSP70 family and cancer. Carcinogenesis. 34. 6: 1181-8.
Narendra D, Tanaka A, Suen D-F, Youle RJ. (2008) Parkin is recruited selectively to impaired mitochondria and promotes their autophagy. The Journal Of Cell Biology. 183. 5: 795-803.
Narendra DP, Jin SM, Tanaka A, Suen DF, Gautier CA, Shen J, et al. (2010) PINK1 is selectively stabilized on impaired mitochondria to activate Parkin. PLoS Biol. 8. 1: e1000298.
Narendra DP, Youle RJ. (2011) Targeting mitochondrial dysfunction: role for PINK1 and Parkin in mitochondrial quality control. Antioxid Redox Signal. 14. 10: 1929-38.
Niescier RF, Kwak SK, Joo SH, Chang KT, Min KT. (2016) Dynamics of Mitochondrial Transport in Axons. Front Cell Neurosci. 10. 123.
Olney JW. (1969) Brain lesions, obesity, and other disturbances in mice treated with monosodium glutamate. Science. 164. 3880: 719-21.
Onteniente B, Couriaud C, Braudeau J, Benchoua A, Guegan C. (2003) The mechanisms of cell death in focal cerebral ischemia highlight neuroprotective perspectives by anti-caspase therapy. Biochemical Pharmacology. 66. 8: 1643-9.
Otera H, Mihara K. (2011) Molecular mechanisms and physiologic functions of mitochondrial dynamics. Journal Of Biochemistry. 149. 3: 241-51.
Palacino JJ, Sagi D, Goldberg MS, Krauss S, Motz C, Wacker M, et al. (2004) Mitochondrial dysfunction and oxidative damage in parkin-deficient mice. J Biol Chem. 279. 18: 18614-22.
Palubinsky AM, Stankowski JN, Kale AC, Codreanu SG, Singer RJ, Liebler DC, et al. (2015) CHIP Is an Essential Determinant of Neuronal Mitochondrial Stress Signaling. Antioxid Redox Signal. 23. 6: 535-49.
Perez FA, Palmiter RD. (2005) Parkin-deficient mice are not a robust model of parkinsonism. Proceedings Of The National Academy Of Sciences Of The United States Of America. 102. 6: 2174-9.
Ploumi C, Daskalaki I, Tavernarakis N. (2017) Mitochondrial biogenesis and clearance: a balancing act. FEBS J. 284. 2: 183-95.
Poole AC, Thomas RE, Andrews LA, McBride HM, Whitworth AJ, Pallanck LJ. (2008) The PINK1/Parkin pathway regulates mitochondrial morphology. Proc Natl Acad Sci U S A. 105. 5: 1638-43.
Poole AC, Thomas RE, Yu S, Vincow ES, Pallanck L. (2010) The mitochondrial fusion-promoting factor Mitofusin is a substrate of the PINK1/Parkin pathway. PLoS ONE. 5. 4: e10054.

Pratt WB, Gestwicki JE, Osawa Y, Lieberman AP. (2015) Targeting Hsp90/Hsp70-Based Protein Quality Control for Treatment of Adult Onset Neurodegenerative Diseases. Annu Rev Pharmacol Toxicol. 55. 353-71.

Pratt WB, Morishima Y, Peng H-M, Osawa Y. (2010) Proposal for a role of the Hsp90/Hsp70-based chaperone machinery in making triage decisions when proteins undergo oxidative and toxic damage. Exp Biol Med. 235. 3: 278-89.

Qian SB, McDonough H, Boellmann F, Cyr DM, Patterson C. (2006) CHIP-mediated stress recovery by sequential ubiquitination of substrates and Hsp70. NATURE. 440. 7083: 551-5.

Quarrie R, Lee DS, Reyes L, Erdahl W, Pfeiffer DR, Zweier JL, et al. (2014) Mitochondrial uncoupling does not decrease reactive oxygen species production after ischemia-reperfusion. Am J Physiol Heart Circ Physiol. 307. 7: H996-H1004.

Radons J. (2016) The human HSP70 family of chaperones: where do we stand? Cell Stress Chaperones. 21. 3: 379-404.

Rappold PM, Cui M, Grima JC, Fan RZ, de Mesy-Bentley KL, Chen L, et al. (2014) Drp1 inhibition attenuates neurotoxicity and dopamine release deficits in vivo. Nat Commun. 5. 5244.

Ravati A, Ahlemeyer B, Becker A, Krieglstein J. (2000) Preconditioning-induced neuroprotection is mediated by reactive oxygen species. Brain Research. 866. 1-2: 23-32.

Ravina B, Janis S, Keleti J, Marler JM. (2004) Funding evidence: the National Institute of Neurological Disorders and Stroke Clinical Trials Program. NeuroRX. 1. 3: 317-22.

Rodrigo R, Fernandez-Gajardo R, Gutierrez R, Matamala JM, Carrasco R, Miranda-Merchak A, et al. (2013) Oxidative stress and pathophysiology of ischemic stroke: novel therapeutic opportunities. CNS Neurol Disord Drug Targets. 12. 5: 698-714.

Rosser MFN, Washburn E, Muchowski PJ, Patterson C, Cyr DM. (2007) Chaperone functions of the E3 ubiquitin ligase CHIP. Journal Of Biological Chemistry. 282. 31: 22267-77.

Rousaki A, Miyata Y, Jinwal UK, Dickey CA, Gestwicki JE, Zuiderweg ER. (2011) Allosteric drugs: the interaction of antitumor compound MKT-077 with human Hsp70 chaperones. J Mol Biol. 411. 3: 614-32.

Rowland RT, Meng X, Cleveland JC, Meldrum DR, Harken AH, Brown JM. (1997) Cardioadaptation induced by cyclic ischemic preconditioning is mediated by translational regulation of de novo protein synthesis. J Surg Res. 71. 2: 155-60.

Sahara N, Murayama M, Mizoroki T, Urushitani M, Imai Y, Takahashi R, et al. (2005) In vivo evidence of CHIP up-regulation attenuating tau aggregation. Journal Of Neurochemistry. 94. 5: 1254-63.

Sardiu ME, Cheung MS, Yu YK. (2007) Cysteine-cysteine contact preference leads to target-focusing in protein folding. Biophys J. 93. 3: 938-51.

Scherz-Shouval R, Shvets E, Fass E, Shorer H, Gil L, Elazar Z. (2007) Reactive oxygen species are essential for autophagy and specifically regulate the activity of Atg4. EMBO Journal. 26. 7: 1749-60.

Schisler JC, Patterson C, Willis MS. (2016) Skeletal Muscle Mitochondrial Alterations in Carboxyl Terminus of Hsc70 Interacting Protein (Chip) -/- Mice. Afr J Cell Pathol. 6. 4: 28-36.

Sengupta S, Badhwar I, Upadhyay M, Singh S, Ganesh S. (2011) Malin and laforin are essential components of a protein complex that protects cells from thermal stress. J Cell Sci. 124. Pt 13: 2277-86.

Sherman MY, Gabai VL. (2015) Hsp70 in cancer: back to the future. Oncogene. 34. 32: 4153-61.

Shi CH, Schisler JC, Rubel CE, Tan S, Song B, McDonough H, et al. (2014) Ataxia and hypogonadism caused by the loss of ubiquitin ligase activity of the U box protein CHIP. Hum Mol Genet. 23. 4: 1013-24.
Shi Q, Xu H, Yu H, Zhang N, Ye Y, Estevez AG, et al. (2011) Inactivation and reactivation of the mitochondrial alpha-ketoglutarate dehydrogenase complex. J Biol Chem. 286. 20: 17640-8.
Shiber A, Ravid T. (2014) Chaperoning proteins for destruction: diverse roles of Hsp70 chaperones and their co-chaperones in targeting misfolded proteins to the proteasome. Biomolecules. 4. 3: 704-24.
Shimshek DR, Mueller M, Wiessner C, Schweizer T, van der Putten PH. (2010) The HSP70 molecular chaperone is not beneficial in a mouse model of alpha-synucleinopathy. PLoS ONE. 5. 4: e10014.
Silva GS, Farrell S, Shandra E, Viswanathan A, Schwamm LH. (2012) The status of telestroke in the United States: a survey of currently active stroke telemedicine programs. STROKE. 43. 8: 2078-85.
Sims NR, Muyderman H. (2010) Mitochondria, oxidative metabolism and cell death in stroke. Biochim Biophys Acta. 1802. 1: 80-91.
Sinor JD, Boeckman FA, Aizenman E. (1997) Intrinsic redox properties of N-methyl-D-aspartate receptor can determine the developmental expression of excitotoxicity in rat cortical neurons in vitro. Brain Res. 747. 2: 297-303.
Song HO, Lee W, An K, Lee HS, Cho JH, Park ZY, et al. (2009) C. elegans STI-1, the homolog of Sti1/Hop, is involved in aging and stress response. J Mol Biol. 390. 4: 604-17.
Stankowski JN, Condreanu GS, Liebler D, McLaughlin BA. Analysis of protein targets by oxidative stress using oxyblot and biotin-avidin capture methodology. In: Aschner M, Price A, Sunol C, editors. Neuromethods: Cell Culture Techniques: Spring Science; 2011.
Stankowski JN, Gupta R. (2011) Therapeutic targets for neuroprotection in acute ischemic stroke: lost in translation? Antioxid Redox Signal. 14. 10: 1841-51.
Stankowski JN, Zeiger SLH, Cohen EL, DeFranco DB, Cai J, McLaughlin BA. (2011) C-Terminus of HSC70 interacting protein increases following stroke and impairs survival against acute oxidative stress. Antioxidants and Redox Signaling. 14. 10: 1787-801.
Su YC, Qi X. (2013) Inhibition of excessive mitochondrial fission reduced aberrant autophagy and neuronal damage caused by LRRK2 G2019S mutation. Hum Mol Genet. 22. 22: 4545-61.
Tabb DL, Fernando CG, Chambers MC. (2007) MyriMatch: highly accurate tandem mass spectral peptide identification by multivariate hypergeometric analysis. J Proteome Res. 6. 2: 654-61.
Tanaka M, Mun S, Harada A, Ohkawa Y, Inagaki A, Sano S, et al. (2014) Hsc70 contributes to cancer cell survival by preventing Rab1A degradation under stress conditions. PLoS ONE. 9. 5: e96785.
Tang YC, Tian HX, Yi T, Chen HB. (2016) The critical roles of mitophagy in cerebral ischemia. Protein Cell. 7. 10: 699-713.
Tani M, Honma Y, Hasegawa H, Tamaki K. (2001) Direct activation of mitochondrial KATP channels mimics preconditioning but protein kinase C activation is less effective in middle-aged rat hearts. Cardiovasc Res. 49. 56.
Teshima Y, Akao M, Li RA, Chong TH, Baumgartner WA, Johnston MV, et al. (2003) Mitochondrial ATP-sensitive potassium channel activation protects cerebellar granule neurons from apoptosis induced by oxidative stress. STROKE. 34. 7: 1796-802.

Tetzlaff JE, Putcha P, Outeiro TF, Ivanov A, Berezovska O, Hyman BT, et al. (2008) CHIP targets toxic alpha-Synuclein oligomers for degradation. J Biol Chem. 283. 26: 17962-8.
Tirapelli DP, Carlotti Jr CG, Leite JP, Tirapelli LF, Colli BO. (2010) Expression of HSP70 in cerebral ischemia and neuroprotetive action of hypothermia and ketoprofen. Arq Neuropsiquiatr. 68. 4: 592-6.
Tokumasu F, Dvorak J. (2003) Development and application of quantum dots for immunocytochemistry of human erythrocytes. J Microsc. 211. Pt 3: 256-61.
Turturici G, Sconzo G, Geraci F. (2011) Hsp70 and its molecular role in nervous system diseases. Biochem Res Int. 2011. 618127.
Twig G, Elorza A, Molina AJ, Mohamed H, Wikstrom JD, Walzer G, et al. (2008) Fission and selective fusion govern mitochondrial segregation and elimination by autophagy. EMBO J. 27. 2: 433-46.
Valente EM, Abou-Sleiman PM, Caputo V, Muqit MM, Harvey K, Gispert S, et al. (2004) Hereditary early-onset Parkinson's disease caused by mutations in PINK1. Science. 304. 5674: 1158-60.
Van Humbeeck C, Waelkens E, Corti O, Brice A, Vandenberghe W. (2008) Parkin occurs in a stable, non-covalent, approximately 110-kDa complex in brain. Eur J Neurosci. 27. 2: 284-93.
van Leyen K, Siddiq A, Ratan RR, Lo EH. (2005) Proteasome inhibition protects HT22 neuronal cells from oxidative glutamate toxicity. J Neurochem. 92. 4: 824-30.
Varcin M, Bentea E, Michotte Y, Sarre S. (2012) Oxidative stress in genetic mouse models of Parkinson's disease. Oxid Med Cell Longev. 2012. 624925.
Wang AM, Miyata Y, Klinedinst S, Peng HM, Chua JP, Komiyama T, et al. (2013) Activation of Hsp70 reduces neurotoxicity by promoting polyglutamine protein degradation. Nat Chem Biol. 9. 2: 112-8.
Wang WW, Chen DZ, Zhao M, Yang XF, Gong DR. (2017) Prior transient ischemic attacks may have a neuroprotective effect in patients with ischemic stroke. Arch Med Sci. 13. 5: 1057-61.
Watkins JC, Jane DE. (2006) The glutamate story. Br J Pharmacol. 147 Suppl 1. S100-8.
Wild P, McEwan DG, Dikic I. (2014) The LC3 interactome at a glance. J Cell Sci. 127. Pt 1: 3-9.
Wisen S, Bertelsen EB, Thompson AD, Patury S, Ung P, Chang L, et al. (2010) Binding of a small molecule at a protein-protein interface regulates the chaperone activity of hsp70-hsp40. ACS Chem Biol. 5. 6: 611-22.
Wisen S, Gestwicki JE. (2008) Identification of small molecules that modify the protein folding activity of heat shock protein 70. Anal Biochem. 374. 2: 371-7.
Wolfe KJ, Ren HY, Trepte P, Cyr DM. (2013) The Hsp70/90 cochaperone, Sti1, suppresses proteotoxicity by regulating spatial quality control of amyloid-like proteins. Mol Biol Cell. 24. 23: 3588-602.
Woo C-H, Le N-T, Shishido T, Chang E, Lee H, Heo K-S, et al. (2010) Novel role of C terminus of Hsc70-interacting protein (CHIP) ubiquitin ligase on inhibiting cardiac apoptosis and dysfunction via regulating ERK5-mediated degradation of inducible cAMP early repressor. The FASEB Journal. 24. 12: 4917-28.
Wu CM, McLaughlin K, Lorenzetti DL, Hill MD, Manns BJ, Ghali WA. (2007) Early risk of stroke after transient ischemic attack: a systematic review and meta-analysis. Arch Intern Med. 167. 22: 2417-22.

Wu Q, Moeller HB, Stevens DA, Sanchez-Hodge R, Childers G, Kortenoeven MLA, et al. (2018) CHIP Regulates Aquaporin-2 Quality Control and Body Water Homeostasis. J Am Soc Nephrol. 29. 3: 936-48.
Yaglom JA, Gabai VL, Sherman MY. (2007) High levels of heat shock protein Hsp72 in cancer cells suppress default senescence pathways. Cancer Res. 67. 5: 2373-81.
Yang Y, Coleman M, Zhang L, Zheng X, Yue Z. (2013) Autophagy in axonal and dendritic degeneration. Trends Neurosci. 36. 7: 418-28.
Yao D, Gu Z, Nakamura T, Shi Z-Q, Ma Y, Gaston B, et al. (2004) Nitrosative stress linked to sporadic Parkinson's disease: S-nitrosylation of parkin regulates its E3 ubiquitin ligase activity. Proceedings of The National Academy of Sciences. 101. 29: 10810-4.
Yoshida KH, T. (2014) Mitochondrial isocitrate dehydrogenase is inactivated upon oxidation and reactivated by thioredoxin-dependent reduction in Arabidopsis. Frontiers in Environmental Science. 2.
Zeiger SLH, McKenzie JR, Stankowski JN, Martin JA, Cliffel DE, McLaughlin B. (2010) Neuron specific metabolic adaptations following multi-day exposures to oxygen glucose deprivation. Biochimica et Biophysica Acta - Molecular Basis of Disease. 1802. 11: 1095-104.
Zhan X, Jickling GC, Tian Y, Stamova B, Xu H, Ander BP, et al. (2011) Transient ischemic attacks characterized by RNA profiles in blood. Neurology. 77. 19: 1718-24.
Zhang J, Liu Q. (2015) Cholesterol metabolism and homeostasis in the brain. Protein Cell. 6. 4: 254-64.
Zhang Q-g, Han D, Wang R-m, Dong Y, Yang F, Vadlamudi RK, et al. (2011) C terminus of Hsc70-interacting protein (CHIP)-mediated degradation of hippocampal estrogen receptor-α and the critical period hypothesis of estrogen neuroprotection. Proceedings of The National Academy of Sciences.
Ziviani E, Tao RN, Whitworth AJ. (2010) Drosophila Parkin requires PINK1 for mitochondrial translocation and ubiquitinates Mitofusin. Proceedings Of The National Academy Of Sciences Of The United States Of America. 107. 11: 5018-23.
Zuiderweg ER, Hightower LE, Gestwicki JE. (2017) The remarkable multivalency of the Hsp70 chaperones. Cell Stress Chaperones. 22. 2: 173-89.